

# S M S

Smart Materials and Surfaces

B A N G K O K 2 0 1 4

---

## International Conference 26 - 28 August 2014

Sheraton Grande Sukhumvit Hotel  
Bangkok - Thailand

Organizer



[www.setcor.org](http://www.setcor.org)

In collaboration with



[www.iaamonline.org](http://www.iaamonline.org)

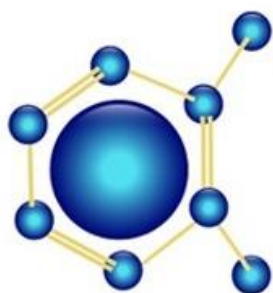


[www.ait.ac.th](http://www.ait.ac.th)



[www.consulting.ait.asia](http://www.consulting.ait.asia)

---



**S M S**  
Smart Materials and Surfaces  
B A N G K O K 2 0 1 4  
26 - 28 August 2014

Sheraton Grande Sukhumvit Hotel - Bangkok-Thailand

## Smart Materials and Surfaces- SMS Bangkok 2014 Conference Program

### Conference General Chairs

**Prof. Ashutosh Tiwari**- Biosensors and Bioelectronics Centre, Linköping University, Sweden

**Dr. Naveed Anwar** - Executive Director/CEO, AIT Consulting Affiliated Faculty, Structural Engineering Director, ACECOMS, Asian Institute of Technology, **Thailand**

**Prof. Joydeep Dutta**- Chair in Nanotechnology Water Research Center, Sultan Qaboos University, **Oman**

### Organizer



### In collaboration with



Tuesday 26 <sup>th</sup> August 2014		
Smart Materials and Surfaces: Fabrication, Characterization & Properties		
7.00 - 9.00	Registration - Welcome coffee	
9.00 - 9.30	Opening Ceremony Chairs: Prof. Ashutosh Tiwari, Sweden and Dr. Naveed Anwar, Thailand	
Keynote talk 9.30 - 10.15	Prof Elias Siores - Provost, Bolton University, <b>United Kingdom</b>	Prof Elias Siores
	Smart functional materials for energy harvesting: from laboratory to commercialisation (E. Siores, N. Soin, T. H. Shah and S. C. Anand)	
10.15 -10.45	Coffee break- Poster Session I	
	Chairs : Prof. Ashutosh Tiwari, Sweden and Dr. Naveed Anwar, Thailand	
Keynote talk 10.45- 11.30	H.N. Alshareef, M.A. Khan and A.J. Caraveo-Frescas Materials Science & Engineering, King Abdullah University of Science & Technology, Thuwal, <b>Kingdom of Saudi Arabia</b>	Prof Husam Alshareef
	Flexible Memory Devices Using Functional Polymers Page. 9	
11.30-11.45	A.S. Dhaliwal, Y. Ali and R.G. Sonkawad Department of Physics, Sant Longowal Institute of Engineering & Technology ((Deemed University) Longowal (Sangrur) -Punjab and Inter University Accelerator Centre, New Delhi, <b>India</b>	Prof Amarjit Dhaliwal
	Galvanostatic fabrication of pTS doped PANI- PPy fiber composite film Page. 10	
11.45- 12.00	A. Yousif, H. C. Swart, O. M. Ntwaeaborwa Department of Physics, University of the Free State, Bloemfontein, <b>South Africa</b>	Dr Abdelrahman Mohammed Yousif
	The role of particulates on the structure and optical properties of Y <sub>3</sub> (Al,Ga) <sub>5</sub> O <sub>12</sub> :Tb films deposited by PLD. Page. 11	
12.00-12.15	E.A.B. Hughes, R. Wise and L.M. Grover University of Birmingham, School of Chemical Engineering, Birmingham and TWI Ltd, Granta Park, Cambridge, <b>United Kingdom</b>	Mr Erik Hughes
	Formulation of covalently linked PEEK/HA composite Page. 12	
12.15-12.30	N.Paleeya, N. Khemasiri, D. S-T Phromyothin, M. Horprathum, S.Porntheeraphat, J.Nukeaw and S. Pratontep National Electronics and Computer Technology Center, Thailand Science Park and College of Nanotechnology, King Mongkut's Institute of Technology, <b>Thailand</b>	Dr Sirapat Pratontep
	Silicon Nitride Protective Coating by Gas-timing RF Magnetron Sputtering Deposition Page. 13	
12.30-12.45	M. Bahrami, A.H. Pakseresht and A. Simchi Department of Material Science and Engineering, Sharif University of Technology, and Department of Ceramics, Materials and Energy Research Center, Karaj, <b>Iran</b>	Mr Mohsen Bahrami
	Application of Spark Plasma Sintering for Fabrication of Functionally Graded Thermal Barrier Coating on a Superalloy Substrate Page. 14	
12.45-14.00	Lunch break- Poster Session I	
	Smart Materials and Surfaces for Energy and Environment	
	Chairs : Prof. Husam Alshareef, Kingdom of Saudi Arabia and Prof. Elias Siores, United Kingdom	
Keynote talk 14.00- 14.45	Prof Joydeep Dutta - Chair in Nanotechnology, Water Research Center, Sultan Qaboos University, <b>Sultanate of Oman</b>	Prof Joydeep Dutta
	Nanotechnology for water treatment and desalination	
14.45-15.15	B. Petter Jelle, T. Gao and A. Gustavsen SINTEF Building and Infrastructure, Department of Materials and Structures, Norwegian University of Science and Technology (NTNU), Department of Civil and Transport Engineering and Norwegian University of Science and Technology (NTNU), Department of Architectural Design, History and Technology, <b>Norway</b> .	Prof Bjorn Petter Jelle
	Electrochromic Materials and their Characterization by Solar Radiation Glazing Factors for Smart Window Applications Page. 15	
15.15- 15:45 Invited talk	P. Hirunsit, W. Soodsawang and J. Limtrakul National Nanotechnology Center (NANOTEC), National Science and Technology Development Agency (NSTDA), Department of Chemistry and NANOTEC Center for Nanoscale Materials Design for Green Nanotechnology, Faculty of Science, Kasetsart University and PTT Group Frontier Research Center, PTT Public Company Limited, Bangkok, <b>Thailand</b> .	Dr Pussana Hirunsit
	Reactivity Trend of CO <sub>2</sub> Electroreduction on Copper Alloys from First Principles Page. 16	

<b>15.45-16:00</b>	Y. Singhvi, I. V. N. Tejasvini and <b>G. Manik</b> Department of Polymer and Process Engineering, IIT Roorkee (Saharanpur Campus), Saharanpur, <b>India</b>	<b>Dr Gaurav Manik</b>
	Molecular Simulations of Anti-stain Polymeric Coatings Page. 17	
<b>16.00-16.15</b>	<b>Coffee break- Poster Session I</b>	
<b>16:15-16:30</b>	<b>K. Koyvanich</b> , N. Muensit and P. Smithmaitrie Center of Excellence in Nanotechnology for Energy (CENE), Physics Department, Faculty of Science and Department of Mechanical Engineering, Faculty of Engineering, Prince of Songkla University (PSU), HatYai, Songkla, <b>Thailand</b> .	<b>Mr Krit Koyvanich</b>
	A Microscale Piezoelectric Harvester for Mechanical Energy from Fluid Flow Page. 18	
<b>16.30-16.45</b>	<b>O. Abbes</b> , A. Portavoce, C. Girardeaux, A. Spiesser, and V. Le Thanh GREMI CNRS-Université d'Orléans, Aix-Marseille Université, CNRS, IM2NP-UMR 6242 and Aix-Marseille Université, CNRS, CINaM-UMR 7325, Marseille, <b>France</b>	<b>Mr Omar Abbes</b>
	Formation of magnetic phases by reactive diffusion between Mn and Ge for Spintronic Applications Page. 19	
<b>16.45-17.00</b>	<b>N. Belkadi</b> , B. Dulmet and T. Baron FEMTO-ST Institute, Time and Frequency Dpt., Besançon, <b>France</b> .	<b>Dr Nesrine Belkadi</b>
	Development of Through Silicon Stacking Technology for Capacitive Acoustical MEMS Resonators Page. 20	
<b>17.00-17.15</b>	N. Jaiswala, S. Upadhyayb, D. Kumarc and <b>O. Parkashd</b> Department of Ceramic Engineering and Department of Physics, Indian Institute of Technology- Banaras Hindu University, <b>India</b>	<b>Prof Om Parkash</b>
	Oxide Ion Conduction in La <sup>2+</sup> and Sr <sup>2+</sup> Co-Doped Ceria/(Li-Na) <sub>2</sub> CO <sub>3</sub> Multifunctional Nanocomposite electrolyte Page. 21	
<b>17.15-17.30</b>	<b>G. R. Dhokane</b> Department of Physics, Arts, Science & Commerce College, Chikhaldara, Maharashtra- <b>India</b>	<b>Dr Gopal. R. Dhokane</b>
	Study of Electrical Conductivity of Polypyridine-PVAc Composite Thin-Film doped with Ni(NO <sub>3</sub> ) <sub>2</sub> Page. 22	
<b>17.30-17.45</b>	<b>M. R. Alenezi</b> , T. H. Alzanki, A. S. Alshammari, S.J. Henley and S. R. P. Silva College of Technological Studies, <b>Kuwait</b> , Nanoelectronics Center, Advanced Technology Institute, University of Surrey, <b>United Kingdom</b> and Department of Physics, College of Science, University of Hail, <b>Kingdom of Saudi Arabia</b>	<b>Dr Mohammad R. Alenezi</b>
	On-Chip Fabrication of High performance Nanostructured Photoetectors Page. 23	
<b>17.45-18.00</b>	V. Yordsri, <b>W. Wongwiriyan</b> and C. Thanachayanont College of Nanotechnology, King Mongkut's Institute of Technology Ladkrabang/ Nanotec-KMITL Center of Excellence on Nanoelectronic Device/ Thailand Center of Excellence in Physics/ National Metal and Materials Technology Center, <b>Thailand</b>	<b>Dr Winadda Wongwiriyan</b>
	Facile growth of carbon nanotube electrode from electroplated Ni catalyst for supercapacitors Page. 24	

Wednesday 27 <sup>th</sup> August 2014		
Smart Materials and Surfaces for life science		
Chairs: Prof Elias Siores- United Kingdom and Suresh Valiyaveettil- Singapore		
Keynote talk 9.00-9.45	<b>Prof Ashutosh Tiwari</b> Biosensors and Bioelectronics Centre, IFM- Linköping University, <b>Sweden</b> <b>Smart Bioengineered Nanosystems for Advanced Healthcare Devices</b>	<b>Prof Ashutosh Tiwari</b>
Keynote talk 9.45-10.15	<b>B. Ayyappa, S. Kanchi, M.I. Sabela, and K. Bisetty</b> Department of Chemistry, Durban University of Technology, Durban, <b>South Africa</b> Electrochemical biosensor based on Cyt-C/GO-AuNPs/ MWCNT modified GCE for determination of Rebaudioside-A Page. 25	<b>Prof Krishna Bisetty</b>
10.15-10.45	<b>Coffee break- Poster Session II</b>	
Keynote talk 10.45-11.15	<b>Prof E. Traversa</b> Division of Physical Sciences and Engineering, King Abdullah University of Science and Technology (KAUST), Thuwal, <b>Kingdom of Saudi Arabia</b> Cerium Oxide Nanoparticles for Antioxidant Therapy Perspectives Page. 26	<b>Prof Enrico Traversa</b>
11.15-11.30	<b>R. Devi, C. Raman Suri and D.K. Sahoo</b> Institute of Microbial Technology (CSIR), Chandigarh, <b>India.</b> An electrochemical polyamines biosensor for biogenic amines determination in biomedical applications based on zinc oxide nanoparticles-polypyrrole modified platinum electrode	<b>Dr Rooma Devi</b> Page. 27
11.30-11.45	<b>S. K. Shukla and A. Tiwari</b> University of Delhi, <b>India</b> and Linköping University, Linköping, <b>Sweden</b> NiO encapsulated polyaniline nanostructure for Non-enzymatic glucose sensing Page. 28	<b>Dr Saroj Shukla</b>
11.45-12.00	<b>C.H. Chia, S.W. Chook and S. Zakaria</b> Materials Science Program, School of Applied Physics, Faculty of Science and Technology, Universiti Kebangsaan Malaysia, Selangor, <b>Malaysia</b> Green approach for the preparation of regenerated cellulose-chitosan membrane containing silver nanoparticles Page. 29	<b>Dr Chin Hua Chia</b>
12.00-12.15	<b>K.Sharma, V. Kumar, B. S. Kaith, S. Kalia and H. C. Swart</b> Department of Physics, University of the Free State, <b>South Africa</b> and Department of Chemistry, Shoolini University of Biotechnology and Management Sciences/ Department of Chemistry, Dr. B.R. Ambedkar National Institute of Technology, Jalandhar/ Department of Chemistry, Bahra University, Wahnaghat (Shimla Hills), <b>India</b> Synthesis of conductive biodegradable hydrogels based on Gum ghatti and their use in colon-specific drug delivery Page. 30	<b>Dr Vijay Kumar</b>
12.15-12.30	<b>J. M. Navarrete and G. Martinez</b> Faculty of Chemistry, National University of Mexico and National Coordination to Restore the Cultural Inheritance, National Institute of Anthropology and History, Mexico City, <b>Mexico</b> Jelly Added with Food Preservatives and Formaldehyde, used as Barrier against Underground Humidity and for Consolidation of Ancient raw Materials Page. 31	<b>Prof Manuel Navarrete</b>
12.30-12.45	<b>M. Kurisawa</b> Institute of Bioengineering and Nanotechnology, <b>Singapore.</b> Enzyme-Mediated Injectable Hydrogels with Independent Tuning of Mechanical Strength and Gelation Rate for Biomedical Applications Page. 32	<b>Dr Motoichi Kurisawa</b>
12.45-14.00	<b>Lunch Break- Poster session II</b>	
<b>Smart Materials and Surfaces for Energy and Environment</b>		
Chairs: Prof. Krishna Bisetty, South Africa and Enrico Traversa- Kingdom of S.A		
Keynote talk 14.00- 14.45	<b>Suresh Valiyaveettil</b> , Department of Chemistry, National University of <b>Singapore</b> <b>Developing new hybrid materials for sensors</b> Page. 33	<b>Prof. Suresh Valiyaveettil</b>
14.45- 15.00 Invited talk	<b>R. K. Gupta</b> Department of Chemical Engineering, Indian Institute of Technology Kanpur, Kanpur, <b>India</b> Photoluminescent Carbon Nanoparticles from Bio-waste Page. 34	<b>Dr Raju Kumar Gupta</b>
15.00- 15.15	<b>S. Chandra and B. Behera</b> Centre for applied Research in Electronics, Indian Institute of Technology Delhi, <b>India.</b> Nanostructured metal oxides: catalyst-free synthesis, characterization and Integration with MEMS processing for gas sensor Page. 35	<b>Prof Sudhir Chandra</b>
15.15-15.30	<b>E. Jankowska, T. Jankowski, W. Zatorski and P. Sobiech</b> Central Institute for Labour Protection - National Research Institute, Warsaw, <b>Poland</b>	<b>Dr Elzbieta Jankowska</b>

	Influence of ventilation on transferring of the nano-sized particles from the fume cupboard to the room air. Page. 36	
<b>15.30-15.45</b>	<b>K. Sivashanmugan</b> , J-D Liao and C-K Yao Department of Materials Science and Engineering, Center for Micro/Nano Science and Technology, Nation-al Cheng Kung University, <b>Taiwan</b> . Smart Focused-Ion-Beam-fabricated Nanostructures for Improving Sur-face Enhanced Raman Scattering on Trace Detection of Single Molecules Page. 37	<b>Mr Sivashanmugan Kundan</b>
<b>15.45-16.00</b>	<b>M. Choudhary</b> , S. S. Siwal and <b>K. Mallick</b> Department of Chemistry, University of Johannesburg, <b>South Africa</b> . Oxidative polymerization of tryptophan: An evidence of PCET reaction mechanism Page. 38	<b>Prof Kaushik Mallick</b>
<b>16.00-16.15</b>	<b>Coffee Break- Poster session II</b>	
<b>16.15-16.30</b>	<b>E. G. Gholami</b> and <b>M. Kadkhodaei</b> Department of Mechanical Engineering, Isfahan University of Technology, Isfahan, <b>Iran</b> Behaviors of Ferromagnetic Shape Memory Alloy Ni–Mn–Ga under Incomplete Biaxial Loadings Page. 39	<b>Dr Mahmoud Kadkhodaei</b>
<b>16.30-16.45</b>	<b>M. R. Alenezi</b> Public Authority for Applied Education and Training, College of Technological Studies, <b>Kuwait</b> . Self-powered Piezoelectric ZnO Nanowire Gas Sensor Page. 40	<b>Dr Mohammad R. Alenezi</b>
<b>16.45-17.00</b>	<b>K. Rudahl</b> and S. E. Goldin Department of Computer Engineering, King Mongkut's University of Technology, Thonburi, <b>Thailand</b> . A Smart Material for Imaging Highway Substructure Damage Page. 41	<b>Prof Kurt Rudahl</b>
<b>17.00-17.15</b>	<b>G. Sthapit</b> and <b>S. Amatya</b> Director of Habitech Center and Architect of AIT Consulting, Asian Institute of Technology, <b>Thailand</b> Soil Cement Interlocking Block: An Alternative Solution to the Reduction of Impacts from Brick-making Industries. Page. 42	<b>Ms. Sudiksha Amatya</b>
<b>17.15-17.30</b>	<b>Q. Hussain</b> , A. Pimanmas and <b>L. Lalin</b> , Sirindhorn International Institute of Technology, Thammasat University, Thailand. Strength and Ductility of SGFRP Confined Concrete Page. 43	<b>Mr Lam Lalin</b>
<b>17.30-17.45</b>	<b>M. Dewan</b> and S. Ram Materials Science Centre, Indian Institute of Technology, Kharagpur, <b>India</b> A facile one-step method to produce nanocrystallites BiFeO <sub>3</sub> -Graphene composite: as a promising energy transfer material Page. 44	<b>Ms Moumita Dewan</b>
<b>17:45-18:00</b>	<b>B. Evangeline</b> and <b>P. Abdul Azeem</b> Department of Physics, National Institute of Technology - India Synthesis and luminescent features of CaZrO <sub>3</sub> nanophosphors Page. 45	<b>Dr. P. Abdul Azeem</b>

Thursday 28 <sup>th</sup> August 2014		
Smart Materials and surfaces for Energy and Environment		
Chairs: Prof. Joydeep Dutta- Oman and Prof Ashutosh Tiwari- Sweden		
Keynote talk 9.00-9.45	<b>M. Syväjärvi</b> Linköping University, Department of Physics, Chemistry and Biology and Graphensic AB, Mjärdevi Science Park, Linköping, <b>Sweden</b>	<b>Dr Mikael Syväjärvi</b>  Page. 46
	<b>Advanced energy and environmental materials concepts from silicon carbide and graphene</b>	
Keynote talk 9.45-10.15	<b>H. C. Swart</b> , Vinod Kumar, Vijay Kumar, S. Som, A. Pandey, J. J. Terblans, O. M. Ntwaaborwa, E. Coetsee and R.E. Kroon Department of Physics, University of the Free State, Bloemfontein, ZA9300, South Africa	<b>Prof Hendrik C Swart</b>  Page. 47
	<b>Role of surface and deep-level defects on the emission and degradation of phosphor materials</b>	
10.15-10.30	<b>Coffee Break</b>	
10.30-10.45	<b>H. Guesmi</b> , B. Zhu, C. Mottet, J. Creuze and B. Legrand ICG, équipe MACS UMR 5253, Montpellier, CINAM UMR 7325, Campus de Luminy Marseille, ICMMO, LEMHE Université Paris-Sud, Orsay and CEA, Service de Recherches de Métallurgie Physique, Saclay, <b>France</b>	<b>Dr Hazar Guesmi</b>  Page. 48
	DFT-based Ising model for the simulation of Au-Pd structure under reaction conditions	
10.45-11.00	<b>S. Fujino</b> and H. Ikeda Kyushu university, Fukuoka, <b>Japan</b>	<b>Prof Shigeru Fujino</b>  Page. 49
	Preparation of SiO <sub>2</sub> /PVA mesoporous and its sintered functional silica glass	
11.00-11.15	<b>T. Kida</b> , H. Furuso, K. Kumamoto, M. Yuasa, and K. Shimano Department of Energy and Material Sciences, Faculty of Engineering Sciences and Department of Molecular and Material Sciences, Interdisciplinary Graduate School of Engineering Sciences, Kyushu University, <b>Japan</b>	<b>Prof Tetsuya Kida</b>  Page. 50
	Polyoxometallate-surfactant hybrid photocatalysts coupled with light antennas	
11.15- 11.30	<b>J. Agrisuelas</b> , R. Catalán, C. Delgado, J. J. García-Jareño, A. F. Roig and <b>F. Vicente</b> Department of Physical Chemistry. University of Valencia, Burjassot and Department of Analytical and Physical Chemistry. UJI, Avda. Sos Bainat, s/n.Castelló, <b>Spain</b> .	<b>Prof Francisco Vicente</b>  Page. 51
	Interfacial role of Cesium in Prussian Blue Films	
11.30-11.45	<b>S. Chaudhary</b> , A. R. Head and J. Schnadt Division of Synchrotron Radiation Research, Lund University, <b>Sweden</b>	<b>Ms Shilpi Chaudhary</b>  Page. 52
	X-ray Photoemission Spectroscopy Study of (3-mercaptopropyl)trimethoxysilane and n-propyltriethoxysilane on Rutile TiO <sub>2</sub> (110)	
11.45-12.00	<b>A. Hozumi</b> , D. F. Cheng, C. Urata and B. Mashed National Institute of Advanced Industrial Sci and Technology (AIST), Shimoshidami, <b>Japan</b> .	<b>Dr Atsushi Hozumi</b>  Page. 53
	Smooth Polydimethylsiloxane Brush Surfaces Showing Unusual Dynamic Dewetting Behavior	
12.00-12.15	<b>Y. Wanna</b> , R. Puingam, J. Nukeaw, A. Chindaduang, G.Tumcharer, S. Porntheerapat and S. Pratontep College of Nanotechnology, King Mongkut's Institute of Technology Ladkrabang/ National Nanotechnology Center (NANOTEC), Thailand Science Park/ Thai Microelectronics Center (TMEC), <b>Thailand</b> and Nara Machinery Co., Ltd, <b>Japan</b> .	<b>Mr Yongyuth Wanna</b>  Page. 54
	Preparation and Characterization of PEG bis(amine) grafted SPION/PMMA nanocomposite	
12.15-12.30	<b>N.S. Kokode</b> , V.R. Panse and S. J. Dhoble N.H.College,Bramhapuri,Gondwana University and Department of Physics, RTM Nagpur University, <b>India</b>	<b>Dr Namdeo Shriram Kokode</b>  Page. 55
	Synthesis and Optical Characterization of Ca <sub>2</sub> PO <sub>4</sub> Cl:Tb <sup>3+</sup> and Mn <sup>2+</sup> Green Emitting phosphor for solid state lighting	
12.30-12.45	<b>T.Venkatappa Rao</b> , N.Rajeswara Rao, SVS Ramana Reddy and B.Sanjeeva Rao National Institute of Technology, Warangal, <b>India</b>	<b>Dr. T.Venkatappa Rao</b>  Page. 56
	Effect of electron beam on thermal, morphological and anti-oxidant properties of kraft lignin	
12.45-13.00	<b>M. Gholampour</b> , A. Abdollah-zadeh, R. Poursalehi and L. Shekari Nanomaterials Group, Department of Materials Engineering, Tarbiat Modares University and Faculty of Energy Engineering and New Technologies, Shahid Beheshti University, <b>Iran</b>	<b>Mr. Mahdi Gholampour</b>  Page. 57
	Porosity Effect on Stoichiometry of GaN Nanostructures by Plasma Enhanced Chemical Vapor Deposition	
13.00-15.30	<b>Lunch break and Awards Ceremony</b>	

## Posters sessions

### Poster session I: 26th August 2014

Poster N°	Abstract's details	Participant
1	Visible-Light-Activated Photocatalytic Hydrogen Production by Hybridized TiO <sub>2</sub> with Tin(IV) Porphyrin Complexes Sung Hyun Kim, Gi-Seon Lee, Beom Hyeok Park, <b>Hee-Joon Kim</b> Department of Applied Chemistry, Kumoh National Institute of Technology, Gumi 730-701, <b>Republic of Korea</b>	<b>Prof Hee-Joon Kim</b>  Page. 59
2	Establishment of Optimized Metallic Contacts on Porous Silicon for Thermoelectric Applications <b>O. Abbes</b> , A. Melhem, K. Snabi, C. Leborgne and N. Semmar GREMI CNRS-Université d'Orléans, Orléans, <b>France</b>	<b>Mr Omar Abbes</b>  Page. 60
3	Photoresponse of Composites of Zinc Oxide and Poly(3-hexythiophene) under Selective UV and White-Light Illumination P. Pattamang, P. Piyakylawat, U. Asawapirom, S. Porntheeraphat, <b>K. Tantisantisom</b> J. Nukeaw and <b>S. Pratontep</b> College of Nanotechnology, King Mongkut's Institute of Technology Ladkrabang, National Nanotechnology Center, National Science and Technology Development Agency Thailand Science Park, National Electronics and Computer Technology Center, National Science and Technology Development Agency Thailand Science Park and ThEP Center, CHE-Bangkok, <b>Thailand</b>	<b>Dr Kittipong Tantisantisom</b>  Page. 61
4	Optical and magnetic properties of doped ZnO: Experiment and Simulation <b>S. Jantrasee</b> , P. Moontragoon and S. Pinitsoontorn Materials Science and Nanotechnology Program, Faculty of Science and Department of Physics, Faculty of Science, Khon Kaen University and Nanotec-KKU Center of Excellence on Advanced Nanomaterials for Energy Production and Storage, <b>Thailand</b> .	<b>Mr Sakwiboon Jantrasee</b>  Page. 62
5	Newly designed $\pi$ -conjugated thiazolo [5,4-d]thiazole based oligomer for efficient small molecule organic solar cells <b>M. Nazim</b> , S. Ameen, H-K. Seo, M. Song, D-R. Park and H-S Shin Energy Materials & Surface Science Laboratory, Solar Energy Research Center, School of Chemical Engineering, Chonbuk National University, <b>Republic of Korea</b>	<b>Mr Mohammed Nazim</b>  Page. 63
6	Fully inorganic tin halides perovskite as light harvesting materials <b>S. Del Gobbo</b> , J. Eid, I. Gereige, S. Masala Solar and Photovoltaic Engineering Research Center (SPERC), King Abdullah University of Science and Technology (KAUST), Thuwal, <b>Saudi Arabia</b>	<b>Dr Silvano Del Gobbo</b>  Page. 64
7	Designing Hierarchical Nanostructures for Enhanced Gas Sensing Properties <b>M. R. Alenezi</b> Public Authority for Applied Education and Training, College of Technological Studies, <b>Kuwait</b> .	<b>Dr Mohammad R. Alenezi</b>  Page. 65
8	The optical and surface properties of Mg <sub>0.3</sub> Zn <sub>0.7</sub> O thin films deposited by PLD methods on the PES substrate <b>H. M. Lee</b> , S. H. Kim, J.H. Ock and N. Jang Division of Electrical and Electronics Engineering Korea Maritime and Ocean University, Busan, <b>Korea</b>	<b>Mr Hyun Min Lee</b>  Page. 66
9	Applicability of PEDOT:PSS Films for Highly Conductive Transparent Electrode by New Effective Dopant <b>Mi-im An</b> , Se-jin Kwon, Seung Young Jeong, Gyojic Shin, Kyung-ho Choi, Sangkug Lee Korea Institute of Industrial Technology, <b>Korea</b>	<b>Ms Mi-im An</b>  Page. 67
10	Novel Photopolymer with High Photosensitivity and Superior Alignment Characteristics for 3D Retardation Film <b>Ju Hui Kang</b> , Si Yeol Yang, Seung Yong Jeong, Sangkug Lee, Kyung Ho Choi, Gyojic Shin Korea Institute of Industrial Technology, <b>Korea</b>	<b>Mr. Gyojic Shin</b>  Page. 68

**Poster session II: 27th August 2014**

Poster N°	Abstract's details	Participant
1	Determination of Copper (II) Ions in Wastewater by Colorimetric Detection <b>P. Muensri</b> and S. Danwittayakul National Metal and Materials Technology Center, Pathumthani, <b>Thailand</b> .	<b>Ms Phitchaya Muensri</b> Page. 69
2	Hansen solubility parameters for an amphiphilic block co-polymer selection for SU-8 modification through self-assembling <b>O. Mednova</b> and K. Almdal Denmark Technical University, Department of Nanotechnology, Copenhagen, <b>Denmark</b>	<b>Mr Olga Mednova</b> Page. 70
3	Spectral selectivity of unbalanced magnetron sputtered TiN, TiAlN and TiAlSiN coatings: XRD, SEM and optical analyses <b>M. Mahbubur Rahman</b> , Zhong-Tao Jiang, Chun Yang Yin, Khalil Ibrahim, Zhonghan Xie, Zhi-feng Zhou, Amun Amri5, Nick Mondinos. School of Engineering & Information Technology, Murdoch University, Murdoch, <b>Australia</b> , School of Science & Engineering, Teesside University, <b>United Kingdom</b> , School of Mechanical Engineering, University of Adelaide, <b>Australia</b> , Department of Mechanical and Biomedical Engineering, City University of Hong Kong, Hong Kong, <b>China</b> , Department of Chemical Engineering, Riau University, <b>Indonesia</b>	<b>M. Mahbubur Rahman</b> Page. 71
4	Immobilization of Urease Based on Adsorption in Eggshell Membrane for Urea Biosensor Application T. Suwanchaituch, S. Imthong and <b>K. Panpae</b> Department of Chemistry, Faculty of Science, King Mongkut's University of Technology Thonburi, KMUTT, Bangkok, <b>Thailand</b>	<b>Prof Kornvalai Panpae</b> Page. 72
5	Effect of the combined radiation and oxidation pretreatment on the surface properties of lignocellulosic materials D.P. Melnikov, Ya.A. Masyutin, A.V. Beskorovaynyy, D.S. Kopitsyn, A.A. Novikov and V.A. Vinokurov1 Gubkin Russian State University of Oil and Gas, Department of Physical and Colloid Chemistry, Moscow, <b>Russia</b>	<b>Mr. Dmitry Kopitsyn</b> Page. 73
6	Antibiotic-Labelled Nanomaterials for the Rapid Detection of Microorganisms by Surface-Enhanced Raman Spectroscopy A.V. Beskorovaynyy, D.S. Kopitsyn, <b>A.A. Novikov</b> , E.A. Bochkova and E.V. Ivanov Gubkin Russian State University of Oil and Gas, Department of Physical and Colloid Chemistry, Moscow, <b>Russia</b>	<b>Dr Andrei Novikov</b> Page. 74
7	Optimization of enzyme immobilization onto nano-structure materials for enhancing bio-gas production from anaerobic digestion C. Kang, K.Y. Lee, .S.J. Kim, K.Y. Park and <b>H.S. Kim</b> Environmental Engineering, Konkuk University and Civil and Environmental System Engineering, Konkuk University, Seoul, <b>Korea</b>	<b>Mr Han Kim</b> Page. 75
8	Needle-less Jet Injection System with Multi-Pore Nozzle for Viscous Drug Delivery Applications <b>Y. C. Jo</b> , H. K. Hong, Y. S. Choi and H. S. Kim Korea Electronics Technology Institute, Medical IT Convergence Research Center, SeongNam-Si and Korea Electronics Technology Institute, Contents Research Center, SeongNam-Si, <b>South Korea</b>	<b>Dr Young-Chang Jo</b> Page. 76
9	Simple Methods to Fabricate Multilayer Microfluidic Devices <b>T. Jiemsakul</b> , C. Kortchana, <b>S. Manakasettharn</b> National Nanotechnology Center, Integrated Nanosystem Laboratory, Pathum Thani and King Mongkut's Institute of Technology Ladkrabang, College of Nanotechnology, Bangkok, <b>Thailand</b>	<b>Mr Thanakorn Jiemsakul</b> Page. 77
10	Effect of Annealing Temperature on Microstructure and Optical Properties of ZnO Thin Films with Mg Dopant <b>K. Verma</b> , B. Chaudhary and M. Kumar Nanomaterial and Environmental Sensors Research Laboratory Department of Physics, University of Lucknow, <b>India</b>	<b>Mr Kartikey Verma</b> Page. 78

# Oral Presentations

# Flexible Memory Devices Using Functional Polymers

H.N. Alshareef, M.A. Khan, A.J. Caraveo-Frescas

Materials Science & Engineering, King Abdullah University of Science & Technology, Thuwal 23955-6900  
Kingdom of Saudi Arabia

**Abstract:** In this talk, we present a review of our recent work on using functional polymers, particularly ferroelectric polymers, for flexible electronic memory applications. Devices based on thin films and nanocomposites have been fabricated. In one case, a ferroelectric diode device based on phase separated blend films of PCBM and P(VDF-TrFE) will be described. This unique memory device relies on ferroelectric polarization to change barrier height at the active material-electrode interface, and can also be used with conducting polymer electrodes. The device shows bi-stable resistive switching operation at low voltage. In addition, we show that blends of P(VDF-TrFE) and selected insulating polymers result in improving the reliability of the P(VDF-TrFE) based flexible memories. Both polarization fatigue, retention, and dielectric breakdown performance is improved. Hybrid devices in which p-type oxide semiconductors (SnO) are combined with P(VDF-TrFE) are shown to give the largest reported mobility of ferroelectric field effect transistors with p-type channel layer. Finally, a single-polymer resistively switched memory device is demonstrated.

Keywords: protein folding, nanoporous

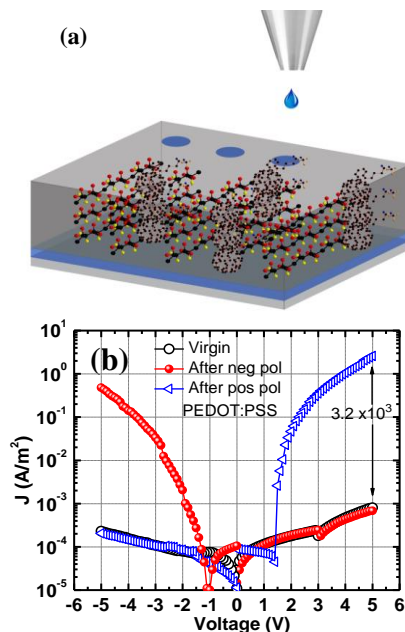


Figure 1: (a) schematic illustration of the PCBM - P(VDF-TrFE) polymer blend device; (b) bipolar resistive switching is observed. Barrier height at active layer/contact interface is tuned by the ferroelectric polarization.

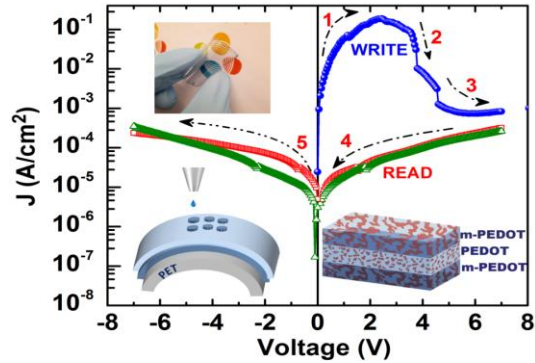


Figure 2: Single polymer resistive memory device is achieved using PEDOT as active layer and PEDOT:PSS as electrodes.

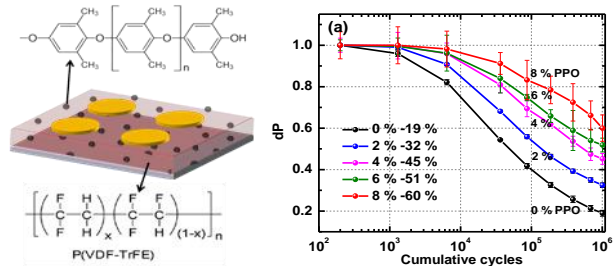


Figure 3: PVDF-PPO composite shows improved ferroelectric memory reliability.

## References:

1. H.N. Alshareef et al, "All-Polymer Bistable Resistive Memory Device Based on Nanoscale Phase-Separated PCBM-Ferroelectric Blends", *Advanced Functional Materials*, 23, 2145 (2013).
2. U. Bhansali, M.A. Khan, Dongkyu Cha, L. Chen, A. Amassian, Ihab N. Odeh, and H.N. Alshareef, "Metal-free, single-polymer device exhibits resistive memory effect", *ACS Nano* 7 (12), 10518-10524.
3. M.A.Khan, Dongkyu Cha, Unnat Bhansali, and H.N. Alshareef, "High-Performance Ferroelectric Memory Based on Phase-Separated Films of Polymer Blends", *Advanced Functional Materials* DOI: 10.1002/adfm.201302056. Cover Page.
4. M. A. Khan, U. Bhansali, and H.N. Alshareef, "High performance ferroelectric memory devices on banknotes", *Advanced Materials* 24, 16, 2165(2012).
5. J.A. Caraveo, P. Nayak, D. Granato, U. Schwingenschlogl, and H.N. Alshareef, "Record Mobility in Fully Transparent p-type Tin Monoxide Films and Devices Processed by Phase Engineering", *ACS Nano* 10, 5160 (2013).

## Galvanostatic fabrication of pTS doped PANI- PPy fiber composite film

A S Dhaliwal<sup>1</sup>Yasir Ali<sup>1</sup>, R G Sonkawade<sup>2</sup>

<sup>1</sup>Department of Physics, Sant Longowal Institute of Engineering & Technology ((Deemed University)  
Longowal(Sangrur) -148106, Punjab, India

<sup>2</sup>Inter University Accelerator Centre, New Delhi 110067, India

\*Email: [Dhaliwalas@hotmail.com](mailto:Dhaliwalas@hotmail.com)

### ABSTRACT

The polymers Polyaniline (PANI) and Polypyrrole (PPy) are treated as outstanding resources due to their promising characteristic properties such as excellent capacity for energy storage, easy synthesis, and higher conductivity. These composites find their applications richly in microelectronics, composite materials, optics and biosensors. Polypyrrol-polyaniline (PANI-PPy) fiber composite films were synthesised on ITO substrates using Galvanostatic technique. It is reported that Galvanostatic deposition of polymer composite film could produce highest electrochemical reactivity in comparison to cyclic voltammetry and potentiostatic deposition methods [1-2]. In Galvanostatic polymerisation the physiochemical properties of the film can suitably be controlled by tuning the synthesis parameters such as current density, monomer concentration, deposition time, electrolyte type, and electrolyte concentration. In previous reported work polyaniline nano fiber were fabricated on ITO conducting glass sheets using the Galvanostatic technique [3].

The PANI-PPy fiber composite films were subjected to various characterisation processes for chemical, structural, morphological studies and conductivity measurements. A rectangular ITO sheet of size 20 × 10 × 0.25 mm was used as working electrode whereas a platinum sheet of size 20 × 40 × 0.25 mm was used as a counter electrode. The chronopotentiogram recorded during electrodeposition of the PANI-PPy fiber composite film on ITO surface is given in Fig.1. The potential versus reference electrode rises to about 0.78 V from the open circuit potential which reflects initiation of the polymerization process, and then immediately comes down to the final stabilization value at about 0.66 V.

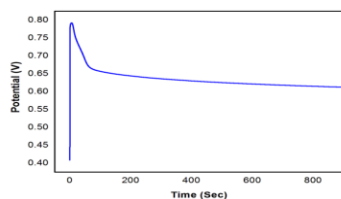


Fig.1

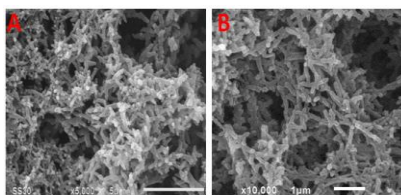


FIG. 2

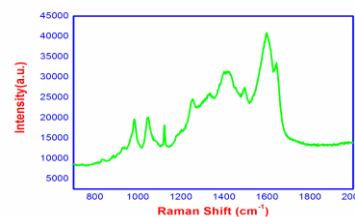


Fig.3

SEM micrographs Fig. 2 (A&B) shows fibrous structures with porous morphology. SEM showed dense network of fibrous structure with greater surface to volume ratio. Ex situ Raman spectra (Fig.3) of PANI-PPy fiber composite films shows formation of composite and significant signatures of polaron and bipolaron states. Raman study confirms the formation of polaron and bipolaron states. The peak observed at 1130 cm<sup>-1</sup> region is the characteristic of conductive state of polymer PPy and is due to the charge delocalization on the polymer backbone. The band formed between the regions 1598-1642 cm<sup>-1</sup> is treated as oxidative state of PPy film. The Raman peak at 1331 cm<sup>-1</sup> is assigned to C-N stretching. Raman band observed at 1504 is treated as skeletal band.

I-V measurement of PANI-PPy fiber composite film showed linear behavior and resembles with Ohm's law. I-V measure showed the conducting nature of PANI-PPy fiber composite and the electrical conductivity of PANI-PPy was found to be 4.8×10<sup>-2</sup> Scm<sup>-1</sup>. A facile method for the synthesis of composite film is reported in this investigation.

### REFERENCES

- [1] R. Rajagopalan, O. Jude, A. Iroh, *Electrochimica Acta* **47** (2002) 1847- 1855
- [2] M. Yamaura, T. Hagiwara, K. Iwata, *Synth. Met.* **26** (1998) 209-224
- [3] Y. Ali, V. Kumar, R.G. Sonkawade, A.S. Dhaliwal, *Adv. Mat. Lett.* **3** (2012) 388-392

# The role of particulates on the structure and optical properties of $Y_3(Al,Ga)_5O_{12}:Tb$ films deposited by PLD.

A. Yousif, H. C. Swart, O. M. Ntwaeaborwa

Department of Physics, University of the Free State, Bloemfontein, ZA9300, South Africa

**Abstract:** Pulsed laser deposition (PLD) is a widely used technique to grow phosphor thin films on solid substrates [1]. The PLD is more efficient than other techniques since high quality films can be deposited at lower substrate temperatures [2]. The  $Y_3(Al,Ga)_5O_{12}:Tb$  thin films were grown in an  $O_2$  working atmosphere on Si (100) substrates using this technique. Micrometer and sub-micrometer sized particulates were detected on the surface and inside the  $Y_3(Al,Ga)_5O_{12}:Tb$  thin films as demonstrated in Figure 1 (a). The presence of these particulates played an important role to induce artificial topographical effects on  $Y_3(Al,Ga)_5O_{12}:Tb$  thin films deposited on Si substrates measured by time-of-flight secondary ion mass spectroscopy (TOF-SIMS). The two and three-dimensional (2D and 3D) images have been recorded in the positive ion mode. Analysis of the 3D images shows big agglomerated particles on the surface of the Si substrate that appears to be embedded in the substrate and the substrate appears to be on the same level as the particles, Figure 1 (b). This phenomenon is due to the artificial topographic effects (ATE) which are attributed to the experimental setup of the TOF-SIMS system. The particulates with different chemical composition were also observed on the film's surface as well as inside the film structures [2]. TOF-SIMS results revealed that the as-deposited film consisted of agglomerated particles of Ga and Al of different sizes. Atomic force microscopy (AFM) images of the as-deposited film show well defined spherically grains that were uniformly distributed over the surface with a root mean square (RMS) roughness value of 9 nm. After annealing at  $800^\circ C$  the surface became smooth as shown in Figure 1 (c) and the RMS value was reduced to 6 nm. The smooth layer was confirmed to be a surface oxide layer enriched with Ga from the images captured using a nano-scanning Auger electron microprobe (NanoSAM). Shifts in the X-ray diffraction (XRD) peak position to lower diffraction angles were observed in the XRD patterns of the annealed film compared to the pattern of the  $Y_3(Al,Ga)_5O_{12}:Tb$  powder [2]. The optical measurements of the Ga enriched film indicated that a new excitation band different from the original  $Y_3(Al,Ga)_5O_{12}:Tb$  powder was obtained.

**Keywords:** PLD, Particulates, TOF-SIMS, Topography, PL, NanoSAM, ATE

## References:

[1] S. Wicklein et. al. Appl. Phys. Lett., 101 (2012) 131601.

[2] A. Yousif et al. Appl. Surf. Sci. 305 (2014) 732.

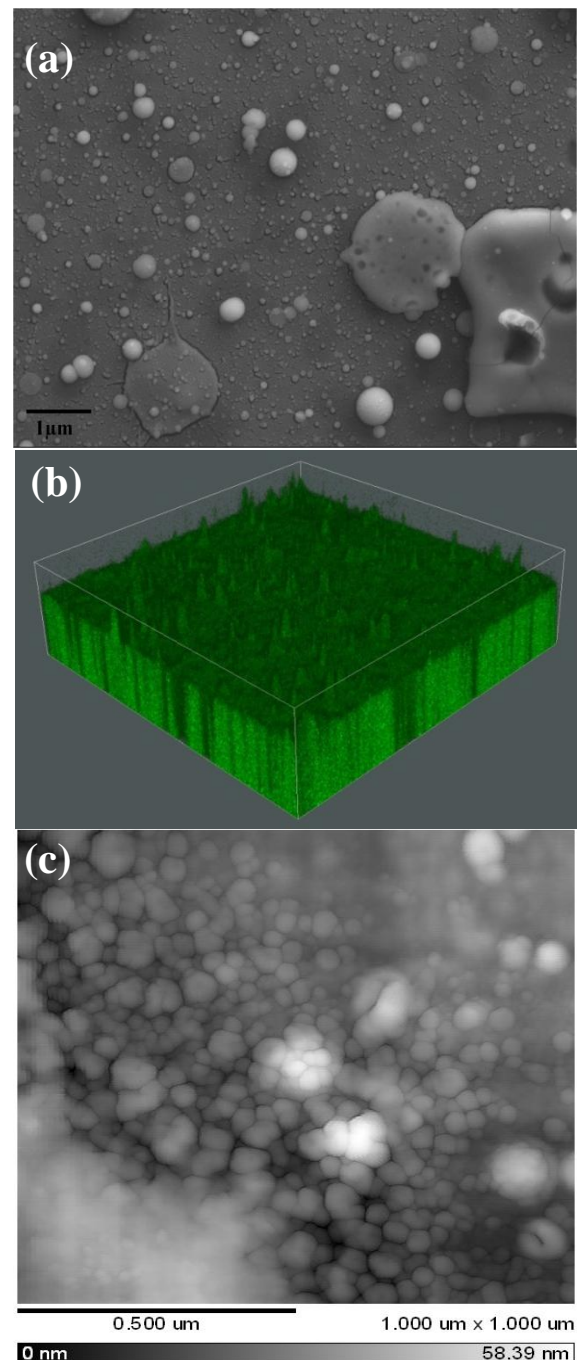


Figure 1: (a) Scanning electron microscopy showing presence of particulates with different features. (b) the TOF-SIMS showing that some areas appear to be higher than the surrounding areas which is due to ATE. (c) AFM showing some regions that appear to have a smoother morphology compared to the rest of the film surface.

# Formulation of covalently linked PEEK/HA composite

E.A.B. Hughes,<sup>1,2,\*</sup>R. Wise,<sup>2</sup>L.M. Grover<sup>1</sup>

<sup>1</sup>University of Birmingham, School of Chemical Engineering, Edgbaston, Birmingham, UK

<sup>2</sup>TWI Ltd, Granta Park, Cambridge, UK

**Abstract:** Poly (etheretherketone) (PEEK) is a high performance polymer used across many industrial sectors as it exhibits impressive mechanical properties, corrosion resistance and thermal stability features. Medical implants that bear considerable load, such as spinal cages, are fabricated from this material and have been shown to perform well following implantation (Kahraman *et al.*, 2006; Ferguson *et al.*, 2006).

PEEK does not allow for bone-growth across its surface. The addition of a bioactive ingredient, such as hydroxyapatite, can engender osteogenic attributes (Roeder *et al.*, 2008; Bakar *et al.*, 2003). The presence of the HA within PEEK has been shown to enable better hard-tissue integration (Bakar *et al.*, 2003).

Additions of high weight fractions of ceramic particles in a polymer matrix can diminish mechanical properties of the composite. This is because, in the absence of strong interaction between the ceramic components, the particles can act as a stress-riser. We postulated that improving the strength of the interface between the ceramic and polymer matrix beyond simple mechanical interlocking would enable us to produce a stronger composite material. Therefore, a composite system was formulated where both the PEEK and HA were modified in order to enable covalent linkage of the two phases (Figure 1).

The one step reduction of PEEK using  $\text{NaBH}_4$  converted a proportion of the ketone moiety on the polymer chain to hydroxyl groups. This made the polymer more accessible to the attachment of further groups without the loss of the desirable properties exhibited by the parent structure.

Hydroxyl groups present on the surface of HA can be exploited as anchorage points for surface modifying agents, such as silane molecules. We demonstrated successful functionalization of HA with amino silanes, thus amino groups were presented on the HA surface. This allowed for a further modification step in the form of a succinylation reaction, which provided terminal carboxylic acid groups. It was found experimental procedures regarding both functionalization steps upon the HA surface required careful pH control in order to optimize the degree of functionalization achievable.

Mild esterification conditions were employed to chemically couple the modified PEEK and functionalized HA through the respective hydroxyl and carboxylic acid moieties available.

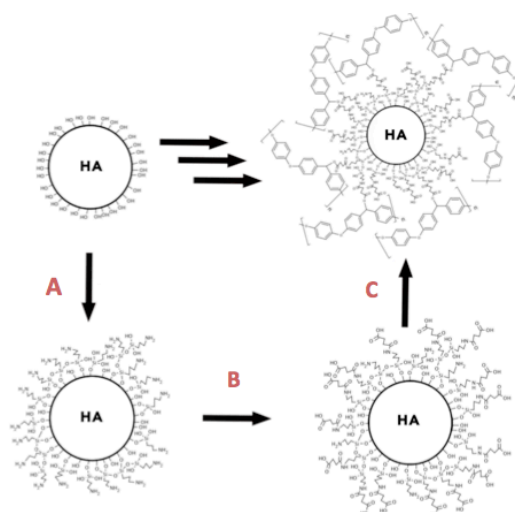


Figure 1: Composite formulation outline: (A) HA was functionalized with an amino silane (3-aminopropyltrimethoxysilane is shown); (B) terminal amino groups provided anchorage points for succinylation by reaction with succinic anhydride, resulting in terminal carboxylic acid groups; (C) esterification between modified PEEK and functionalized HA resulting in chemical coupling between polymer and ceramic filler.

Keywords: PEEK, hydroxyapatite, chemical modification, surface functionalization, amino silanes, bio active composites

## References:

- Abu Bakar, M., Cheng, M., Tang, S., Yu, S.C., Liao, K., Tan, C.T., Khor, K.A., Cheang, P. (2003) Tensile properties, tension-tension fatigue and biological response of polyetheretherketone-hydroxyapatite composites for load-bearing orthopedic implants. *Biomaterials.*, 24, 2245–2250.
- Ferguson, S.J., Visser, J.M.A., Polikeit, A. (2006) The long-term mechanical integrity of non-reinforced PEEK-OPTIMA polymer for demanding spinal applications: experimental and finite-element analysis. *Eur Spine Journal.*, 15, 149–156.
- Kahraman, S., Daneyemez, M., Kayali, H., Solmaz, I., Bedük, A., Akay, M. (2006) Polyetheretherketone (Peek) Cages For Cervical Interbody Replacement: Clinical Experience. *Turk Neurosurg.*, 28, 120–123.
- Roeder, R., Converse, G., Kane, R., Yue, W. (2008) Hydroxyapatite-reinforced Polymer Biocomposites for Synthetic Bone Substitutes. *Biological Materials Science*, 28–45

# Silicon Nitride Protective Coating by Gas-timing RF Magnetron Sputtering Deposition

N.Paleeya<sup>1,\*</sup>, N. Khemasiri<sup>1</sup>, D. Sae-tang Phromyothin<sup>1</sup>, M. Horprathum<sup>2</sup>, S.Porntheeraphat<sup>2</sup>, J.Nukeaw<sup>1</sup>, S. Pratontep<sup>1,\*</sup>

<sup>1</sup>National Electronics and Computer Technology Center, Thailand Science Park, Paholyothin Rd., Klong 1, Klong Luang, Prathumthani, 12120, Thailand

<sup>2</sup>College of Nanotechnology, King Mongkut's Institute of Technology Ladkrabang, Chalongkrung Rd., Ladkrabang, Bangkok 10520, Thailand

**Abstract:** Protective coatings based on silicon nitride are a promising alternative to carbon based coatings, owing to its compatibility with existing semiconductor technology. However, the fabrication of silicon thin films with high nitrogen content, such as reactive sputtering, often face difficulties in obtaining desirable properties of the films, owing to oxygen contamination. Here we explore a method to incorporate nitrogen into sputtered silicon thin films by gas-timing RF magnetron sputtering on glass and Si substrates. The gas-timing sputtering technique controls the on-off sequence of the reactive sputtering gases during deposition. In this study, the Ar gas was employed in the plasma sputtering of a pure silicon target. The Ar gas was injected in alternation with the N<sub>2</sub> gas using an on-off sequence (in seconds) of Ar:N<sub>2</sub> from 10:0, 10:1, 10:3, 10:5, 10:7 and 10:10. The effect of the gas-timing ratio on the properties of silicon nitride films was investigated by Atomic Force Microscopy (AFM), Raman Spectroscopy, Auger Electron Spectroscopy, X-ray Diffraction. The chemical resistance was measured by electrochemical corrosion test in sulfuric acid, while the hardness was obtained by the nano-indentation technique. The results reveal that the gas timing technique is able to produce the films with high nitrogen content and enhanced crystallinity. The acid corrosion resistance and the hardness properties (Fig. 1) are also significantly improved by controlling the gas-timing ratio.

Keywords: hard coatings, silicon nitride

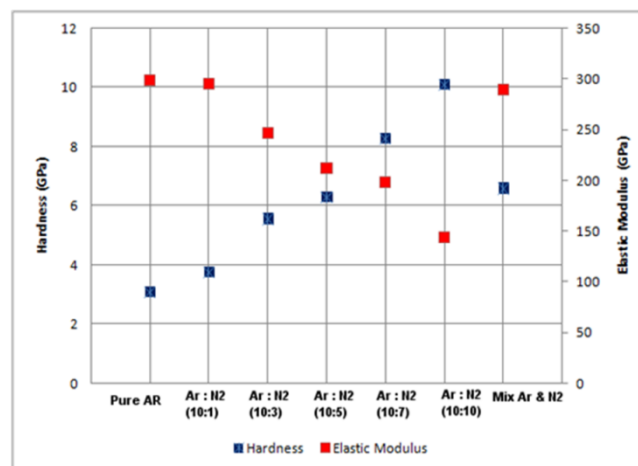


Figure 1: Hardness and elastic modulus of nitrogen-doped silicon oxide deposited by gas-timing reactive RF magnetron sputtering at different Ar:N<sub>2</sub> ratios in comparison to a conventional method with mixed Ar and N<sub>2</sub> gases.

## References:

- Nukeaw, J., Sungthong, A., T-Thienprasert. *et al.* (2008), Local structure of Indium Oxynitride from X-Ray absorption spectroscopy, *App. Phys. Lett.* 93, 051903.
- Kietipaisalsophon, N., Bunjongpru, W., Nukeaw, J. (2002), Photoreflectance study of AlN thin film grown by RF magnetron sputtering, *Int. J. Mod. Phys. B*, 16, 4418-4422.
- Klaitabtim, D., Pratontep, S., Nukeaw, J. (2008), Effect of gas-timing technique on structure and optical properties of sputtered zinc oxide films, *Ceramics International*, 34, 1103-1107.

# Application of Spark Plasma Sintering for Fabrication of Functionally Graded Thermal Barrier Coating on a Superalloy Substrate

M. Bahrami<sup>1</sup>, A.H. Pakseresht<sup>2</sup>, A. Simchi<sup>1</sup>

<sup>1</sup>Department of Material Science and Engineering, Sharif University of Technology, Tehran, Iran

<sup>2</sup>Department of Ceramics, Materials and Energy Research Center, Karaj, Iran

**Abstract:** Thermal barrier coating (TBC) are commonly used in high temperature components of gas turbine engines such as blades, vanes and nozzles, for aeronautic and energy production applications. These coatings consist of superalloy substrate, metallic layer called bond coat and ceramic layer called top coat. The difference between the thermal expansion coefficient of ceramic and metallic layer is an unfavorable parameter leading to an extensive usage of Functionally Graded Material (FGM) coatings. This kind of coating reduces the residual and thermal stresses and enhances bonding strength along the interface of the coating and the substrate. Recently, the spark plasma sintering (SPS) technique has been utilized to improve coatings with a complex structure. In comparison with other conventional methods (e.g. air plasma spray (APS) and physical vapour deposition (PVD)) this technique brings significant advantages, such as a higher heating rate, shorter dwell time, fast processing and limited grain growth. In this paper, a new fabrication method is proposed using the FGM-TBC coating, including nanostructured materials in the top layer, on a Ni-based superalloy substrate in a single short production step by SPS. Prepared coatings are dense and they does not have the common defects which can be observed in conventional coatings. Also the nanostructure of top coat is retained after SPS process. The microstructure and the phases in the bond coat with element dispersion in various layers have been analysed by secondary electron microscope (SEM) equipped with an EDX and Mapping analyser.

**Keywords:** Thermal barrier coating, Spark plasma sintering, Functionally graded materials.

## References:

- Thomas.Kh.G, Haindl.H, Fu.D, (1997), Modifications of thermal barrier coatings (TBCs), *Surf. Coat. Technol.* 94-95, 149-154.
- Hejwowski.T, (2010), Comparative study of thermal barrier coatings for internal combustion engine, *Vacuum.* 85, 5, 610-616.
- Lee.Y.D, Erdogan.F, (1994/1995), Residual/thermal stresses in FGM and laminated thermal barrier coatings, *Int. J. Fract.* 69, 2, 145-165.
- Jiang.Y, Yang.J.F, Zhuang.Z, Liu.R, Zhou.Y, Wang.X.P, Fang.Q.F, (2013), Characterization and properties of tungsten carbide coatings fabricated by SPS technique, *J. Nucl. Mater.* 433, 1-3, 449-454.

# Electrochromic Materials and their Characterization by Solar Radiation Glazing Factors for Smart Window Applications

Bjørn Petter Jelle <sup>ab\*</sup>, Tao Gao <sup>c</sup> and Arild Gustavsen <sup>c</sup>

<sup>a</sup> SINTEF Building and Infrastructure,  
Department of Materials and Structures, NO-7465 Trondheim, Norway.

<sup>b</sup> Norwegian University of Science and Technology (NTNU),  
Department of Civil and Transport Engineering, NO-7491 Trondheim, Norway.

<sup>c</sup> Norwegian University of Science and Technology (NTNU),  
Department of Architectural Design, History and Technology, NO-7491 Trondheim, Norway.

\* Corresponding author: bjorn.petter.jelle@sintef.no (e-mail), +47-73593377 (phone).

## Abstract

Electrochromic materials (ECM) and windows (ECW) are able to regulate the solar radiation throughput by application of an external electrical voltage. Hence, as smart window applications, the ECWs may decrease heating, cooling and electricity loads in buildings by admitting the optimum level of solar energy and daylight into the buildings at any given time, e.g. cold winter climate versus warm summer climate demands. In order to achieve as dynamic and flexible solar radiation control as possible, the ECWs may be characterized by solar radiation glazing factors, i.e. ultraviolet solar transmittance ( $T_{uv}$ ), visible solar transmittance ( $T_{vis}$ ), solar transmittance ( $T_{sol}$ ), solar material protection factor (SMPF), solar skin protection factor (SSPF), external visible solar reflectance ( $R_{vis,ext}$ ), internal visible solar reflectance ( $R_{vis,int}$ ), solar reflectance ( $R_{sol}$ ), solar absorbance ( $A_{sol}$ ), emissivity ( $\epsilon$ ), solar factor (SF) and colour rendering factor (CRF). Comparison of these important solar quantities for various ECM and ECW combinations and configurations enables one to select the most appropriate ones for specific smart window and building applications. In Figure 1 there are given measured transmittance spectra for an electrochromic window at different applied potentials, with corresponding calculated solar radiation glazing factors in Table 1. This particular ECW based on the ECMs polyaniline (PANI), prussian blue (PB) and tungsten oxide ( $WO_3$ ) is e.g. able to regulate as much as 60 % ( $\Delta T_{vis}$ ) of the visible and 59 % ( $\Delta T_{sol}$ ) of the total solar radiation, whereas the solar factor regulation is as high as 44 % ( $\Delta SF$ ).

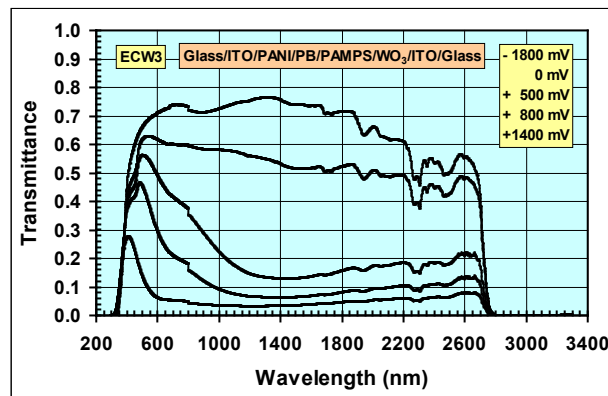


Figure 1. Transmittance versus wavelength in the whole solar spectrum measured for an ECW at different applied potentials. Highest colouration level is at +1400 mV.

Table 1. Calculated solar radiation glazing factors for an ECW at two different colouration levels (transparent and coloured), i.e. at two different applied potentials. Corresponding transmittance spectra are given in Figure 1.

Glass Configuration	n	$T_{uv}$	$T_{vis}$	$T_{sol}$	SMPF	SSPF	$R_{vis,ext}$	$R_{vis,int}$	$R_{sol}$	$A_{sol}$	$\epsilon$	SF	CRF
ECW3 (-1800 mV)	1	0.08	0.69	0.67	0.59	0.97	0.09	0.09	0.08	0.25	0.836	0.74	0.96
ECW3 (+1400 mV)	1	0.12	0.09	0.08	0.83	0.97	0.09	0.09	0.08	0.84	0.836	0.30	0.59

# Reactivity Trend of CO<sub>2</sub> Electroreduction on Copper Alloys from First Principles

Pussana Hirunsit<sup>1,\*</sup>, Wiwaporn Soodsawang<sup>1</sup>, Jumras Limtrakul<sup>2,3</sup>

<sup>1</sup> National Nanotechnology Center (NANOTEC), National Science and Technology Development Agency (NSTDA), Pathumthani, Thailand

<sup>2</sup> Department of Chemistry and NANOTEC Center for Nanoscale Materials Design for Green Nanotechnology, Faculty of Science, Kasetsart University, Bangkok, Thailand

<sup>3</sup> PTT Group Frontier Research Center, PTT Public Company Limited, Bangkok, Thailand

**Abstract:** The electroreduction of CO<sub>2</sub> to valuable hydrocarbon products is a promising process that would allow recycling waste CO<sub>2</sub> into usable hydrocarbons without high temperature reactions requirement and the production rate can be varied to follow the availability of electricity produced from clean resources such as solar cells. The critical challenges for the CO<sub>2</sub> electroreduction process are that the reaction must be at a low overpotential as well as being selective. The electrode material is crucial in that it plays essential roles in determining the overpotential, efficiency and selectivity. A Copper electrode was found to perform the direct reduction of CO<sub>2</sub> to hydrocarbons (methane and ethylene) with a reasonable rate but very low efficiency (Hori *et al.*, 1986). It is an important challenge to discover promising electrode materials (electrocatalysts) which provide high efficiency and high hydrocarbon product selectivity. In this talk, we will present the thermodynamic investigation of CO<sub>2</sub> conversion to CH<sub>4</sub> on copper-based alloy with transition metals in group 9-11 using density functional theory calculations associated with standard hydrogen electrode model (Nørskov *et al.*, 2004) (Hirunsit, 2013). The key intermediate species, the theoretical overpotential, the potential-limiting step and the theoretical onset potential of key elementary steps are discussed. The scaling correlation of the key intermediate adsorbed free energies and their electronic structures provide the fundamental understanding of the interaction with surfaces. Also, the reactivity toward the competitive reaction of hydrogen evolution and the favorability of OH\* surface poisoning will be discussed.

**Keywords:** density functional theory, heterogeneous catalysis, electrocatalysts, CO<sub>2</sub> reduction, and copper alloys.

## References:

- Hori, Y.; Kikuchi, K.; Murata, A.; Suzuki, S. (1986), Production of methane and ethylene in electrochemical reduction of carbon dioxide at copper electrode in aqueous hydrogencarbonate solution, *Chem. Lett.*, 897-898
- Nørskov, J. K.; Rossmeisl, J.; Logadottir, A.; Lindqvist, L.; Kitchin, J. R.; Bligaard, T.; Jónsson, H. (2004), Origin of the Overpotential for Oxygen Reduction at a Fuel-Cell Cathode, *J.Phys.Chem.B*, 108 (46), 17886-17892
- Hirunsit, P. (2013), Electroreduction of Carbon Dioxide to Methane on Copper, Copper–Silver, and Copper–Gold Catalysts: A DFT Study, *J.Phys.Chem.C*, 117 (16), 8262-8268.

# Molecular Simulations of Anti-stain Polymeric Coatings

Y. Singhvi,<sup>1</sup> I. V. N. Tejasvini,<sup>1</sup> G. Manik<sup>1\*</sup>

<sup>1</sup>Department of Polymer and Process Engineering, IIT Roorkee (Saharanpur Campus), Saharanpur, India

**Abstract:** There has been an immense interest in the development of anti-stain polymeric coatings in the past (Fong *et al.*, 2012 and Robert *et al.*, 1999). Polyvinyl acetate (PVA) based coatings find extensive use in various coating and paints industries globally. Blending and copolymerization of PVA with oleophobic polymers/monomers has resulted in potential coating formulations that possess enhanced stain-resistance. Molecular simulations have been long used to understand the behaviour of specialty polymers and their blends. In this work, we employ molecular simulations to understand the effect of blending/copolymerization of fluoro based monomers with PVA on the oleophobic behaviour of formulated coatings. Material Studio™ software available from Accelrys™ has been employed for running Molecular Dynamics (MD) simulations to describe polymer coatings behavior under stain-like conditions (using a decane molecule). Simulation results described in terms of movement of oil-representative molecules away from the formulated coatings surface clearly demonstrates the effect of selective fluorine based comonomers/blends on PVA matrix (figure 1). Simulated density of coatings was found to confirm to the experimentally derived values. Formulated coatings of some of such fluoro containing compounds have been simulated and oleophobic properties quantified.

Simulation results have been quantified in terms of movement of oil-representative molecules away from the formulated coatings surface, and clearly demonstrate the effect of selective fluorine based blends with PVA matrix. To confirm accuracy of the simulation protocol, the simulated density of coatings is found to confirm to the experimentally derived values. Formulated coatings of some of such compounds have been simulated and oleophobic properties quantified in terms of msd of decane molecule. Results demonstrate that with increasing fluoro content the oleophobic behaviour is improved as found by increased msd values.

Keywords: oleophobic, anti-stain, molecular simulations,

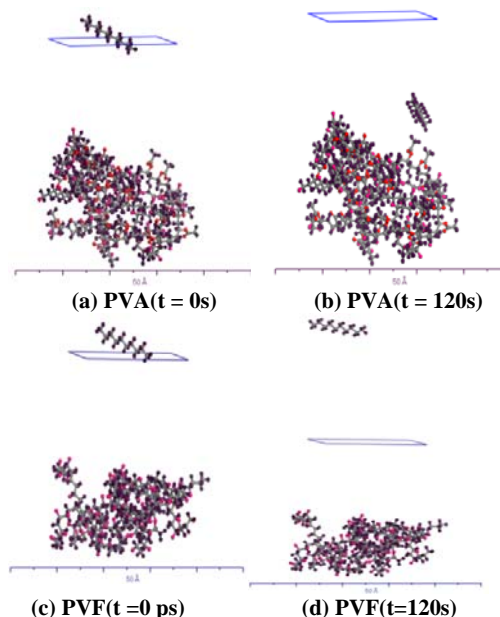


**Figure 1:** Illustration of behavior of a decane molecule against pure PVA coating (a & b) compared with pure PVF coating (c & d) at  $t = 0$ ps and 120ps simulation times.

## References:

- Fong, B. C., Huang, T-L. J., Ko, J.H., Zhu, D-W., (2001), Patterned article having alternating hydrophilic and hydrophobic surface, regions. Patent Number EP1084178A1.
- Robert H. B., Perlman, D., (1999) Improved anti-graffiti coatings and method of graffiti removal, . Patent Number EP0912260A1.
- Material studio™ (licensed by IIT Roorkee), owned by dassault systemes, UK (previously Accelrys™). <http://accelrys.com/products/materials-studio/>

# A Microscale Piezoelectric Harvester for Mechanical Energy from Fluid Flow

K. Koyvanich,<sup>1,2,\*</sup> N. Muensit,<sup>1,2</sup>, P. Smithmaitrie,<sup>1,3</sup>

<sup>1</sup>Center of Excellence in Nanotechnology for Energy (CENE),

Prince of Songkhla University (PSU), Hat Yai, Songkhla, THAILAND

<sup>2</sup>Physics Department, Faculty of Science, Prince of Songkhla University (PSU), Hatyai, Songkhla, THAILAND

<sup>3</sup>Department of Mechanical Engineering, Faculty of Engineering, Prince of Songkla University (PSU),  
HatYai, Songkla, THAILAND

**Abstract:** We have developed a new design energy harvester for utilization energy from the under water flow and vortex base on cantilever beam energy conversion (Muensit, 2011). It converts fluid flows energy into electrical energy through the vibration of a piezoelectric film. The full wave oscillation of piezoelectric film was induced by dolphin flukes which attached at the cantilever end of the piezoelectric film sheet. The variation of frequencies vibration had been created by pressures fluctuation in vortex of fluid flow from bluff body (Wang, *et al.*, 2011). The attachment was obtain a larger energy output. The coupling mathematical model of energy harvesting technique and experimental were established (Kanjaporn *et al.*, 2010). The finite element analysis was performed to exploit the stream line of velocity fluctuation of fluid flow into the harvester. Experiments were carried out to verify the validity of the numerical simulation results (Smithmaitrie, 2011). It shows that the power output and the peak frequency obtained from the numerical analysis was in good agreement with the experimental results. This approach leading to the potential of hydropower harvesting convert to electrical energy for powering wireless devices. The microscale of the output power from this harvesting can be improved by increasing the piezoelectric constant of piezoelectric materials or by an optimization of design harvesting process. The multiply arrays of this harvester together with rectifier which available to be a part the hydropower harvesting device placed into a flowing river.

## References:

- Muensit, N. (2011). "Energy harvesting materials" Muensit, N.(ed.) *Energy Harvesting with Piezoelectric and Pyroelectric Materials* (Vol.72, 1<sup>st</sup> ed., pp 1-34). Switzerland: Trans Tech Publications Ltd.
- Smithmaitrie, P. (2011) "Vibration theory and design of piezoelectric energy harvesting structures" Muensit, N.(ed.) *Energy Harvesting with Piezoelectric and Pyroelectric Materials* (Vol.72, 1<sup>st</sup> ed., pp. 58-77). Switzerland: Trans Tech Publications Ltd.
- Kanjaporn, W., Maliwan, K. and Smithmaitrie, P., (2010), "The Effect of Mechanical Vibration on Minimum Fluidization Velocity," Proceeding of the 8<sup>th</sup> PSU-Engineering Conference (PEC8), April 22-23, 2010, Hatyai, Thailand.
- Wang, D.A., Pham, H.T., Chao, C.W., Chen, J.M., (2011), "A Piezoelectric Energy Harvester Based on Pressure Fluctuations in Kármán Vortex Street," Proceeding of the *World Renewable Energy Congress 2011* (WREC2011), May 8-11, 2011, Linköping, Sweden.

Keywords: piezoelectric, fluid flow, energy harvesting, vortex, hydraulic energy

# Formation of magnetic phases by reactive diffusion between Mn and Ge for Spintronic Applications

O. Abbes,<sup>1,\*</sup> A. Portavoce,<sup>2</sup> C. Girardeaux,<sup>2</sup> A. Spiesser,<sup>3</sup> and V. Le Thanh,<sup>3</sup>

<sup>1</sup>GREMI CNRS-Université d'Orléans, 14 Rue d'Issoudun, 45067 Orléans, France

<sup>2</sup>Aix-Marseille Université, CNRS, IM2NP-UMR 6242, Saint Jérôme Case 142, 13397 Marseille, France

<sup>3</sup>Aix-Marseille Université, CNRS, CINaM-UMR 7325, Luminy Case 913, 13288 Marseille, France

**Abstract:** The synthesis of an epitaxial ferromagnetic silicide or germanide, exhibiting a high Curie temperature, is an important issue in order to efficiently inject spin-polarized currents into standard semiconductors (Dietl *et al.*, 2010). Among the different compounds, the Mn-Ge system presents a particular interest since it provides many phases with different magnetic properties. The most interesting phase is the intermetallic phase  $\text{Mn}_5\text{Ge}_3$ , which has been shown to epitaxially grow on germanium (Olive Mendez *et al.*, 2008) and has a Curie temperature at room temperature (Sawatzky *et al.*, 1971). Hence, it is opening the road for spin injection into group IV semiconductors. The phase diagram of the bulk Mn-Ge system contains a number of phases:  $\text{Mn}_{3,4}\text{Ge}$ ,  $\text{Mn}_5\text{Ge}_2$ ,  $\text{Mn}_7\text{Ge}_3$ ,  $\text{Mn}_2\text{Ge}$ ,  $\text{Mn}_5\text{Ge}_3$  and  $\text{Mn}_{11}\text{Ge}_8$ , but data on thin films in the Mn-Ge system are relatively scarce. Therefore studying the phase formation sequence is of high interest. Furthermore, the current microelectronic technology uses the self-aligned silicide (SALISIDE) process (Chen *et al.*, 2008), to establish silicide contacts on silicon by solid state reaction. In our case, the reaction between a thin Mn metal layer and the germanium substrate gives a phase formation sequence of only some Mn germanides. In fig. 1, we present First results of in-situ X-ray diffraction measured during thermal annealing of 50 nm thick Mn layer deposited on 150 nm amorphous Ge are presented (Figure 1). The annealing temperature range was from 30 °C to 280 °C. These in-situ XRD measurements indicate that the Mn layer is stable on the Ge film until a temperature of about 130 °C, beyond which Mn starts to be consumed. The first phase to be observed is the  $\text{Mn}_5\text{Ge}_3$  one, which appears in the phase sequence diagram. After that, at about 210 °C, we observe peaks characteristic of the  $\text{Mn}_{11}\text{Ge}_8$  phase.

Numerous characterization techniques, including in-situ X-Ray Diffraction (XRD), Atomic Force Microscopy (AFM), and Transmission Electron Microscopy (TEM), were combined to study the sequential formation of Mn-Ge phases during reactive diffusion.

**Keywords:** intermetallic phase, Mn, Ge, reactive diffusion, Spintronics, in-situ XRD diffraction, surface and interface characterizations.

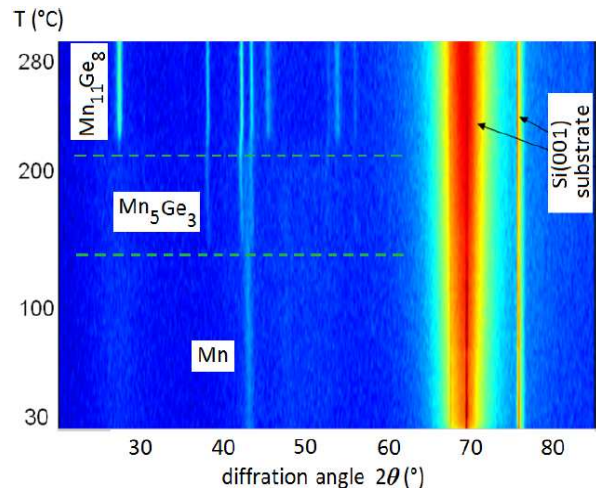


Figure 1: Figure illustrating the planar view of diffraction peaks corresponding to sequential formation of  $\text{Mn}_5\text{Ge}_3$  and  $\text{Mn}_{11}\text{Ge}_8$  during thermal annealing reaction of 50 nm thick Mn film with 150 nm thick film of amorphous Ge deposited on  $\text{SiO}_2/\text{Si}(001)$  substrate.

## References:

- Dietl T. (2010), A ten-year perspective on dilute magnetic semiconductors and oxides. *Nature Mater.* 9, 965-974.
- Olive-Mendez S. F., Spiesser A., Michez L. A., Le Thanh V., Glachant A., Derrien J., Devillers T., Barski A., Jamet M. (2008), Epitaxial growth of  $\text{Mn}_5\text{Ge}_3/\text{Ge}(111)$  heterostructures for spin injection. *Thin Solid Films*, 517, 191.
- Sawatzky E., (1971), Magneto - Optical Properties of Sputtered  $\text{Mn}_5\text{Ge}_3$  Films. *J. Appl. Phys.* 42, 1706.
- Chen Y. N., Lippitt M. W., Chew H. Z., Moller W. M., (2003), Manufacturing enhancements for CoSi<sub>2</sub> self-aligned silicide at the 0.12- $\mu\text{m}$  CMOS technology node. *IEEE Trans. Electron Devices* 50, 2120-5.

# Development of Through Silicon Stacking Technology for Capacitive Acoustical MEMS Resonators

N. Belkadi\*, B. Dulmet\*, T. Baron\*

\*FEMTO-ST Institute, Time and Frequency Dpt., 26, chemin de l'épitaphe – 25030 Besançon Cedex, France.

**Abstract:** This article describes the key process to realize conductive vias in silicon MEMS resonators. Cancelling out the resistance of interconnections in micro-acoustic resonators structures is mandatory to improve their performances because electrostatic generation of elastic waves results into relatively small values of the electromechanical coupling factor (Ivan *et al.*; 2012). Via techniques so-called TSS (Through-Silicon Stacking or Thru-Silicon Stacking) were developed for 3D integration. The physical constitution of these conductive via generally consists of a set of four generic steps. The holes are machined by deep reactive ion etching (DRIE), most often with the help of the Bosch process. This technique allows to elaborate structures with high aspect ratio and optimally vertical edges. An initial wet etching in KOH bath can be performed in order to decrease the depth machined by DRIE (Rousseau *et al.*; 2009). This etching step represents somehow the skeleton of the TSS. Once it is achieved, it becomes necessary to prepare the edges for subsequent operations. The first step of this preparation consists in achieving an electrical insulation of the via sidewalls from the silicon substrate in order to prevent any risk of short circuit. After this insulating coating, a barrier material is deposited to prevent atomic diffusion by substitution. The ultimate step in the realization of the TSS is that of filling by a conductive material. Electrochemical deposition is a well suited technique to perform this step in the frame of silicon resonators development. The electrolytic solution mainly consists of additives determined by the influence on the deposition kinetics. We briefly describe their role and their deposition conditions as well. A compound metallic seed layer is deposited on the bottom face of the silicon wafer in order to improve the uniformity of the electrodeposited copper filling. Eventually, we conclude the paper by summarizing the results from the electrical characterisations of the developed structures.

**Keywords:** MEMS resonators, TSS, TSV, Interconnection technology.

## References:

- Ivan, M., Dulmet, B., Martin, G., Abbe, P., Robert, L., Ballandras, S. (21-24 may 2012), "A new electrostatically-excited silicon structure for CMUT and TE-mode resonators and sensing applications", Proc. 2012 IEEE International Frequency Control Symposium, Baltimore, MD, USA, DOI: 10.1109/FCS.2012.6243724
- Rousseau, M. (2009), Impact des technologies d'intégration 3D sur les performances des composants CMOS (Doctoral dissertation, Université Paul Sabatier-Toulouse III).

# Oxide Ion Conduction in La<sup>2+</sup> and Sr<sup>2+</sup> Co-Doped Ceria/(Li-Na)<sub>2</sub>CO<sub>3</sub> Multifunctional Nanocomposite electrolyte

Nandini Jaiswal<sup>a</sup>, Shail Upadhyay<sup>b</sup>, Devendra Kumar<sup>c</sup> and Om Parkash<sup>d</sup>  
<sup>a,c,d</sup>Department of Ceramic Engineering, Indian Institute of Technology  
(Banaras Hindu University), Varanasi- 221005, (India).  
<sup>b</sup>Department of Physics, Indian Institute of Technology  
(Banaras Hindu University), Varanasi- 221005, (India).

## Abstract

Nanocomposite electrolyte in the system Ce<sub>0.85</sub>La<sub>0.125</sub>Sr<sub>0.025</sub>O<sub>1.9125</sub>/(Li-Na)<sub>2</sub>CO<sub>3</sub> has been synthesized by mixing nanosized co-doped ceria powder prepared by citrate-nitrate gel auto-combustion method with eutectic mixture of carbonates. Synthesized powder has been characterized via TGA/DTA, XRD, SEM, thermal expansion and impedance spectroscopy. Single phase formation has been confirmed by XRD which suggested that carbonates exist as an amorphous phase. SEM micrograph shows a percolated network of ceria and carbonates in which carbonates covers the surface of ceria particle. Complex plane impedance spectra show a complex nature. The main feature of impedance spectra is the absence of distinct grain boundary arc in contrast to doped ceria where distinct grain and grain boundary arcs have been observed. Conductivity increases very rapidly around the melting temperature of carbonate due to superionic transition at the interfaces formed between the ceria and carbonate phases. At the interfaces a space charge layer is formed consists of large number of mobile defects than that of the bulk.

**Keywords:** Co-doped ceria; Nanocomposite; LT-SOFC, Electrical conductivity.

Conductivity of 0.12 S/cm has been observed at 500 °C with an activation energy 0.50 eV of conduction.

## References:

- Y. Zhao et al. (2012) Quantifying multi-ionic conduction through doped ceria carbonate composite electrolyte by a current interruption technique and product analysis, *Int. J. of Hydrogen Energy* 37 8556-61.
- L. Fan et al. (2013) Recent development of ceria-based (nano) composite materials for low temperature ceramic fuel cells and electrolyte-free fuel cells, *Journal of Power Sources* 234 154-74.

# Study of Electrical Conductivity of Polypyridine-PVAc Composite Thin-Film doped with Ni(NO<sub>3</sub>)<sub>2</sub>

Gopal. R. Dhokane \*

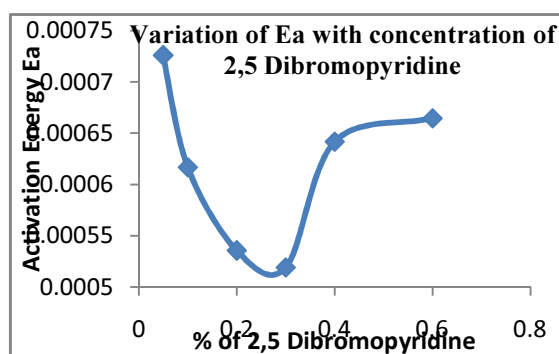
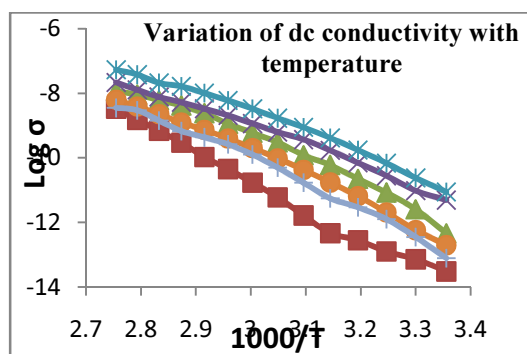
\* Department of Physics, Arts, Science & Commerce College, Chikhaldara, Maharashtra 444807 (India)  
E-mail: [grdhokane@gmail.com](mailto:grdhokane@gmail.com), [grdhokane\\_2007@india.com](mailto:grdhokane_2007@india.com).

---

## Abstract:

Pyridine shows interesting properties due to hetroaromatic nature combined to its electron deficient nitrogen and molecular simplicity. Herein Ni doped Polypyridine-PVAc composite films were prepared by isothermal evaporation technique with varying concentration of 2,5-Dibromopyridine as well as oxidizing agent Ni(NO<sub>3</sub>)<sub>2</sub>. In XRD spectra sharp reflection peaks are observed at  $2\theta$  value of 26.46 and 29.78<sup>0</sup>, and 26.51, and 29.81<sup>0</sup>, corresponding to d-spacing of 3.36 and 3.00, and 3.36 and 2.99 Å<sup>0</sup> respectively, may be due to the phases of polypyridine. The dc conductivity of polypyridine-PVAc composite films depends on temperature and increases with increase in temperature, indicating negative temperature coefficient (NTC) of resistance. This shows the semiconducting nature of the films. Ac electrical conductivity is measured for all prepared samples in the frequency range 100 Hz to 200 KHz. As frequency increases the ac electrical conductivity  $\sigma_{ac}$  increases linearly according to equation  $\sigma_{ac} = A \omega^s$ . The frequency exponent 's' was calculated for all the investigated samples and the frequency is found to have a pronounced effect on conductivity at relatively lower temperature.

**Keywords:** Composites; Conducting polymer; Polypyridine; XRD; Conductivity



# On-Chip Fabrication of High performance Nanostructured Photoetectors

Mohammad R. Alenezi,<sup>\*,1,2</sup> Talal H. Alzanki,<sup>1</sup> Abdullah S. Alshammari,<sup>2,3</sup> Simon J. Henley,<sup>2</sup> S. R. P. Silva<sup>2</sup>

[Mr.alenezi@paaet.edu.kw](mailto:Mr.alenezi@paaet.edu.kw)

<sup>1</sup> College of Technological Studies, PAAET, P.O. Box 42325 Shuwaikh, Kuwait  
<sup>2</sup> Nangelectronics Center, Advanced Technology Institute, University of Surrey, Guildford, GU2 7XH, UK  
<sup>3</sup> Department of Physics, College of Science, University of Hail, P.O. Box 2440, Hail, KSA

## Abstract:

Low temperature hydrothermal synthesis methods of different ZnO nanostructures where rational control over their morphology and size is important for a wide range of sensing applications.<sup>1-4</sup> A controlled, seedless and site selective hydrothermal technique to fabricate high performance ZnO nanostructured photodetectors directly on chip is reported. We demonstrate that by controlling the nanowires growth process, via tuning the experimental parameters such as the concentration of reactants and the growth time, the device structure efficiency can be increased and significantly enhance its performance (sensitivity, detectability, response-time, and recovery-time). Using on-chip fabrication technique, bridging NWs (BNWs) photodetectors are fabricated on flexible and transparent substrates. The fabricated BNWs devices are then compared with other photodetectors having different device structures, NW array (NWA) and single NWs (SNWs) device. The BNWs photodetector demonstrates improved sensitivity, nanowatts detectability, and ultrafast response time and recovery time. The improvement in response time and recovery time is attributed to the unique NW-NW junction barrier dominating the charge transport in the BNWs devices and the direct contact between the ZnO nanowires and the Au electrode which are not available for the other devices. The enhanced photosensitivity and nanowatts detectability of the BNWs device are due to the reduction in dimensionality and ultrahigh surface-to-volume ratio compared to the other tested structures. This work paves the way toward low cost, large scale, low temperature, seedless and site-selective fabrication of high performance ZnO NW sensors on flexible and transparent substrates.<sup>1,2</sup>

Keywords: ZnO, hydrothermal synthesis, photodetectors, nanowires, seedless synthesis, bottom up.

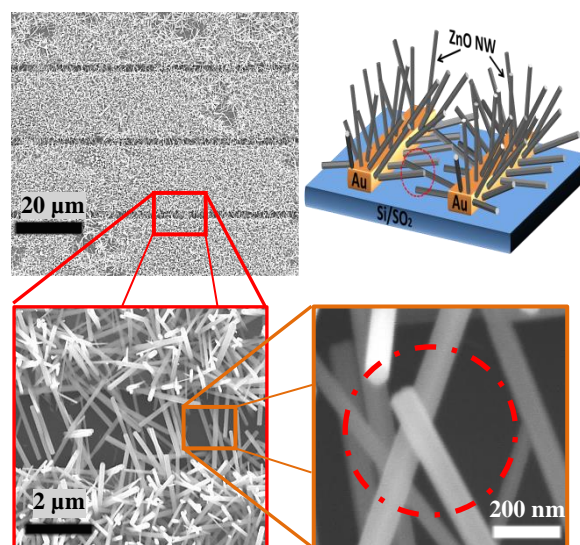


Figure 1: SEM images at different magnifications and schematic diagram of the bridging nanowires photodetectors.

## References:

1. Alenezi, M. R.; Alshammari, A. S.; Jayawardena, K. D. G. I.; Beliatas, M. J.; Henley, S. J.; Silva, S. R. P. *J. Phys. Chem. C* **2013**, 117, 17850–17858.
2. Alenezi, M. R.; Abdullah S. Alshammari, Peter D. Jarowski, Talal H. Alzanki, Simon J. Henley, and S. R. P. Silva. *Langmuir*, **2014**, 30, 3913–3921.
3. Alenezi, M. R.; Henley, S. J.; Emerson, N. G.; Silva, S. R. P. *Nanoscale*, **2014**, 6, 235–247.
4. Alenezi, M. R.; Alzanki, T. H.; Almeshal, A. M.; *International Journal of Science and Research*. **2014**, 3, 588–591.

# Facile growth of carbon nanotube electrode from electroplated Ni catalyst for supercapacitors

V. Yordsri,<sup>1,4</sup> W. Wongwiriyan,<sup>1-3\*</sup> C. Thanachayanont<sup>4</sup>

<sup>1</sup>College of Nanotechnology, King Mongkut's Institute of Technology Ladkrabang, Chalokkrung Rd., Ladkrabang, Bangkok, Thailand

<sup>2</sup>Nanotec-KMITL Center of Excellence on Nanoelectronic Device, Chalokkrung Rd., Ladkrabang, Bangkok, Thailand

<sup>3</sup>Thailand Center of Excellence in Physics, CHE, Si Ayutthaya Rd., Bangkok, Thailand

<sup>4</sup>National Metal and Materials Technology Center, 114 Thailand Science Park, Paholyothin Rd., Klong 1, Klong Luang, Pathumthani, Thailand

**Abstract:** Carbon nanotube (CNT) is one of the most promising materials in nanotechnology due to its large effective surface, excellent mechanical and electrical properties. CNT shows a great potential to apply in various applications to improve device properties such as electronics devices, energy storage devices and sensors (Steve *et al.*, 2013). For practical application, a simple method to synthesize a mass production of CNT is required. Chemical vapor deposition (CVD) is one of the main methods for CNT synthesis. Metal catalyst is an essential ingredient for CVD approach (Lee *et al.*, 2002, Muangrat, *et al.*, 2013). Normally, evaporation and sputtering techniques are utilized for catalyst film preparation. However, these techniques are time-consuming process and high cost. In this study, a facile growth of CNT using electroplated Ni as catalyst was proposed. Ni catalyst layers were deposited on Cu sheet by direct-current electroplating technique. Morphology of Ni layers were controlled by the applied voltage during electroplating. The applied voltages were varied at 1.0, 1.5 and 2.0 V. Next, Ni catalyst-deposited Cu sheet was set into a quartz tube reactor for CVD process using ethanol as carbon source. Scanning electron microscope (SEM), atomic force microscopy (AFM), transmission electron microscope (TEM) and Raman spectroscopy were utilized for the characterization of electroplated Ni catalyst and synthesized CNTs. The optimum condition for CNTs synthesis is electroplated Ni at 1.5 V. CNTs with a uniform diameter of approximately 54 nm with graphene layers being parallel to CNT axis, corresponding to multi-wall CNTs, were obtained (Figure 1). Moreover, for supercapacitor demonstration, the CNTs synthesized using electroplated Ni at 1.5 V were used as electrodes for the electrical double-layer capacitor (EDLC) structure. Filter paper was used as separator and 1 M of H<sub>2</sub>SO<sub>4</sub> was used as electrolyte. The capacitive characteristics were characterized by cyclic voltammetry and the galvanostatic charge/discharge techniques.

**Keywords:** Electroplating, Carbon nanotube, Chemical vapor deposition, Electrical double-layer capacitor.

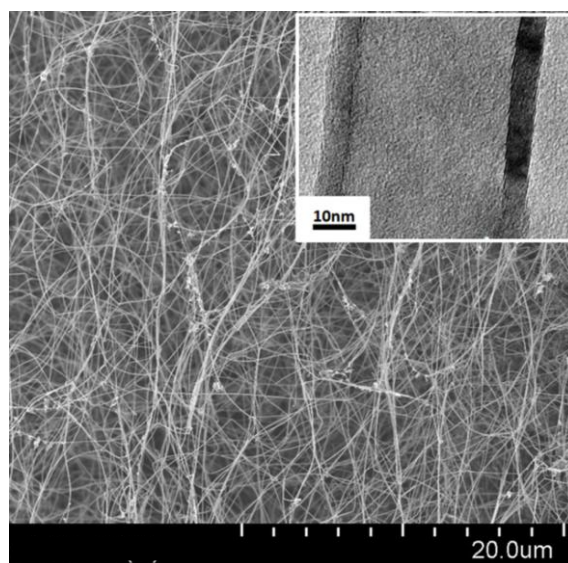


Figure 1: SEM image of multi-wall CNTs synthesized from electroplated Ni at 1.5 V. Inset is its high resolution TEM image.

## References:

- Pask, S., Vosguerichian, M., Bao, Z., (2013), A review of fabrication and applications of carbon nanotube film-based flexible electronics, *Nanoscale*, 5, 1727-1752.
- Lee, C.J., Park, J., Yu, J.A. (2002), Catalyst effect on carbon nanotubes synthesized by thermal chemical vapor deposition, *Chem. Phys. Lett.*, 360, 250-255.
- Muangrat, M., Porntheeraphat, S., Wongwiriyan, W. (2013), Effect of metal catalysts on synthesis of carbon nanomaterials by alcohol catalytic chemical vapor deposition, *Engineering Journal*, 17, 35-39.

# Electrochemical biosensor based on Cyt-C/GO-AuNPs/MWCNT modified GCE for determination of Rebaudioside-A

B. Ayyappa, S. Kanchi, M.I. Sabela, and K. Bisetty\*

\*Department of Chemistry, Durban University of Technology P.O. Box 1334, Durban 4000 South Africa

**Abstract:** The main purpose of this study was to develop a suitable electro-analytical method under optimum experimental conditions for the determination of Reb-A which is a main sweetening component in steviol glycosides. Hence, an electrochemical biosensor based on Cytochrome-c immobilized on gold nano particles decorated graphene oxide/ multiwall carbon nano tube has been developed. This material was characterized by means of frontier transition infrared spectroscopy (FTIR), scanning electron microscope (SEM) and energy dispersive spectroscopy (EDS). The electrochemical behaviour of the modified electrode was investigated in 0.1 M borate buffer solution (PBS) at pH 11.0 by cyclic voltammetry and differential pulse voltammetry. The DPV results reveal that, the gold nano particles decorated graphene oxide modified GCE shows catalytic activity towards the quasireversible reduction of Reb-A at  $-0.1\text{ V}$ . The addition of multiwall carbon nanotubes provides the highest edge density per unit nominal area causing to increase in the sensitivity of the electrode. Further, Cyt-c was adsorbed tightly on the surface of the modified electrode and it shows an enzyme-like activity for the reduction of Reb-A (Figure. 1). By employing, Cyt-C/GO-AuNPs/MWCNT modified electrode a 10-fold enhancement in DPV signal was observed than GCE and this indicates the direct electron transfer of Cyt-c. Under the optimized conditions  $I_p$  ( $\mu\text{A}$ ) was proportional to the concentration of Rub-A in the range

of  $1.0 \times 10^{-6}$  to  $4.5 \times 10^{-5}\text{ M}$  ( $R^2 = 0.9991$ ) with a low detection limit ( $S/N = 3$ ) of  $2.6 \times 10^{-7}\text{ M}$ . The analytical applications of the modified electrode were demonstrated by the determination of Reb-A in different real food samples.

**Keywords:** Rebaudioside-A, cytochrome-c, graphene oxide, cyclic voltammetry, differential pulse voltammetry, real food samples.

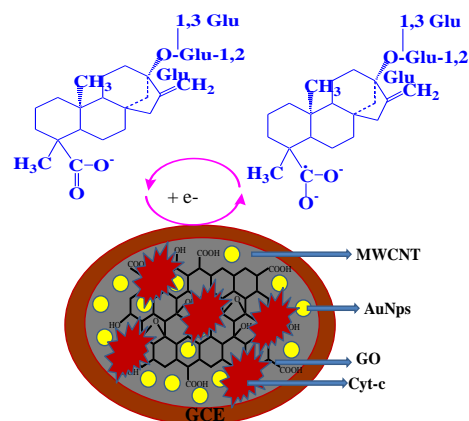


Figure 1: A schematic representation for the typical electroreduction of Reb-A at Cyt-C/GO-AuNPs/MWCNT modified GCE.

# Cerium Oxide Nanoparticles for Antioxidant Therapy Perspectives

Enrico Traversa

Division of Physical Sciences and Engineering, King Abdullah University of Science and Technology (KAUST), Thuwal, Saudi Arabia

**Abstract:** Nanotechnology is offering unprecedented tools to medicine over the last few years. The extensive use of nanoparticles for therapy and/or diagnostics has unveiled a new generation of nanobiomaterials for medical applications. The general trend is towards the development of bioactive rather than bio-inert materials, with materials directly triggering or participating to cellular reaction pathways. Nanostructured oxides play also an important role in this scenario, and not only as inert materials as one would expect. Recently, cerium oxide nanoparticles (nanoceria) have been reported to show outstanding biomedical activity, acting as well tolerated anti-age and anti-inflammatory agents (Chen *et al.*, 2006). Potential pharmacological applications are proposed due to redox changes in the Ce oxidation state ( $Ce^{4+}/Ce^{3+}$ ) that trigger the abatement of intracellular reactive oxygen species (ROS), hindering the oxidative stress cytotoxic effects (Celardo *et al.*, 2011a). The search for reliable and effective antioxidant therapy is a focus of current pharmacological research, since many serious diseases imply oxidative stress. However, the comprehension of the biological antioxidant mechanisms of nanoceria is at an early stage and controversial results are reported in the literature. This talk will summarize our recent studies on the antioxidant effects of nanoceria. It was found that nanoceria reduce the oxidative status and the extent of damage-induced apoptosis, in various cellular systems, including cardiac progenitor cells, subjected to various oxidative stresses (Celardo *et al.*, 2011b; Pagliari *et al.*, 2012).

Keywords: cerium oxide nanoparticles, oxidative stress, nanomedicine, stem cells, apoptosis.

## References:

Celardo, I., Pedersen, J.Z., Traversa, E., Ghibelli, L. (2011a), Pharmacological potential of cerium oxide nanoparticles, *Nanoscale*, 3, 1411-1420.

Celardo, I., De Nicola, M., Mandoli, C., Pedersen, J.Z., Traversa, E., Ghibelli, L. (2011b),  $Ce^{3+}$  ions determine redox-dependent anti-apoptotic effect of cerium oxide nanoparticles, *ACS Nano*, 5, 4537-4549.

Chen, J.P., Patil, S., Seal, S., McGinnis, J.F. (2006), Rare earth nanoparticles prevent retinal degeneration induced by intracellular peroxides, *Nature Nanotech.*, 1, 142-150.

Pagliari, F., Mandoli, C., Forte, G., Magnani, E., Pagliari, S., Nardone, G., Licocchia, S., Minieri, M., Di Nardo, P., Traversa, E. (2012), Cerium oxide nanoparticles protect cardiac progenitor cells from oxidative stress, *ACS Nano*, 6, 3767-3775.

# An electrochemical polyamines biosensor for biogenic amines determination in biomedical applications based on zinc oxide nanoparticles-porphyrrole modified platinum electrode

Rooma Devi, C. Raman Suri, Debendra.K. Sahoo  
Institute of Microbial Technology (CSIR), Sector 39-A, Chandigarh 160036,

**Abstract:** Biogenic polyamines (i.e., putrescine, spermidine, and spermine), which are found in a wide variety of organisms and tissues, play a pivotal role in the regulation of many cellular processes, such as cell growth and differentiation (Stefanelli *et al.*; 1998) Elevated levels of these polyamines in the tissue or blood are intimately associated with the presence of many types of cancers( Fujita *et al.*; 1976, Stefanelli *et al.*; 1998). Zinc oxide nanoparticles (ZnO-NPs) were synthesized from zinc nitrate by simple and efficient method in aqueous media at 55 °C without any requirement of calcinations step. A mixture of ZnO-NPs and pyrrole was eletropolymerized on Pt electrode to form a ZnO-NPs-polypyrrole (PPy) composite film. The determination of polyamines via enzymatic analysis using the enzymes polyamine oxidase (POx) and diamine oxidase (DOx). Our work consisted in the construction and assembling of a highly specific and sensitive amperometric biosensor for spermidine and spermine using the enzyme POx purified from oat seedling and putrescine using the enzyme DOx purified seedlings of *Pisum Sativum*. Enzymes were immobilized onto this nanocomposite film through physisorption. The ZnONPs/polypyrrole/Pt electrode was characterized by Fourier transform infrared (FTIR), cyclic voltammetry (CV), X-ray diffraction (XRD), scanning electron microscopy (SEM), transmission electron microscopy (TEM) and electrochemical impedance spectroscopy (EIS) before and after immobilization of enzymes. The Enzymes/ZnO-NPs-PPy/Pt electrode as working electrode, Ag/AgCl as reference electrode and Pt wire as auxiliary electrode were connected through a potentiostat to construct a polyamines biosensor. Polyamines content were determined in various urine samples of healthy and patients of cancer disease of various age group and sex employing the proposed method.

**Keywords:** zinc oxide nanoparticles, pyrrole, polyamine oxidase, diamine oxidase, polyamines biosensor, biomedical applications.

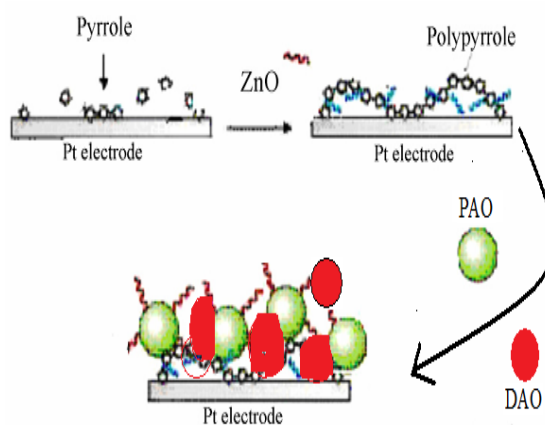


Figure 1: Scheme of construction of Polyamines biosensor

## References:

- Fujita, K., Nagatsu, T., Maruta, K., Ito, M., Senba, H., Miki, K. (1976) Urinary putrescine, spermidine, and spermine in human blood and solid cancers and in an experimental gastric tumor of rats, *Cancer Res.*, 36, 1320-1324.
- Stefanelli, C., Bonavita, F., Stanic, I., Mignami, M., Facchinin, A., Pignatti, C., Flamigni, F., Calderera, C. (1998) Spermine causes caspase activation in leukaemia cells, *FEBS Lett.*, 437, 233-236.

# NiO encapsulated polyaniline nanostructure for Non-enzymatic glucose sensing

S. K. Shukla<sup>1</sup> and Ashutosh Tiwari<sup>2</sup>

<sup>1</sup>Department of Polymer science, Bhaskaracharya College of Applied Sciences, University of Delhi, Delhi 110075, India

<sup>2</sup>Biosensors and Bioelectronics Centre, IFM, Linköping University, 581 83 Linköping, Sweden

\*Corresponding author. Tel: (+91) 11-20507597; E-mail: sarojshukla2003@yahoo.co.in

## Abstract

Quantitative assessment glucose is a practical need for medical diagnostics and the food processing industries [Gerard 2002]. The most of previous studies on glucose sensor are based on glucose oxidase (GOx), but its greatest drawback is stability and therefore, the development of different types of non-enzymatic sensors are current need of analytical chemistry [Shukla, Park, 2012, 2006]. In the present work, a high sensitive and selective potentiometric non-enzymatic glucose developed using nickel oxide encapsulated polyaniline nanostructures. The enzyme-free sensing electrode was fabricated through *in situ* electrochemical polymerisation of polyaniline in the presence of NiO on ITO coated glass. The obtained electrode was characterized by scanning electron microscopy (SEM), transmission electron microscopy (TEM), powder X-ray diffractometry (XRD), and Infrared spectroscopy (FT-IR). Potentiometric measurement reveals the catalytic properties of the prepared sensing electrode for glucose electro-oxidation in both buffer at biological pH and blood serum. Under optimized conditions, the developed enzyme less sensor exhibited better performance for glucose analysis selectively than its constituents, offering a wider linear range (from 20 to 400 ppm), with an low detection limit of 5 ppm. The further, favorable reproducibility and long-term performance stability were checked from the robust nanostructured frameworks for about 60 days.

## References

- Gerard, M.A.; Chaubey A.; Malhotra, B. D.; Biosensors & Bioelectronics 17( 2002) 345-359.  
Shukla, S. K.; Deshpande, S. R.; Shukla, S. K.; and Tiwari, A.; Talanta 99 (2012) 283-287.  
Park, S.; Boo, H.; Chung, T. D.; Anal. Chim. Acta 556 (2006) 46–57.

# Green approach for the preparation of regenerated cellulose-chitosan membrane containing silver nanoparticles

C.H. Chia, S.W. Chook, S. Zakaria

Materials Science Program, School of Applied Physics, Faculty of Science and Technology,  
Universiti Kebangsaan Malaysia, 43600 Bangi, Selangor, Malaysia

**Abstract:** Immobilization of nanoparticles, such as silver, gold, titanium dioxide on polymeric substrate would introduce new functionality such as antibacterial properties for various applications, including such as antimicrobial (Dastjerdi *et al.*, 2010), food packaging (Duncan 2011) and wound dressing (Maneerung *et al.* 2008). For the past decades, silver nanoparticles (AgNP) has been extensively studied for wide range of applications especially for biomedical purposes due to its strong antibacterial activity (Chook *et al.* 2012; Rai *et al.* 2009; Ravindran *et al.* 2013). Synthesis of AgNP usually involved a chemical reduction of  $\text{Ag}^+$  precursor using strong but hazardous reducing agent, such as sodium borohydrate or hydrazine (Kumar *et al.* 2008). Thus, a more environmental friendly method to produced AgNP was developed by reducing Tollens reagent or silver ammonia complex with reducing sugar such as glucose (Yin *et al.* 2002). The present study demonstrates the preparation of chitosan coated regenerated cellulose membrane by coagulating cellulose solution into an acetic acid solution containing chitosan. The membrane is subsequently served as the substrate for immobilization of AgNP via *in situ* synthesis method. Fig. 1 shows the schematic diagram of the procedure for the preparation of the antibacterial cellulose membrane containing chitosan and AgNP. The concentration chitosan on the cellulose membrane can be adjusted by varying the concentration of chitosan in the acetic acid solution. The greater chitosan content on the cellulose membrane has enhanced more AgNP to be deposited on the membrane, which can be explained by the electrostatic charges interaction between the negative charged AgNP and positive charged amine groups on the chitosan. The surface morphology of membrane obtained by SEM, showed that the presence of chitosan has affected the porous structure of membranes and the formation of AgNP. Additionally, AFM revealed that the surface roughness of each membranes increased as a result of the increase of the immobilized AgNP on the membrane. Furthermore, the membranes exhibited improved antibacterial activity against *S. aureus* and *E. coli* by increasing the chitosan and AgNP concentrations. A green approach for the preparation regenerated cellulose membrane containing chitosan was developed for the significant improvement on the antibacterial properties of regenerated cellulose membrane.

**Keywords:** cellulose, chitosan, *in situ* synthesis, regenerated cellulose, silver nanoparticle

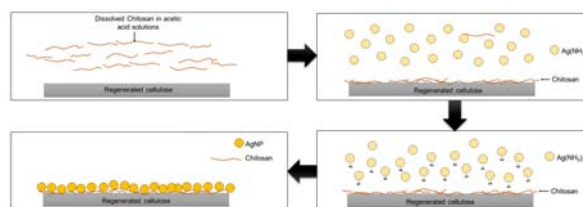


Figure 1. Preparation of regenerated cellulose membrane containing chitosan and AgNP.

## References:

- Chook, S., Chia, C.H., Zakaria, S., Ayob, M., Chee, K.L., Huang, N.M., Neoh, H.M., Lim, H.N., Jamal, R., Rahman, R. (2012). Antibacterial performance of Ag nanoparticles and AgGO nanocomposites prepared via rapid microwave-assisted synthesis method, *Nanoscale Res. Lett.*, 7, 541.
- Dastjerdi, R., Montazer, M. (2010), A review on the application of inorganic nano-structured materials in the modification of textiles: Focus on anti-microbial properties, *Colloid. Surf. B*, 79, 5-18.
- Duncan, T.V. (2011), Applications of nanotechnology in food packaging and food safety: Barrier materials, antimicrobials and sensors, *J. Colloid Inter. Sci.*, 363, 1-24.
- Kumar, A., Vemula, P.K., Ajayan, P.M., John, G. (2008). Silver-nanoparticle-embedded antimicrobial paints based on vegetable oil, *Nat. Mater.*, 7, 236-241.
- Maneerung, T., Tokura, S., Rujiravanit, R. (2008), Impregnation of silver nanoparticles into bacterial cellulose for antimicrobial wound dressing, *Carbohydrate Polym.*, 72, 43-51.
- Rai, M., Yadav, A., Gade, A. (2008). Silver nanoparticles as a new generation of antimicrobials, *Biotechnology Advances*, 27, 76-83.
- Ravindran, A., Chandran, P., Khan, S.S. (2013), Biofunctionalized silver nanoparticles: Advances and prospects, *Colloid. Surf. B*, 105, 342-352.
- Yin, Y., Li, Z.-Y., Zhong, Z., Gates, B., Xia, Y., Venkateswaran, S. 2002. Synthesis and characterization of stable aqueous dispersions of silver nanoparticles through the Tollens process, *J. Mater. Chem.*, 12, 522-527.

# Synthesis of conductive biodegradable hydrogels based on *Gum ghatti* and their use in colon-specific drug delivery

Kashma Sharma<sup>1,2</sup>, Vijay Kumar<sup>2</sup>, B. S. Kaith<sup>3</sup>, S. Kalia<sup>4</sup> and H. C. Swart<sup>2</sup>

<sup>1</sup>Department of Physics, University of the Free State, Bloemfontein ZA9300, South Africa

<sup>2</sup>Department of Chemistry, Shoolini University of Biotechnology and Management Sciences, Solan, Himachal Pradesh, India

<sup>3</sup>Department of Chemistry, Dr. B.R. Ambedkar National Institute of Technology, Jalandhar, Punjab-144011, India

<sup>4</sup>Department of Chemistry, Bahra University, Wahnaghat (Shimla Hills) 173234, Distt. Solan, H.P., India

**Abstract:** A conductive superabsorbent hydrogel was developed based on interpenetrating network that was formed as a result of concurrent free radical polymerization of aniline (ANI) onto Gg-cl-poly(MAA) using N, N'-methylene-bis-acrylamide (MBA), as cross-linker and ammonium persulfate (APS), as an initiator system (Sharma et al., 2013; Tiwari and Singh, 2008). Gg-cl-poly(MAA) was prepared by free-radical copolymerization of methacrylic acid onto Gum ghatti in aqueous media with optimized process parameters, using MBA and APS as an initiator-crosslinker system. The resulting cross-linked hydrogels structure, morphology, thermal and swelling behaviour were investigated. It was found that incorporating ANI into Gg-cl-poly(MAA) causes an increase in the value of equilibrium swelling as compared with Gg-cl-poly(MAA). Biodegradation studies of the cross-linked hydrogel samples were carried out by composting soil test for a period of 60 days (Mittal et al., 2013). Percent weight loss was measured as a function of the number of days and it was observed that percent weight loss increased with increasing number of days. The evidence for biodegradability has been confirmed by carrying out the FTIR and SEM techniques. The cross-linked hydrogels has further been applied for colon specific drug delivery of amoxicilline trihydrate under different pH conditions at 37 °C (Kaith et al., 2012). The initial diffusion coefficient has been found to show greater values than late diffusion coefficient confirming greater release at the early stages of the drug release than that in the late stages.

**Keywords:** Smart polymers, *Gum ghatti*, biodegradability, drug release, pH sensitive.

## References:

Sharma, K., Kaith, B.S, Kumar, V., Kumar, V., Som, S., Kalia, S., Swart, H.C. (2013) Synthesis and properties of poly(acrylamide-aniline)-grafted gum ghatti based nanospikes, *RSC Advance* 3, 25830-25839.

Tiwari, A., Singh, S.P. (2008) Synthesis and characterization of biopolymer-based electrical conducting graft copolymers, *J. Appl. Polym. Sci.*, 108, 1169–1177.

Mittal, H., Mishra, S.B., Mishra, A.K., Kaith, B.S., Jindal, R., Kalia, S. (2013) Preparation of poly(acrylamide-co-acrylic acid)-grafted gum and its flocculation and biodegradation studies, *Carbohydr. Polym.* 98, 397-404.

Kaith, B.S., Saruchi, Rajeev, J., Manpreet, S.B. (2012) Screening and RSM optimization for synthesis of a Gum tragacanth–acrylic acid based device for in situ controlled cetirizine dihydrochloride release, *Soft Matter* 8, 2286-2293.

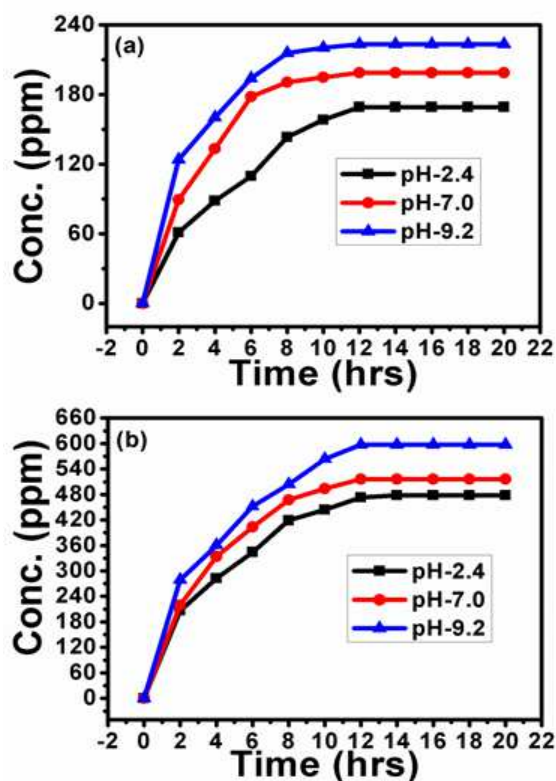


Figure 1: The effect of pH value on amoxicillin trihydrate release behaviour through (a) Gg-cl-poly(MAA) and (b) Gg-cl-poly(MAA-ipn-aniline).

# Jelly Added with Food Preservatives and Formaldehyde, used as Barrier against Underground Humidity and for Consolidation of Ancient raw Materials

J. M. Navarrete<sup>1</sup>, G. Martínez<sup>1,2+</sup>

<sup>1</sup>Faculty of Chemistry, National University of Mexico, Mexico City, Mexico

<sup>2</sup>National Coordination to Restore the Cultural Inheritance, National Institute of Anthropology and History, Mexico City, Mexico

**Abstract:** Surfaces of ancient raw materials are usually very strongly attacked by humidity coming up from underground, causing salts deposition and material losing, which is definitely more regrettable for mural paintings and special plasters used in historical times. Few examples of these conservation problems are so important monuments as Ajanta caves and Matuti Temple in India, Xiang warriors in China, Sukothai Kingdom in Thailand and recently discovered Cacaxtla ruins in Tlaxcala, Mexico, where impressive mural paintings have been partially destroyed mainly by underground humidity. So, it was laboratory tested one procedure to diminish the porosity of several mineral samples used as raw materials in the past, such as fired plain mud, feldspar, quarries, bricks, limestone etc. It was used the hot solution of an organic, soft polymer called French gelatin, added with food preservatives, plus formaldehyde just before solidification. When this hot, colorless solution, is spread out with a hand pump atomizer over the surface materials, its penetration results directly proportional to porosity and hence capacity to absorb underground and environmental humidity, besides of compacting lose material, and forming

an elastic barrier which preserves materials surface for long time, about 8 years by now, with no need of any extra treatment.

Keywords: preservation, ancient, ruins, destroyed, underground, humidity.



Fig 1.- Guadalupe Virgin's Image before treatment



Fig. 2.- Same religious Image after 8 years of treatment

## References

Navarrete, M., Martínez, G.(2012), Consolidation of ancient raw material, using a reversible, elastic, soft polymer, *Adv.in Mat.Phys.and Chem.*, 2, 37-42

# Enzyme-Mediated Injectable Hydrogels with Independent Tuning of Mechanical Strength and Gelation Rate for Biomedical Applications

Motoichi Kurisawa

Institute of Bioengineering and Nanotechnology, 31 Biopolis Way, The Nanos, #04-01 Singapore 138669

Email: mkurisawa@ibn.a-star.edu.sg

**Abstract:** Recently, enzymes such as transglutaminase and horseradish peroxidase (HRP) have been utilized to form chemically-crosslinked hydrogels. We have developed hydrogels based on the HRP-mediated oxidative coupling of phenol moieties that conjugated to biodegradable polymers. The oxidative reaction of hydrogen peroxide ( $H_2O_2$ ) and horseradish peroxidase (HRP) catalyzed the crosslinking of the phenol moieties and allowed the independent tuning of the mechanical strength and gelation rate. This system does not involve toxic chemicals or reactions in the hydrogel formation process, thus allowing therapeutic proteins, growth factors and cells to be incorporated without damaging these biological molecules. In addition, Recently, we have developed a novel approach to improve the anticancer efficacy of protein drugs in liver cancer therapy by using an injectable hydrogel system that incorporates protein therapeutics. Also, we have studied the effect of hydrogel stiffness on the maintenance of chondrocyte phenotype in a 3D environment and in the cartilage tissue repair using the chondrocyte-laden hydrogels. We found that the appropriate stiffness of hydrogel exhibited a superior 3D environment in maintaining the chondrogenic phenotype and favored the regeneration of cartilage tissue in vivo. In view of the injectable enzymatically cross-linked hydrogel system's promising properties, our novel hydrogel is expected to be an important tool in the field of biomaterial science and medicine.

**Keywords:** Injectable, hydrogel, drug delivery system (DDS), tissue engineering, biodegradable, biomedical applications.

## References:

M. Kurisawa, J. E. Chung, Y. Y. Yang, S. J. Gao, H. Uyama, Injectable biodegradable hydrogels composed of hyaluronic acid-tyramine conjugates for drug delivery and tissue engineering, *Chem. Commun.* 4312-4314 (2005).

L. S. Wang, J. Boulaire, P. P. Y. Chan, J. E. Chung, M. Kurisawa, The roll of stiffness of gelatin- hydroxyphenylpropionic acid hydrogels formed by enzyme-mediated crosslinking on the differentiation of human mesenchymal stem cell, *Biomaterials* 31, 8608–8616 (2010).

K. Xu, F. Lee, S. J. Gao, J. E. Chung, H. Yano, M. Kurisawa, Injectable hyaluronic acid-tyramine hydrogels incorporating interferon- $\alpha$ 2a for liver cancer therapy, *J. Control. Release* 166, 203–210 (2013).

K. H Bae, L. S. Wang, M. Kurisawa, Injectable biodegradable hydrogels: Progress and Challenges, *J. Mater. Chem. B* 1, 5371-5388 (2013).

L. S. Wang, C. Du, W. S. Toh, A. C. A Wan, S. J. Gao, M. Kurisawa, Modulation of chondrocyte functions and stiffness-dependent cartilage repair using an injectable enzymatically crosslinked hydrogel with tunable mechanical properties, *Biomaterials* 35, 2207–2217 (2014).

## Developing new hybrid materials for sensors

Suresh Valiyaveetil

Department of Chemistry, National University of Singapore,  
3 Science Drive 3, Singapore 117543  
Email. chmsv@nus.edu.sg

Manufacturing complex structures from soft materials with long range order and orientation have been investigated by many research groups. The bottom up approach, less prevalent approach, makes use of self - organizing intriguing components, wherein control only involves selection of choice of material and self-assembly conditions. The self-assembly approach is currently being actively investigated to achieve interesting structures and properties in thin films. Subtle adjustments in casting environment conditions allow remarkable control in the consequent thin film morphologies. The present study focuses on the fabrication of micro-structured blue light-emitting thin films of novel, functionalized amphiphilic poly(*p*-phenylene)s (PPPs) which are being investigated as potential candidates for advanced polymer electronic and optical applications. In addition to this, we demonstrate how interplay of inter-chain interaction forces influence the formation of large area of periodic and intricately patterned conjugated thin polymer-nanoparticle hybrid films. Recently, we have developed hybrid organo-silica hybrid materials and investigating their properties for gas sensing. The present talk will focus on the design and synthesis of conjugated polymers, hybrid materials and fabrication of self-organized patterned functional microstructured thin films incorporated with nanoparticles.

# Photoluminescent Carbon Nanoparticles from Bio-waste

Raju Kumar Gupta

Department of Chemical Engineering, Indian Institute of Technology Kanpur, Kanpur - 208016, U.P., India

[guptark@iitk.ac.in](mailto:guptark@iitk.ac.in)

**Conference theme: Development and Characterization of Multifunctional and Smart Materials/ Surfaces/ Coatings (Nanostructured, nanoporous, etc)**

**Abstract:** Recent advances in the field of carbon based nano-materials with diverse morphologies generated a great concern in the advanced scientific research owing to their excellent and unique properties, since their discoveries. Such as fullerenes (Kroto *et al.*; 1985), multiwalled (Pastorin *et al.*; 2006) and single walled carbon nano-tubes (Jeng *et al.*; 2006), carbon nano-onions (Dubey *et al.*; 2014), carbon nano-spheres, carbon nanorods, graphene, (Cushing, *et al.*; 2006) and recently discovered graphene quantum dots (GQDs) (Park *et al.*; 2013).

The size and shape of carbon nanoparticles (CNPs) have strong influence on their electrical, optical and sensing properties (Albanese *et al.*; 2012). So, morphology-controlled fabrications of carbons nano particles as well as broadening their practical applications are in great demand. Up to now, chemical modification and template based synthesis have been extensively used to fabricate desired morphology of CNPs.

In this presentation, we will talk about synthesis of water soluble photoluminescent carbon nanoparticles from “bio-waste” like almond husk. During synthesis, there was significant effect of temperature on carbonization, resulting in the formation of different shaped carbon nano particles. At higher temperature nano-carbons formed are smaller in shape and spherical in morphology in comparison to those formed at lower, rod shaped. Further oxidative treatment of as synthesized nano-carbons imparts water solubility along with the photo-luminescent properties extended over the visible/NIR region of spectrum. The proposed method is very useful and could be scaled up for gram scale synthesis of carbon nano-particles. These water soluble carbon dots were used for p-nitrophenol dye removal as an adsorbent and observed ~82 % removal with these carbon dots. These carbon nanoparticles can be useful in other applications like bio imaging, photocatalysis, energy storage etc.

**Keywords:** Green synthesis; Fluorescent material; Carbon nanoparticles; Carbon dots; p-nitrophenol; Adsorption

## References:

Kroto, H. W., Heath, J. R., O'Brien, S. C., Curl, R. F., Smalley, R. E. (1985) C<sub>60</sub>: Buckminsterfullerene *Nature*, 318, 162.

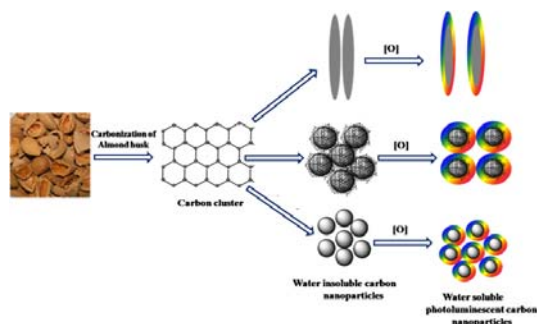


**Figure:** Schematic representation for the synthesis of shape variant photoluminescent carbon nanoparticles by almond husk at different carbonization temperatures.

Pastorin, G., Wu, W., Wieckowski, S., Briand, J.-P., Kostarelos, K., Prato, M., Bianco, A. (2006) Double functionalization of carbon nanotubes for multimodal drug delivery, *Chem. Commun.*, 1182.

Jeng, E. S., Moll, A. E., Roy, A. C., Gastala, J. B., Strano, M. S. (2006) Detection of DNA hybridization using the near-infrared band-gap fluorescence of single-walled carbon nanotubes, *Nano Letters*, 6, 371.

Dubey, P., Tripathi, K. M., Sonkar, S. K. (2014) Gram scale synthesis of green fluorescent water-soluble onion-like carbon nanoparticles from camphor and polystyrene foam, *RSC Adv.*, 4, 5838.

Cushing, S. K., Li, M., Huang, F., Wu, N. (2014) Origin of strong excitation wavelength dependent fluorescence of graphene oxide, *ACS Nano*, 8, 1002.

Park, J.-E., Grayfer, E. D., Jung, Y., Kim, K., Wang, K.-K., Kim, Y.-R., Yoon, D., Cheong, H., Chung, H.-E., Choi, S.-J., Choy, J.-H., Kim, S.-J. *J. Mater. Chem. B*, (2013) Photoluminescent nanographitic/nitrogen-doped graphitic hollow shells as a potential candidate for biological applications, 1, 1229.

Albanese, A., Tang, P. S.; Chan, W. C. W. (2012) The Effect of Nanoparticle Size, Shape, and Surface Chemistry on Biological Systems, *Annu. Rev. Bio-med. Eng.* 14, 1.

# Nanostructured Metal oxides: Catalyst-free Synthesis, Characterization and Integration with MEMS Processing for Gas Sensor

S. Chandra, B. Behera

Centre for Applied Research in Electronics, Indian Institute of Technology Delhi,  
HauzKhas, New Delhi-110016, India

**Abstract:** Thin films of metal oxides (such as tin oxide, indium tin oxide, zinc oxide, tungsten oxide etc.) are potential candidates for gas and VOC (volatile organic compound) sensing applications (Eranna G). In nanostructure form, these materials are more sensitive as gas sensor due to their much higher surface-to-volume ratio compared to their corresponding thin films. For efficient operation, it is a requirement that the gas sensor, incorporating metal oxide material, is heated upto 350 °C. The power consumption is an important issue in sensor design. Sensors made on suspended thin diaphragm of silicon using MEMS (Micro-Electro-Mechanical-Systems) technologies consume much less power due to thermal isolation. There is thus twin advantage in using nanostructured metal oxides integrated with MEMS technologies for gas and VOC sensing (Gong et al.). There is a challenge in developing these MEMS based sensors using low cost and easy-to-manufacture technologies (Pandya et al.).

In the present work, we report a novel catalyst-free low cost technique for synthesis of nanostructured ZnO and its integration with MEMS processing to demonstrate a sensor for VOC detection. For this purpose, thin films of Zn were prepared by RF sputtering method on oxidized silicon substrates. These were then subjected to an annealing cycle in oxidizing ambient in the temperature range of 400-550 °C in a horizontal tube furnace resulting in the growth of nanostructured ZnO. The effect of parameters such as initial Zn film thickness, sputtering parameters (RF power, pressure), annealing time, ambient (dry O<sub>2</sub>, wet O<sub>2</sub>, atmospheric air, synthetic air, wet N<sub>2</sub> etc.) were investigated in detail on the nature of nanostructures formed by the annealing step. The process was optimized to yield long nanowires of ZnO. The characterization included: Scanning Electron Microscopy (SEM) and X-ray diffraction (XRD) studies on the synthesized nanostructured ZnO material. A complete sensor, schematically shown in Fig. 1 incorporating an on-chip heater and inter digital electrode (IDE) for sensing on a MEMS platform using bulk micromachining is demonstrated.

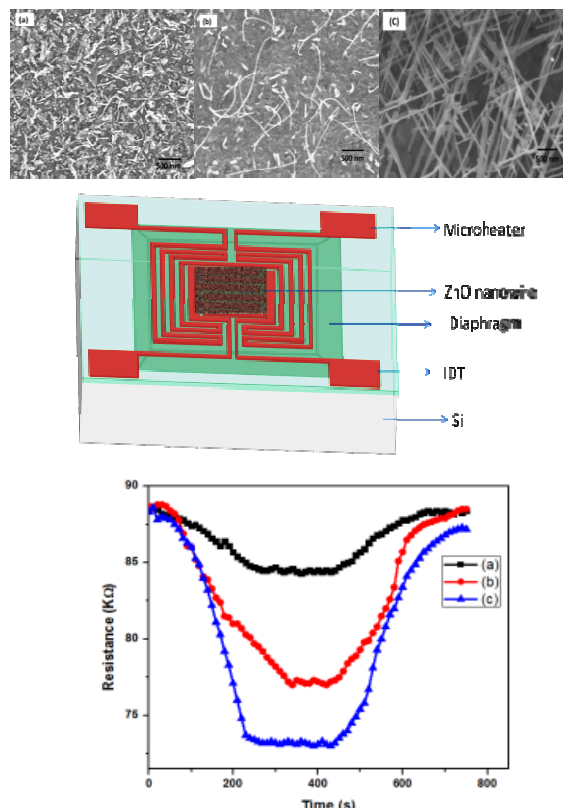


**Fig. 1** (i) SEM images of three different types of ZnO nanostructures. (ii) The schematic layout of the MEMS based gas sensing device and (iii) sensor responses for 50 ppm of ethanol at 100 °C.

**Keywords:** nanostructured metal oxides, catalyst-free synthesis, VOC-gas sensor, MEMS technologies.

Eranna G 2011 *Metal Oxide Nanostructures as Gas Sensing Devices* (Boca Raton, FL: CRC Press)

Gong J, Chen Q, Fei W and Seal S 2004 Micromachined nanocrystalline SnO<sub>2</sub> chemical gas sensors for electronic nose *Sensors Actuators B Chem.* 102 117–25

Pandya H J, Chandra S and Vyas A L, 2012 Integration of ZnO nanostructures with MEMS for ethanol sensor *Sensors Actuators B Chem.* 161, 923–8

# Influence of ventilation on transferring of the nano-sized particles from the fume cupboard to the room air

E. Jankowska, T. Jankowski, W. Zatorski, P. Sobiech

Central Institute for Labour Protection - National Research Institute, Czerniakowska 16, 00-701 Warsaw, Poland

**Abstract:** On the particles emitted during processes can be exposed not only workers performing work associated with the process but also another workers in the room. The aim of the investigation was to determine the influence of switched-off/on of fume cupboard - with switched-off general ventilation, on parameters of particles spread in the room air, when processes of mixing commercially available nano-materials powders were conducted inside the fume cupboard (1) - see Figure 1. Another five measuring points were located outside of the fume cupboard: points (2), (3) and (4) close to the fume cupboard and points (5) and (6) far from the point (1) in the distance 3.8m point (5) and 6.3m point (6).

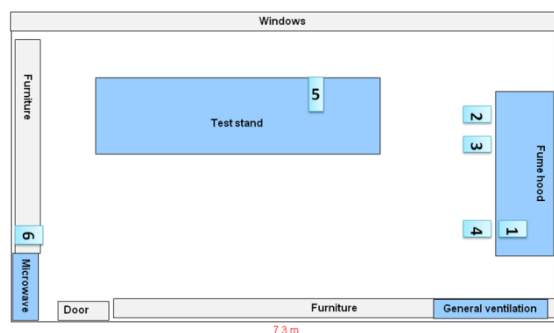


Figure 1. Location of measuring points in the room.

Measurements of particles parameters in all six points were done with portable devices DiscMini's (Matter Aerosol) when additionally in point (1) with devices from TSI: SMPS, P-Trak and Aero-Trak. As an example in Figure 2 are presented number concentrations determined with DiscMini's before, between and during processes of mixing of nanocly - nanomer I.34MN when fume cupboard was switched-off (two processes) and switched-on (two processes). Data presented in Figure 2 shown that when fume cupboard was switched-off particles transferred to the room air during both processes, even far from place where the processes of mixing were conducted. When fume cupboard was switched-on, and air was exhaust with flow rate  $931\text{m}^3/\text{h}$ , only a little transferring particle to the room was observed. However, when fume cupboard was switched-on, increase concentrations of particles in the room air compare to background was observed - the reason can be suspension in the air of particles settled on the surfaces in the room.

Keywords: nanomaterials, transferring of particles, ventilation, particle parameters

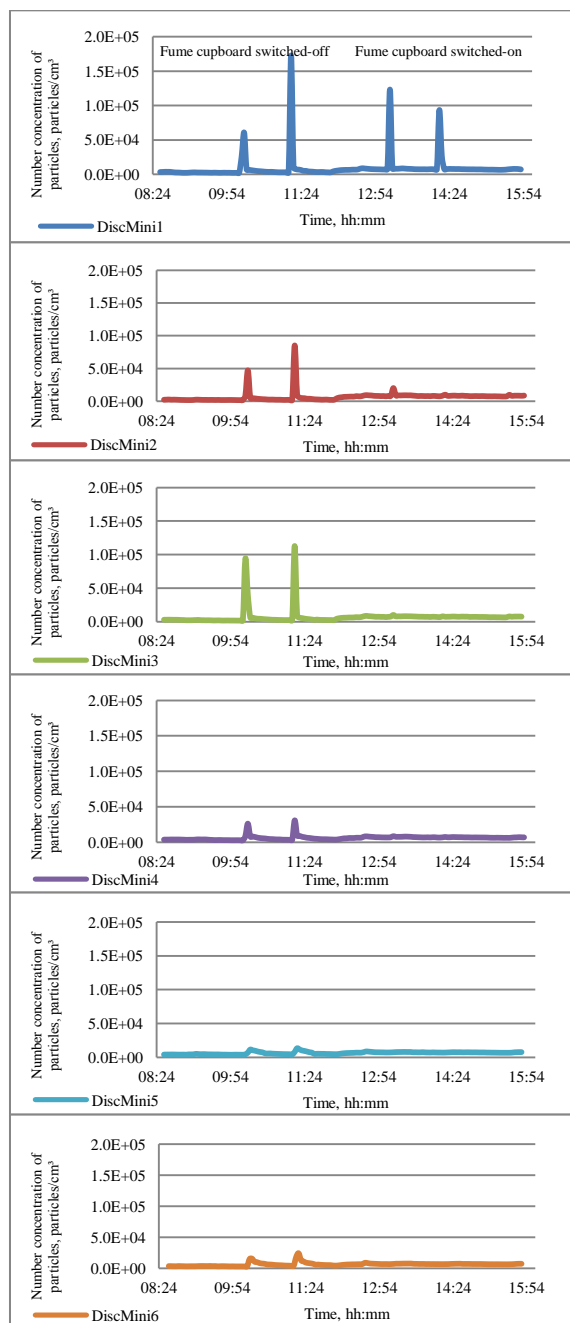


Figure 2. Number concentrations of particles 10-700nm in the fume cupboard (1) and in the five other points located in the room - DISCmini's results.

## Acknowledgements

This study has been prepared within projects SCAFFOLD (280535) and I.P.02 carried out within the National Programme "Safety and working conditions improvement", funded in the years 2014-2016 by the MNiSW.

# Smart Focused-Ion-Beam-fabricated Nanostructures for Improving Surface Enhanced Raman Scattering on Trace Detection of Single Molecules

Kundan Sivashanmugan<sup>1</sup>, Jiunn-Der Liao<sup>1,2,\*</sup>, Chih-Kai Yao<sup>1</sup>

<sup>1</sup> Department of Materials Science and Engineering, <sup>2</sup> Center for Micro/Nano Science and Technology, National Cheng Kung University, 1 University Road, Tainan 70101, Taiwan.

\* Corresponding author: jdliao@mail.ncku.edu.tw

**Abstract:** Surface-enhanced Raman scattering (SERS) is a label-free and extremely selective spectroscopic tool for analyzing a wide variety of chemical or biological species owing to its excellent sensitivity to molecular vibrations (Nusz *et al.*). The effect of SERS is mainly attributed to two primary mechanisms, namely chemical and electromagnetic (EM) effects. The interaction of noble metal nanoparticles (NPs) or nanostructure (NSs) with a laser with a constant wavelength can result in a collective oscillation caused by an excitation of conduction electrons and a subsequent electric field in the vicinity of NPs or NSs owing to the induction of localized surface plasmon resonance (LSPR). The frequency of LSPR strictly depends on the composition and geometry of NPs or NSs as well as the refractive index of the localized environment and that allows single molecule detection (Campion *et al.*). The optical properties of FIB-fabricated NSs may be suitable for Raman-active substrates (Sivashanmugan *et al.*). There still occur some drawbacks to NSs for use as photonic components. For example, FIB-fabricated NSs are strongly influenced by the residual Ga concentration and have a limited aspect ratio (Tao *et al.*).

In this work, Au and Au/Ag nanorod arrays (*fib*Au<sub>NR</sub> and *fib*Au/Ag<sub>NR</sub>) were fabricated by focused ion beam (FIB) with low and high ion energy. The formation of AuGa<sub>2</sub> alloys on *fib*Au<sub>NR</sub> was controlled by ion energy and temperature treatment. On the other hand, *fib*Au/Ag<sub>NR</sub> embedded nanovoids were generated with an increase in stress mostly caused by the effects of oxidation and heat expansion. In addition, the nanovoids formed in the embedded Ag layer. However, Au and Ag interface have different diffusion rates of the metal atoms and temperature treatment where atomic diffusion is possible; the interface could be moved and produce the alloys and voids in Au/Ag. Moreover, AuGa<sub>2</sub> on *fib*Au<sub>NR</sub>s was anticipated to increase the LSPR due to the matched photon energy between Au and AuGa<sub>2</sub>. The embedded nanovoids increased the available space for the interaction analyses with laser light and a strong EM field effect is generated in and around these nanovoids, creating LSPR (Figure 1). The *fib*Au<sub>NR</sub> and *fib*Au/Ag<sub>NR</sub> SERS properties were investigated using crystal violet as molecular test probes. The enhancement factor

reached up to 10<sup>7</sup>. Furthermore, an optimized *fib*Au<sub>NR</sub> and *fib*Au/Ag<sub>NR</sub> SERS-active substrate was applied to the detection of melamine cyanurate (MEL-CA) in milk solution at low concentration (pM). Results show that SERS-active *fib*Au<sub>NR</sub> and *fib*Au/Ag<sub>NR</sub> have potential for rapidly detecting low-concentration samples.

**Keywords:** Focused ion beam; Nanorods; Surface-enhanced Raman scattering; Crystal violet; Melamine-cyanurate

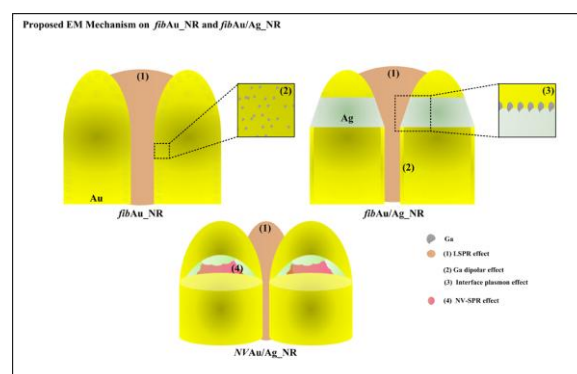


Figure 1 Brief description of proposed EM mechanism for *fib*Au<sub>NR</sub> and *fib*Au/Ag<sub>NR</sub>.

## References:

- Nusz, G. J., Curry, A. C., Marinakos, S. M., Wax, A., Chilkoti, A. (2009), Rational selection of gold nanorod geometry for label-free plasmonic biosensors. *ACS Nano* 3, 795-806.
- Campion, A., Kambhampati, P. (1998), Surface-enhanced Raman scattering. *Chem. Soc. Rev.* 27, 241-250.
- Sivashanmugan, K., Liao, J. D., You, J. W., Wu, C. L. (2013), Focused ion beam fabricated Au/Ag multilayered nanorod array as SERS-active substrate for virus strain detection. *Sens. Act. B: Chem.* 181, 361-367.
- Tao, H. H., Ren, C., Feng, S., Liu, Y. Z., Li, Z. Y., Cheng, B. Y., Zhang, D. Z., Jin, A. Z. (2007), Optical improvement of photonic devices fabricated by Ga + focused ion beam micromachining. *J. Vac. Sci. Technol. B* 25, 1609-1614.

## **Oxidative polymerization of tryptophan: An evidence of PCET reaction mechanism**

Meenakshi Choudhary, Samarjeet Singh Siwal, Kaushik Mallick\*

Department of Chemistry, University of Johannesburg, P.O. Box 524, Auckland Park 2006, South Africa.

E-mail: kaushikm@uj.ac.za

**Abstract:** Metal nanoparticles are of significant interest as they show exceptional electronic, optical, and catalytic properties due to their quantum size effects. Nanoparticles are currently under intensive study for applications in optical and electronic devices, sensors, bio-medical applications and as catalysts in different types of chemical reactions. The main challenge in the application of nanomaterials is agglomeration and that can be overcome through using suitable stabilizer. Polymer stabilized metal nanoparticles have attracted much attention recently as a new research direction in catalysis [1]. The polymer matrices serve both as the support as well as the stabilizer of the nanoparticles thus providing a mechanism to prevent particle agglomeration. During the synthesis of metal-polymer composite material using *in-situ* polymerization and composite formation (IPCF) technique [2], the proton and the electron are released and the charged particles are involved for proton coupled electron transfer (PCET) reaction [3]. The PCET is an important mechanistic route of charge transfer in a variety of biochemical, organic, inorganic and electrochemical reactions. The conversion of energy during photosynthesis and the respiration process also follows the PCET mechanism.

In the present investigation, we have synthesized poly-tryptophan encapsulated gold nanoparticles using an *in-situ* polymerization and composite formation method. The gold precursor (auric acid) acts as an oxidizing agent that facilitates the oxidative polymerization of tryptophan, on the other hand, the reduction of gold precursor produces gold nanoparticles. During the IPCF process, the bleaching of methylene blue colour (a reduction process) supports the evidence of a proton-coupled electron transfers reaction.

**Keywords:** poly-tryptophan, gold nanoparticles, *in-situ* polymerization and composite formation (IPCF), proton coupled electron transfer (PCET) reaction.

### **References:**

- [1] Mahato, S., Islam, R., Acharya, C., Witcomb, M., Mallick, K. (2014) ChemCatChem, 6, 1419.
- [2] Mallick, K., Witcomb, M., Erasmus, R., Strydom, A. (2009) J. Appl. Phys., 106, 074303.
- [3] Choudhary, M. Shukla, S., Islam, R., Witcomb, M., Holzapfel, C., Mallick, K. (2013) J Phys. Chem. C, 117, 23009.

# Behaviors of Ferromagnetic Shape Memory Alloy Ni–Mn–Ga under Incomplete Biaxial Loadings

E. G. Gholami,<sup>1</sup> M. Kadkhodaei<sup>1,\*</sup>

<sup>1</sup>Department of Mechanical Engineering, Isfahan University of Technology, Isfahan, 84156-83111, Iran

**Abstract:** High-frequency response (about 1000 Hz) and large reversible strain of Ferromagnetic (or magnetic) Shape Memory Alloys (FSMAs) makes them proper candidates for sensors and actuators. Although they have been usually investigated under the simultaneous application of magnetic field and mechanical stress (Halder *et al.*, 2014), recent experiments on biaxial compression of FSMAs shows that these alloys still keep their advantages under biaxial stresses (Chen *et al.*; 2014, 2013). In the present work, martensite reorientation in a single crystal tetragonal five-layered modulated martensitic (5M) Ni–Mn–Ga was experimentally studied under complete and incomplete biaxial loadings. To this end, shown in Figure 1, a special test rig was designed and manufactured to equip a uniaxial compression testing machine with apparatus for applying a constant lateral compressive load. Different dead loads were applied in the specimen's lateral direction, and stress–strain responses in the axial direction were obtained at different conditions. Quasiplastic response was seen when no lateral stress was applied, but transition to pseudoelasticity was observed by gradually increasing the constant lateral compression. Moreover, by increasing the applied lateral compressive load, higher axial stresses were shown to be required for start and finish of martensite reorientation. Interruptions were further induced in the course of loading and unloading, and the so-called strain-hardening and return point memory phenomena were observed in the alloy. Different behaviors were also seen between elastic and inelastic interruptions.

**Keywords:** Ferromagnetic shape memory alloy, Martensite reorientation, Biaxial compression, Incomplete Loading.

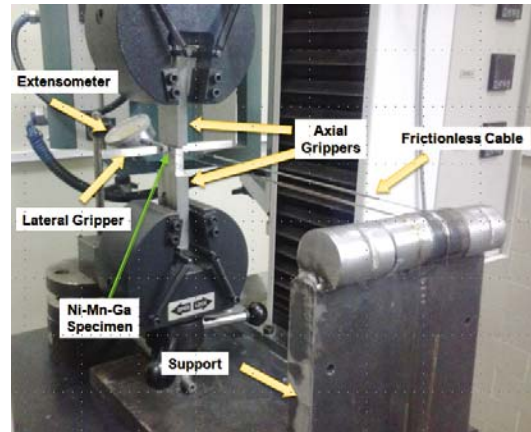


Figure 1: Special test rig for biaxial loading.

## References:

- Chen, X., Moumni, Z., He, Y., Zhang, W. (2014) A three-dimensional model of magneto-mechanical behaviors of martensite reorientation in ferromagnetic shape memory alloys, *Journal of the Mechanics and Physics of Solids*, 64, 249–286.
- Chen, X., He, Y., Moumni, Z. (2013) Twin boundary motion in NiMnGa single crystals under biaxial compression, *Materials Letters*, 90, 72–75.
- Haldar, K., Lagoudas, D. C., Karaman, I. (2014) Magnetic field-induced martensitic phase transformation in magnetic shape memory alloys: Modeling and experiments, *Journal of the Mechanics and Physics of Solids*, 69, 33–66.

# Self-powered Piezoelectric ZnO Nanowire Gas Sensor

Mohammad R. Alenezi

Public Authority for Applied Education and Training, College of Technological Studies,  
P.O. Box 42325 Shuwaikh, (Kuwait)

[Mr.alenezi@paaet.edu.kw](mailto:Mr.alenezi@paaet.edu.kw)

## Abstract:

Nanogenerators (NGs) based on the piezoelectric, triboelectric or pyroelectric effect, which can convert different forms of energy in the environment into electric energy, are great candidates to be used as an effective source of energy for nanodevices and nanosystems. There are many examples in the literature of self-powered nanosystems including self-powered pH sensors, UV sensors, self-charging power cells, small liquid crystal displays, commercial laser diodes, etc. [1]

Smart sensors, providing real-time analysis of gaseous chemical analytes, are necessary for environmental emissions monitoring, fossil fuel combustion control, medical diagnosis, artificial olfaction and homeland security. [2-5]

The output of a piezoelectric nanogenerator (PNG) fabricated based ZnO nanowire array is largely influenced by the density of the surface charge carriers at the nanowire surfaces. Adsorption of gas molecules could modify the surface carrier density through a screening effect. Thus, the output of the PNG is sensitive to the gas concentration. Based on this mechanism, the responses of an unpackaged PNG to oxygen, H<sub>2</sub>S and water vapor were studied. The fabricated PNG demonstrated sensitivity to H<sub>2</sub>S at a level as low as 100 ppm. Therefore, the generated piezoelectric signal by ZnO NWs can be treated not only as a power source, but also as a response signal to the gas, demonstrating a possible approach as a self-powered active gas sensor.

Keywords: Self-powered, Piezoelectric, ZnO, Gas Sensor, Nanowire.

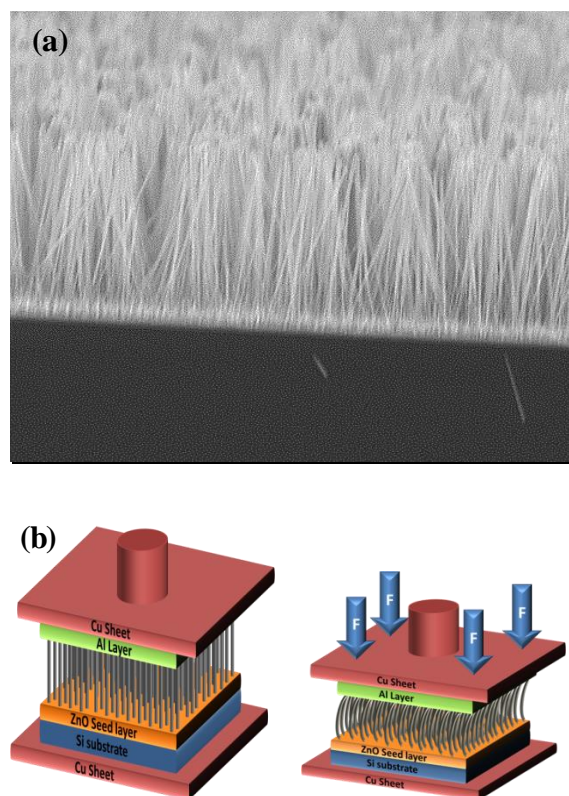


Figure 1: (a) ZnO nanowire array, (b) schematic of the fabricated PNG.

## References:

1. Z. L. Wang, *J. Phys. Condens. Matter.* **2004**, 16, 829
2. Alenezi, M. R.; Alshammari, A. S.; Jayawardena, K. D. G. I.; Beliatis, M. J.; Henley, S. J.; Silva, S. R. P. *J. Phys. Chem. C* **2013**, 117, 17850–17858.
3. Alenezi, M. R.; Abdullah S. Alshammari, Peter D. Jarowski, Talal H. Alzanki, Simon J. Henley, and S. R. P. Silva. *Langmuir*, **2014**, 30, 3913–3921.
4. Alenezi, M. R.; Henley, S. J.; Emerson, N. G.; Silva, S. R. P. *Nanoscale*, **2014**, 6, 235–247.
5. Alenezi, M. R.; Alzanki, T. H.; Almeshal, A. M.; *International Journal of Science and Research.* **2014**, 3, 588–591.

## A Smart Material for Imaging Highway Substructure Damage

Kurt Rudahl, M.S.\* and Sally E. Goldin, Ph.D.  
Department of Computer Engineering  
King Mongkut's University of Technology, Thonburi  
\* ktr@goldin-rudahl.com

**Abstract:** Roads, highways, airport runways, railways, and levees (dikes) all consist of carefully designed and built layers which ultimately rest on an earthen subbase. Over time, erosion, nearby construction, weather, seismic activity, and other causes can weaken or create gaps in the subbase. Initially there is no sign of this on the surface, until a collapse suddenly occurs. This collapse entails expenses for immediate repair, and direct and indirect costs to the surrounding communities due to disruption of transport and damage to buildings. In some cases there can be environmental damage or human casualties.

At present there is no practical way to monitor the condition of the earthen subbase. Surveys are periodically made on important roads to detect pavement distress, and railway staff are continually monitoring the state of the railway track. However, subsurface degradation or cavities which form in the subbase are not detectable from visible pavement distress. Furthermore, existing techniques such as ground-penetrating radar, which allow indirect examination of the highway structural condition, are not appropriate for routine, repeated use.

In this paper we describe a "smart" material that addresses this problem. This material can be embedded into roads and highways during construction or reconstruction. Subsequently, an easy-to-use and inexpensive sensor array can be used to verify the integrity of the highway subbase. We describe the theory and design of the material and sensor array, and the computer processing used to create the subsurface images. We then describe a simple setup for testing the material *in-vitro* in a laboratory, and present the positive results of this testing. We also describe plans for the next stages of testing, which will require incorporating the material into large-scale highway construction followed by a multi-year testing program.

**Keywords:** highway testing, road collapse, subsurface imaging, smart material

## **Soil Cement Interlocking Block: An Alternative Solution to the Reduction of Impacts from Brick-making Industries**

**Mr. Gyanendra Sthapit and Ms. Sudiksha Amatya**

Director of Habitech Center and Architect of AIT Consulting, Asian Institute of Technology, Thailand

### **Abstract:**

The rapid urbanization in many developing countries is demanding for sustainable solutions for affordable and social housing for the masses, as well as the higher-end housing needs meet by the commercial developer, through tall buildings. The solution should be not only affordable, but also use material and technology that favors environmental sustainability and health impact, disaster resilience and local adaptability.

This paper presents one of the alternate solution, Soil Cement Interlocking Block developed and applied to various housing needs in the region by the Habitech Center at Asian Institute of Technology, Thailand. The block is modular type and uses locally available soil and other materials which has been effectively used for Residential, School, Medical Clinics, Offices and Resort Buildings and other community based projects in many countries in Asia and Africa. The block doesn't go through any burning process nor uses any fuel which eliminates any type of gas production during entire process of manufacture. They can be manufactured at or close to the site, eliminating in need for transportation. Production process is very simple and can be used by any unskilled labor with little training. Laterite soils are mixed with a part of cement and little water is added to the mixer and then compressed with manual or hydraulic press. After 24 hours of air-curing and 3 weeks of water-curing, the bricks are ready to use for construction.

These aspects considerably improve the environmental sustainability and health impact. The blocks are put together using a dry process, reducing the water demand. The robust nature of the interlocking mechanisms provide a robust construction and the system has been used effectively for the Post-Tsunami and hurricane relief shelter as well as permanent housing. The lower cost of the block makes it affordable, without reducing the quality or durability. The block is being improved and enhanced continuously for various innovative application through research and development.

**Keywords:** Soil Cement Interlocking Block, Environmental Sustainability and Health impact, Disaster resilience, Local adaptability, Affordable, Social and Permanent Housing

# Strength and Ductility of SGFRP Confined Concrete

Q. Hussain,<sup>1</sup> A. Pimanmas<sup>2\*</sup>

<sup>1</sup>Graduate Student, Sirindhorn International Institute of Technology, Thammasat University

<sup>2</sup>Associate Professor, Sirindhorn International Institute of Technology, Thammasat University

\*Corresponding author email: amom@siit.tu.ac.th

**Abstract:** During last decade, external confinement of concrete using different uni-directional fiber reinforced polymer composites (FRP) is proved successful to enhance strength and ductility of concrete. FRP are high strength and low weight compared with steel and concrete. In contrast to the uni-directional FRP composites, sprayed glass fiber reinforced polymer composites (SGFRP) are comprised of randomly distributed chopped fibers. In SGFRP, the fibers are sprayed using spraying and pumping equipment (Figure 1).

In this study the behavior of concrete confined with SGFRP is evaluated in terms of strength and ductility enhancement. Both circular and square concrete cylinders externally strengthened with different SGFRP thickness were investigated. Further, the effect of length of chopped fibers in SGFRP was also examined on strength and ductility of confined concrete. Total 24 concrete cylinders were tested under axial compression loading. All SGFRP confined and control specimens were loaded to failure. The response of loaded specimens were investigated both in axial and transverse direction. The experimental investigations clearly show that sprayed glass fiber reinforced polymer composites are significantly effective to enhance strength of concrete. The external confined with SGFRP is also resulted into increased ductility of confined concrete. There is found momentous increase in load carrying capacity and ductility with increasing thickness of SGFRP. However increase in strength and ductility is more significant for circular specimens compared with square.

**Keywords:** sprayed glass fibers, strength, ductility concrete, confinement.



Figure 1: Figure showing the pumping and spraying equipment for sprayed glass fiber reinforced polymer composites (SGFRP).

# A facile one-step method to produce nanocrystallites BiFeO<sub>3</sub>-Graphene composite: as a promising energy transfer material

M. Dewan,<sup>1\*</sup> and S. Ram,<sup>1</sup>

<sup>1</sup>Materials Science Centre, Indian Institute of Technology, Kharagpur-721 302, India

**Abstract:** Graphene (GR) has become a most promising material in the field of material science recent years. Due to its unique planar structure, excellent transparency, superior electron conductivity, mobility, high specific surface area and high chemical stability, GR is regarded as an ideal high performance candidate to prepare GR-based nanocomposites for energy storage and conversion (Zhang et al., 2012). In addition, GR also has excellent optical properties (Singh et al., 2011). It could be used with nanoparticles to form GR-nanoparticles composites and as a high quality coating materials to enhance the performances in the fields of photocatalysts and fuel cells (Liang et al., 2011 and Li et al., 2013). BiFeO<sub>3</sub> based photocatalysts are highly responsive to visible light and exhibit higher photocatalytic efficiency in the visible range as compared with TiO<sub>2</sub> based photocatalysts (Gao et al., 2011). Here GR has been incorporated with BiFeO<sub>3</sub> for the improvement of photocatalytic and photovoltaic activity. In these graphene-photocatalyst composites, photogenerated electrons can be readily captured by graphene layer which acts as electron acceptor, thus more photogenerated holes are increasingly available for the photocatalytic reactions. Also it reduces the recombination rate of electron-hole pairs due to its high charge mobility and high electric conductivity (Stengl et al., 2011). Up to now, the BiFeO<sub>3</sub>-GR composites are often prepared by introducing BiFeO<sub>3</sub> precursors into the dispersed aqueous of graphene or graphene oxide, followed by two-step hydrothermal reaction (Li et al., 2013). In this study, nanocrystallites BiFeO<sub>3</sub> are prepared by a one-step hydrothermal reaction with an organic carbon source of glycine, where BiFeO<sub>3</sub> nanocrystallites are densely embedded with graphene sheet or a graphene like surface layer. TEM observation demonstrates that the GR-BiFeO<sub>3</sub> consisted of single-layer 2D graphene sheets decorated with nanocrystallites BiFeO<sub>3</sub> (Figure 1) and HRTEM also shows good crystallinity with clear lattice fringes. Phonon bands and photoluminescence spectra incur in support of the chemical bonding between graphene and nanocrystallites BiFeO<sub>3</sub> by the formation of Fe-O-C bonds. The band gaps of the GR-BiFeO<sub>3</sub> composites could be successfully tuned to 2.0 eV, which makes it a potential material towards solar applications. The composite shows moderately effective to

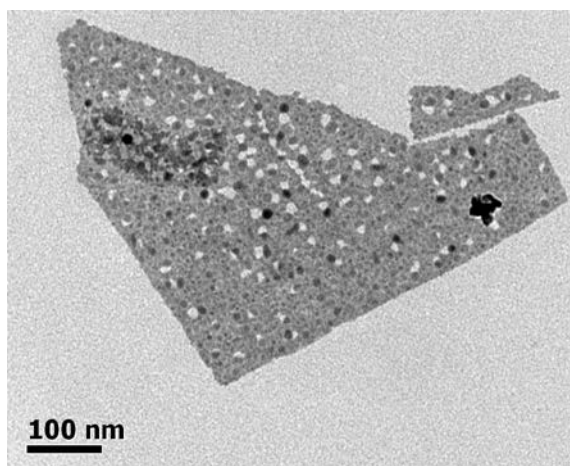


Figure 1: TEM image of a GR-BiFeO<sub>3</sub> sheet with densely embedded with nanocrystallites BiFeO<sub>3</sub>

generate clean H<sub>2</sub> energy by photocatalytic water splitting. This information coupled with the cost efficient synthesis process may lead to the fabrication of new devices for harvesting solar energy and other optoelectronic purposes.

Keywords: Bismuth ferrite, Graphene, hydrothermal synthesis, Photocatalytic activity

## References:

- Zhang N., Zhang Y. and Xu Y-J, *Nanoscale*, 2012, 4, 5792.
- Singh V., Joung D., Zhai L., Das S., Khondaker SI, Seal S., *Prog. Mater. Sci.* 2011,56, 1178-1271.
- Li Z., Shen Y., Yang C., *J. Mater. Chem. A*, 2013, 1, 823-829.
- Liang Y., Li Y., Wang H., *Nat. Mater.*, 2011, 10, 780-786.
- Gao F., Chen X. Y., Yin K. B., Dong S., Ren Z. F., Yuan F., Yu T., Zou Z. and Liu J. M., *Adv. Mater.*, 2011, 19, 2889.
- Stengl V., Popelkova D. and Vlácil P., *J. Phys. Chem. C*, 2011,115, 25209-25218.
- Li T., Shen J., Li N., and Ye M., *Mater. Lett.*, 2013, 91, 42-44.

## Synthesis and luminescent features of CaZrO<sub>3</sub> nanophosphors

B. Evangeline, P. Abdul Azeem  
Department of Physics  
National Institute of Technology,  
Warangal-506004, A.P., India.  
Email:drazeeem2002@gmail.com

**Abstract:** CaZrO<sub>3</sub> nanophosphors were synthesized by a citrate based sol-gel method using citric acid as chelating agent. The prepared powders were annealed at different temperatures i.e. 600°C, 700°C, 800 °C and 900 °C. The powders were characterized by X-ray Diffraction (XRD), Field Emission Scanning Electron Microscope (FE-SEM), Fourier Transform Infrared (FTIR) and Photoluminescence (PL) spectroscopic techniques to study the structural and optical properties and comparative studies were made to optimize the temperature. The XRD pattern shows broad peaks indicating nano crystalline nature of the samples and well resolved peaks were obtained at 900 °C with orthorhombic structure. The FTIR spectrum confirms the presence of functional groups related to metal oxide and inorganic molecular groups. FE-SEM images shows agglomerated nature with irregular morphology and non-uniform particle size distribution. The average size of the particles is 85 nm for the samples annealed at 900 °C. The samples were excited with 241nm and the emission spectra at 900 °C revealed a broad band having its maximum intensity at 399 nm. The CIE chromaticity coordinates were also calculated from emission spectrum for the sample annealed at 900° C (x = 0.151 and y = 0.112). By the above studies the desired CaZrO<sub>3</sub> is obtained at 900 °C and the results indicate that the prepared sample is suitable material for application in UV LEDs.

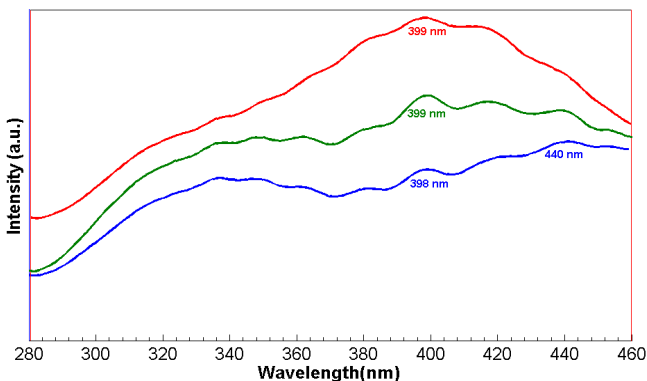


Fig (i) Photoluminescence spectrum of CaZrO<sub>3</sub> annealed at 600°C, 700°C, 800 °C and 900 °C

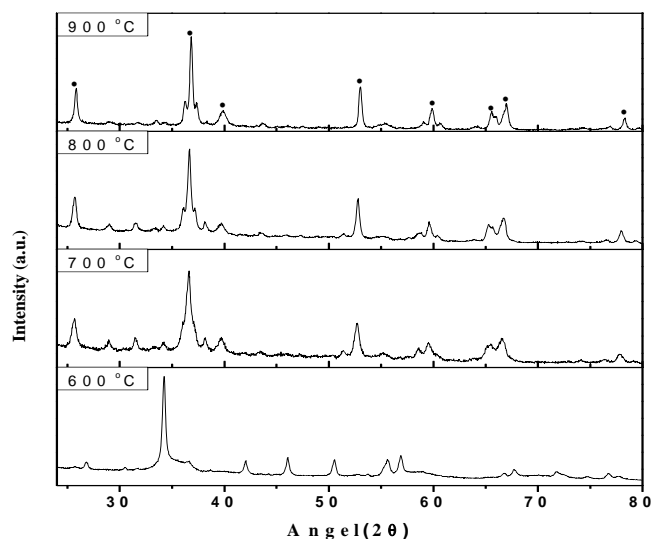


Fig (ii) XRD pattern CaZrO<sub>3</sub> annealed at 600 °C, at 700 °C, 800 °C and 900 °C

### References

- [1] Hongwu Zhanga, Xiaoyan Fub, Shuyun Niub, Qin Xina, Blue luminescence of nanocrystalline CaZrO<sub>3</sub>:Tm phosphors, synthesized by a modified Pechini sol-gel method, Journal of Luminescence 2008;128, 1348–1352.
- [2] V.H. Romero, E. De la Rosa, P. Salas, J.J. Vela´zquez-Salazar. Strong blue and white photoluminescence emission of BaZrO<sub>3</sub> undoped and lanthanide doped phosphor for light emitting diodes application, Journal of Solid State Chemistry 2012;196, 243–24
- [3] D.V. Sunitha, H. Nagabhushana, S.C. Sharma, B.M. Nagabhushana, B. Daruka Prasad, R.P.S. Chakradhar, Study on low temperature solution combustion synthesized Sr<sub>2</sub>SiO<sub>4</sub>:Dy<sup>3+</sup> nano phosphor for white LED, Spectrochimica Acta Part A: Molecular and Biomolecular Spectroscopy 2014;127, 381–387.
- [4] P. Stoch, J. Szczerba, J. Lis, D. Madej, Z. P. edzich. Crystal structure and *ab initio* calculations of CaZrO<sub>3</sub>, Journal of the European Ceramic Society, 2012;32, 665–670.

# Advanced energy and environmental materials concepts from silicon carbide and graphene

M. Syväjärvi,<sup>1,2,\*</sup>

<sup>1</sup> Linköping University, Department of Physics, Chemistry and Biology, Linköping, Sweden

<sup>2</sup> Graphensic AB, Mjärdevi Science Park, Linköping, Sweden

\* mikael.syvajarvi@ifm.liu.se

**Abstract:** Silicon carbide emerged in beginning of 1990's as a promising material for electronics, in particular high power and high frequency applications. The SiC boule growth was developed to manage the macroscopic defect control, and progress in substrates in hexagonal polytypes made wafers to become commercially available. Still there exist defects in wafers but on a level with substantially reduced impact in comparison to the macroscopic defects that were initially present.

Silicon carbide is now emerging in optoelectronics applications. In 2006, 6H-SiC was shown to be a very efficient material for white light emitting diodes (Kamiyama *et al*; 2006). In this technology, the critical challenge is in control of the fluorescent properties of silicon carbide (Syväjärvi *et al*; 2012). The combination of nitrogen and boron doping in a thick layer, and nitrogen and aluminum doping in a second layer, produces a combination of white light that has a high color rendering index (Kamiyama *et al*; 2011). Also, it is a monolithic semiconductor structure that does not use phosphor and rare earth metals.

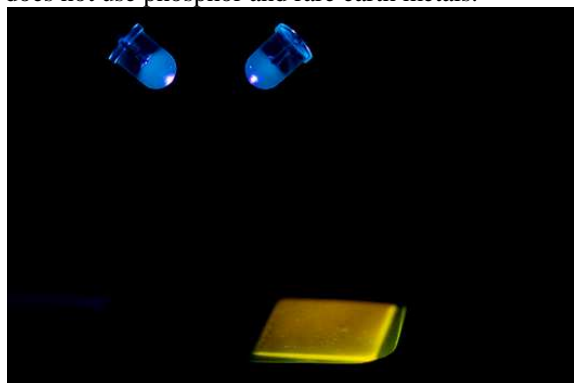


Figure 1: Fluorescent silicon carbide excited by two near UV LEDs.

The cubic silicon carbide is a challenging material to grow, but has very interesting concept for high efficiency photovoltaics based on the intermediate bandgap theory (Syväjärvi 2012). The material is metastable and challenging to fabricate in high quality. A main issues has been the lack of 3C-SiC substrates. Recently we have developed a method that makes it possible to grow high quality cubic silicon carbide as bulk material. Freestanding material have been produced, and can now be applied as substrate in various epitaxial approaches.

Finally, graphene on silicon carbide has demonstrated the possibility to produce large area high quality

graphene. While the graphene may not be transferred, there are a number of applications where the silicon carbide has advantages. In electrochemistry, the solvents may cause that the graphene flakes or graphene transferred from metal substrates floats away from the substrate. This is not the case in graphene on silicon carbide since the graphene forms from the carbon atoms in the silicon carbide and is bound to the SiC substrate. In addition, the silicon carbide processing experience may be applied to produce structures and tailor electrodes. Therefore, the graphene on silicon carbide is highly interesting as electrode material in biofuels cells, and in biosensor applications.

In this paper we will overview the silicon carbide history and describe the new materials sciences in optoelectronics and graphene.

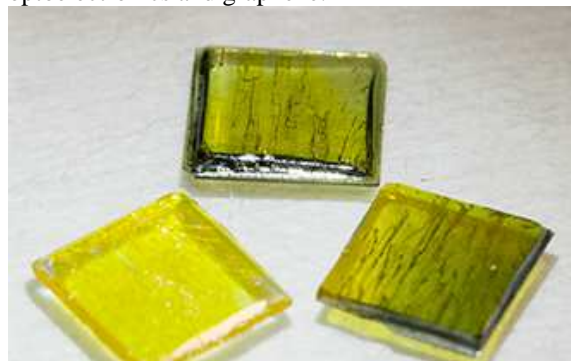


Figure 2: Free standing cubic silicon carbide substrates.

Keywords: energy materials, optoelectronics, biofuels cells, new materials, graphene, biosensors.

## References:

Kamiyama, S. *et al* (2006), Extremely high quantum efficiency of donor-acceptor-pair emission in N-and-B-doped 6H-SiC, *J. Appl. Phys.* 99, 93108.

Kamiyama, S. *et al* (2011), Fluorescent SiC and its application to white light-emitting diodes", *J. Semiconductors* 32, 13004.

Syväjärvi, M. *et al* (2012), Fluorescent SiC as new material for white LEDs, *Physica Scripta* T148, 14002.

Syväjärvi, M. (2012), Perspectives of fluorescent and cubic silicon carbide, *Adv. Mat. Lett.* 3, 175

# Role of surface and deep-level defects on the emission and degradation of phosphor materials

H. C. Swart\*, Vinod Kumar, Vijay Kumar, S. Som, A. Pandey, J. J. Terblans, O. M. Ntwaeaborwa, E. Coetsee and R.E. Kroon

Department of Physics, University of the Free State, Bloemfontein, ZA9300, South Africa

**Abstract:** Luminescent compounds and materials have numerous uses, most notably in detectors of various sorts, but also in consumer products such as displays, light emitting diode (LED) lighting and watches. The emission properties, whether of a fast decay rate fluorescent material or a slow decay rate phosphorescent material, are defined by the chemical composition and the physical structure of the luminescent material [1]. Surface characterization techniques play a vital role in the complete understanding of the luminescent properties of phosphor materials. Zinc oxide (ZnO) nanophosphors were synthesized with different techniques for UV, blue, green, red and near white light emission applications. X-ray photo electron spectroscopy (XPS) indicated that the O1s peak consists of three different components. These were O1 (oxide) and O2 (deficient oxygen; OH groups) and O3 (chemisorbed species). All samples showed near band edge (NBE) and defect level emission (DLE). The DLE enhancement was due to the increase in oxygen related defects such as oxygen vacancies/interstitials. Different defect level emissions that varied from the blue to red visible range were observed. Due to the combination of the NBE and DLE, near white light emission was observed in some cases [1]. The emission could be tuned by varying preparation parameters such as different ultrasonic times, combustion temperatures, dopant concentration and different precursors. Figure 1 illustrating the tunability of the colour obtained from ZnO after different preparation conditions as indicated: The defect emission wavelengths have changed and so was the colour on the CIE coordinate diagram. Auger electron spectroscopy (AES) and cathodoluminescence (CL) both excited by the same electron beam, were used to monitor changes in surface composition and luminous efficiency during electron bombardment of different phosphor materials. Degradation was manifested by a non-luminescent ZnO layer that formed on the surface of ZnS phosphors according to electron stimulated surface chemical reactions (ESSCRs). By comparing the experimental and Monte Carlo simulation results, it is predicted that a diffusion interface forms between the ZnO layer and the ZnS bulk that broadens during the degradation process. Due to the formation of defects and the dissociation of the ZnS at the diffusion interface the region is non-luminescent [2]. Figure 2 illustrating the defect and non luminescent layer that formed during the electron bombardment.

**Keywords:** ESSCR, defect emission, ZnO, ZnS, degradation.

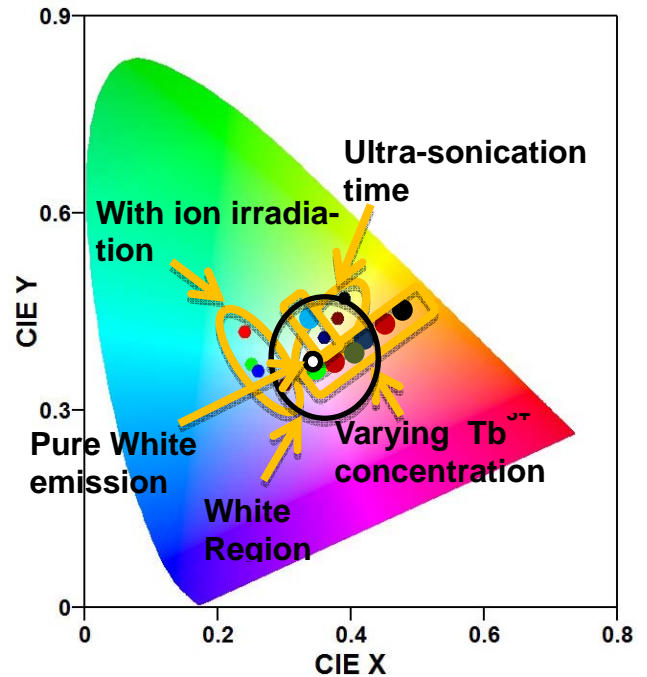


Figure 1: Figure illustrating the tunability of the colour obtained from ZnO after different preparation conditions as indicated:

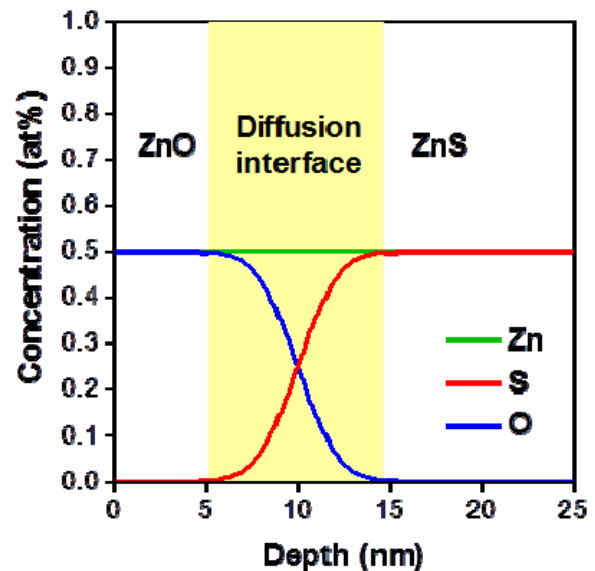


Figure 2: Figure illustrating the defect and non luminescent layer that formed during electron bombardment of ZnS.

## References:

- [1] Vinod Kumar et al. *Materials Letters*. 110(15) (2013) 57
- [2] SH Chen et al. *J. of Luminescence*. 113/3-4 (2005) 191

# DFT-based Ising model for the simulation of Au-Pd structure under reaction conditions

H. Guesmi,<sup>\*a</sup> B. Zhu,<sup>a</sup> C. Mottet,<sup>b</sup> J. Creuze,<sup>c</sup> B. Legrand<sup>d</sup>

<sup>a</sup> ICG, équipe MACS UMR 5253, 8 rue de l'Ecole Normale 34296, Montpellier, France

<sup>b</sup> CINAM UMR 7325, Campus de Luminy 13288 Marseille, France

<sup>c</sup> ICMMO, LEMHE Bâtiment 410, Université Paris-Sud, 91405 Orsay, France

<sup>d</sup> CEA, Service de Recherches de Métallurgie Physique, Saclay, France

**Abstract:** Gold-based nanoalloys (or gold alloy nanoparticles) are attracting growing attention due to their specific properties as optical, catalytic and electro-catalytic materials. In heterogeneous catalysis, bimetallic gold nanoparticles have shown high reactivity in a number of catalytic reactions including the direct synthesis of hydrogen peroxide from H<sub>2</sub> and O<sub>2</sub>, synthesis of vinyl acetate, selective hydrogenation of butadiene and so forth. In the context of CO reforming, recent experiments on gold nanoparticles with different Ni contents show an improvement of the CO oxidation rate. Palladium and platinum also emerge as good candidates for the enhancement of such reaction.

Surface structures, compositions and segregation properties of nanoalloys are of prior interest as they are important in determining chemical reactivity and especially catalytic activity. Moreover, the adsorbate-induced segregation of metal alloys under the reaction conditions and thus the changes in local atomic composition and surface structure have been predicted and demonstrated to occur for a number of gold alloy systems [1]. In particular, for Au-Pd nanoalloys although the gold surface enrichment is predicted to be thermodynamically favourable under vacuum conditions, a reversed segregation of Pd as a more active component to the surface is reported to occur in the presence of adsorbates [2-4].

The aim of our theoretical work is to develop an accurate approach able to model the surface of alloys and their change during reaction conditions. Such approach should allow as the knowledge of both the molecular coverage (O<sub>2</sub> or CO) and the surface concentration of the AuPd alloy depending on the partial pressure and the bulk concentration of the alloy at given temperatures. To reach this goal we derive an effective Ising model [5] in which the energetic parameters (segregation enthalpies and metal-metal pair interactions, both in the infinite dilute limits) are obtained after relaxations at T=0 K, via DFT calculations (instead of the commonly used Tight Bonding potential). In addition, DFT calculations of the adsorption energies ( $E_{ads}$ ) of CO on flat surfaces of Au, Pd and Au-Pd alloys with various Pd surface concentrations and CO coverage were performed. Then we fitted two effective pair potentials according to these energies for CO-metal interaction and CO-CO interaction respectively. This allows us to run Monte

Carlo simulations within the semi-grand canonical ensemble and to get the segregation-adsorption isotherms under CO pressure (Figure 1).

**Keywords:** Heterogeneous catalysis, DFT, nanoalloys, segregation, reactive gas, Ising model, Monte Carlo.

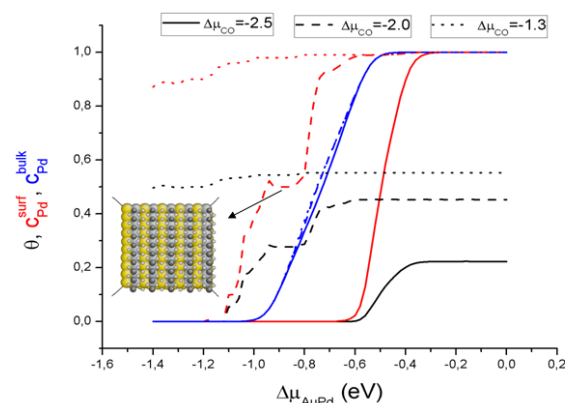


Figure 1: Isotherms of CO/AuPd(100) at 300K.

The molecular coverage (CO) and the surface concentration of the AuPd alloy depending on the partial pressure and the bulk concentration

## References:

- [1] H. Guesmi, Gold Bulletin, **46** (2013) 213-219
- [2] H. Guesmi, C. Louis, L. Delannoy, Chem. Phys. Lett., **503** (2011) 97
- [3] A. Dhouib, H. Guesmi, Chem. Phys. Lett., **521** (2012) 98.
- [4] B. Zhu, G. Thirumurthu, L. Delannoy, C. Louis, C. Mottet, J. Creuze, B. Legrand and H. Guesmi, J. Catal., **308** (2013) 272-281.
- [5] V. Moreno, J. Creuze, F. Berthier, C. Mottet, G. Tréglia, B. Legrand, Surf. Sci., **600** (2006) 22.

# Preparation of SiO<sub>2</sub>/PVA mesoporous and its sintered functional silica glass

Shigeru Fujino and Hiroshi Ikeda

Kyushu university, 6-1 Kasuga, Fukuoka, Japan  
[fujino@astec.kyushu-u.ac.jp](mailto:fujino@astec.kyushu-u.ac.jp)

## Abstract

A preparation process of a monolithic mesoporous for a silica glass precursor was developed. A (100-x)SiO<sub>2</sub>-xPVA suspension was prepared using SiO<sub>2</sub> nanoparticles, poly(vinyl alcohol) (PVA), and water adjusted to pH 2–8. Subsequently, the suspension was dried to form a SiO<sub>2</sub>-PVA nanocomposite. The dispersion or aggregation state of the SiO<sub>2</sub> nanoparticles and PVA in the suspension was controlled by the amount of PVA and the pH value. The suspension, of which the composition was x=20 with below pH 3, was preferred to aggregation of the SiO<sub>2</sub> nanoparticles and PVA because of the hydrogen bond, resulting in fabrication of the monolithic nanocomposite without cracks after drying the suspension. The samples show mesoporous structure by TEM[1]

To obtain monolithic transparent silica glass by sintering SiO<sub>2</sub> nanoparticles, we prepare an SiO<sub>2</sub>/PVA nanocomposite. We demonstrated fabrication of submicron patterns on silica glass by room-temperature imprinting method. Micropatterns on the nanocomposite are fabricated by imprinting a mold at room temperature for 5 MPa in air atmosphere. The nanocomposite has a strong network made of hydrogen bonding interactions between the silanol groups of SiO<sub>2</sub> nanoparticles and the hydroxyl groups of PVA. This strong network structure prevents destruction of the nanocomposite due to compressive stress during imprinting. After sintering the nanocomposite at 1100 °C, micropatterned silica glass is obtained[2]. The process described, herein, provides an attractive, low-temperature alternative to fabricate micropatterns on silica glass. Nano metals can be printed on the surface or inside of nano composite and can form circuit pattern by co-sintering. Thus circuit on glass can be formed[3]. These various application concepts will be created and verified such as printable photoelectronics

## References

- [1] H. Ikeda, S. Fujino, and T. Kajiwara, "Preparation of SiO<sub>2</sub>-PVA Nanocomposite and Monolithic Transparent Silica Glass by Sintering," *J. Ceram. Soc. Jpn.*, 119[1] (2011) 65–69.
- [2] H. Ikeda, S. Fujino, and T. Kajiwara, "Fabrication of Micropatterns on Silica Glass by a Room-Temperature Imprinting Method," *J. Am. Ceram. Soc.*, 94[8] (2011)2319–2322.
- [3] H. Ikeda, S. Fujino, and T. Kajiwara, "Fabrication of Au Nanoparticles Doped Bulk Silica Glass by using SiO<sub>2</sub>-PVA Nanocomposite," *J. Ceram. Soc. Jpn.*, 120[1402] (2012)238–242.

# Polyoxometallate-surfactant hybrid photocatalysts coupled with light antennas

Tetsuya Kida<sup>a</sup>, Hiromasa Furuso<sup>b</sup>, Kota Kumamoto<sup>b</sup>, Masayoshi Yuasa<sup>a</sup>, and Kengo Shimano<sup>e</sup>

<sup>a</sup>Department of Energy and Material Sciences, Faculty of Engineering Sciences, Kyushu University, Kasuga, Fukuoka 816-8580, Japan

<sup>b</sup>Department of Molecular and Material Sciences, Interdisciplinary Graduate School of Engineering Sciences, Kyushu University, Kasuga, Fukuoka 816-8580, Japan

[kida@mm.kyushu-u.ac.jp](mailto:kida@mm.kyushu-u.ac.jp)

## Abstract

Using photocatalysts to reduce metal ions and recover noble metals has been recognized as a green process. One of the major photocatalysts is heterogeneous  $\text{TiO}_2$ . However, noble metal particles reduced by  $\text{TiO}_2$  particles cover the surface of the photocatalyst during photo-recovery processes, which leads to poisoning of the photocatalytic activity. Furthermore,  $\text{TiO}_2$  can utilize only UV light, which limits the photo-recovery under sunlight. In this study, we propose a photo-recovery of noble metal ions from solution using a polyoxometalate (POM) as a homogenous catalyst. Using an inorganic-organic hybrid photocatalyst based on  $\alpha\text{-SiW}_{12}\text{O}_{40}^{4-}$  coupled with a cationic surfactant, the photocatalyst can be dissolved in the organic phase and metal ions can be reduced at the aqueous/organic interface to produce metal particles, as shown in Fig.1. In this study, in order to improve the reduction activity, the photocatalyst was coupled with a light antenna that can absorb visible light. We confirmed that under visible light irradiation ( $\lambda > 420 \text{ nm}$ ), the concentration of  $\text{AuCl}_4^-$  were decreased as gold particles produced at the interface, as shown Fig.2.

## References

- [1] T. Kida, H. Matsufuji, M. Yuasa, and K. Shimano, *Langmuir*, **29** (2013) 2128.  
 [2] T. Triantis, E. Gkika, G. Alexakos, N. Boukos, E. Papaconstantinou, and A. Hiskia. *Catalysis today*, **144** (2009) 2.

## Figures

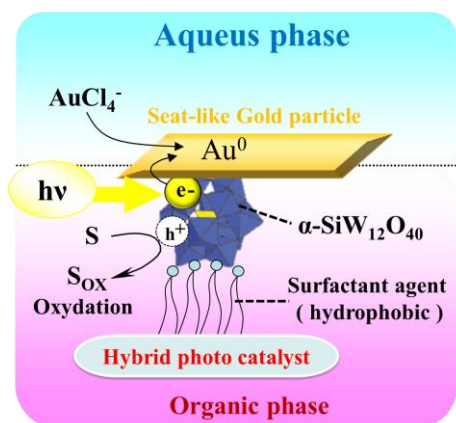


Fig. 1 Photo-recovery process using an  $\alpha\text{-SiW}_{12}\text{O}_{40}$ -surfactant hybrid photocatalyst.

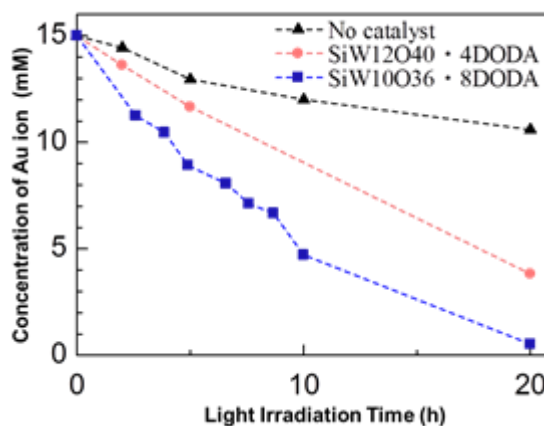


Fig. 2 Changes in  $\text{AuCl}_4^-$  concentration in the aqueous phase under visible light irradiation ( $\lambda > 420 \text{ nm}$ )

# Interfacial role of Cesium in Prussian Blue Films

J. Agrisuelas<sup>1</sup>, R. Catalán<sup>1</sup>, C. Delgado<sup>1</sup>, J. J. García-Jareño<sup>1</sup>, A. F. Roig<sup>2</sup>, F. Vicente<sup>1</sup>.

<sup>1</sup>Department of Physical Chemistry. University of Valencia. C/. Dr. Moliner,50. 46100-Burjassot (Spain)

<sup>2</sup>Department of Analytical and Physical Chemistry. UJI, Avda. Sos Baina, s/n.Castelló (Spain)

**Abstract:** Hexacyanometallate-like materials have raised intense interests because of their electrocatalytic, electrochromic, ion-exchange, ion-sensing or photomagnetic properties. Nano-electrogravimetric measures during the electrochemical stabilization process of Prussian Blue (PB) in CsCl aqueous solution yields interesting information about the insertion role of the Cs into the crystalline structure through the interfacial regions (García-Jareño *et al.*, 2003). In addition to the intrinsic scientific interest of this topic, many works have suggested that hexacyanoferrate compounds can be used as precipitants for cesium removal from aqueous radioactive wastes (Thammawong *et al.*, 2013). This work was carried out by means of simultaneous measurements of resonant frequency of quartz as well as the motional resistance of the Butterworth-Van Dyke equivalent circuit model measured by means of an electrochemical quartz crystal microbalance (R-EQCM) during successive cyclic voltammograms. The simultaneous measure of current, mass and motional resistance magnitudes allows to explain the differences between the electrochemical cation insertion processes in a solution of CsCl salt with respect to the cation insertion observed in KCl aqueous solutions (J.J. García-Jareño *et al.*, 1998). Accordingly, the main goal of this work was to study in depth the different processes which involve the PB electrochemistry during the PB $\leftrightarrow$ ES switch, where ES is the reduced form (Everitt's salt).

Cesium counterions show two different sites for their insertion: one located into the crystalline framework and other into ferrocyanide vacancies. PB deposits were voltammetrically cycled or only immersed in CsCl aqueous solutions. In both cases, their respective motional resistances  $R$  increase about 300  $\Omega$ . Simultaneously, a decrease in the resonance frequency is also recorded, suggesting that in both cases a spontaneous entrance of Cs should be considered. Then, two different types of cesium exchange are postulated: one associated to the electrochemical reaction during the first scan, (Figure 1), and another spontaneous non-stoichiometric entrance where the Cs is located inside the inner water cluster. This means that a part of the water molecules are expelled from the cluster and consequently the film loses electrical conductance as well as their mechanical rigidity increases.

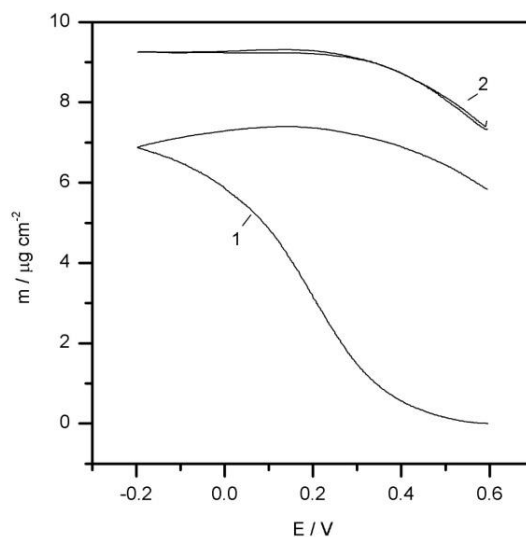


Figure 1. Mass variation during voltammograms of the PB $\leftrightarrow$ ES switch (Au electrode, surface area 20.02 mm<sup>2</sup>) in 0.5 M CsCl (pH = 2.7); reference electrode Ag/AgCl/KCl (sat),  $v = 20 \text{ mV s}^{-1}$ ,  $T = 26.2 \text{ }^\circ\text{C}$ . 1 is the first cycle; and 2 is the ninth cycle.

**Keywords:** smart material, Prussian Blue, motional resistance, cesium removal, electrochemical microbalance, interfacial region, ion insertion.

**Acknowledgements:** Part of this work was supported by CICYT project FEDER-CTQ2011-28973/BQU. J. Agrisuelas acknowledges his position to the *Ajuntament de Valencia*.

## References:

- J.J. García-Jareño, D. Giménez-Romero, F. Vicente, C. Gabrielli, M. Keddad, H. Perrrot (2003). EIS and ac-electrogravimetry study of PB films in KCl, NaCl and CsCl solutions. *J. Phys. Chem. B* 107, 11321-11330.
- C.Thammawong, P. Opaprakasit, P. Tangboribonrat, P. Sreerunothai (2013). PB-coated magnetic nanoparticles for removal of cesium from contaminated environment. *Journal of Nanoparticles Research* 15 1689.
- J. García-Jareño, J. Navarro-Laboulais, A. Sanmatias, F. Vicente (1998). The correlation between electrochemical impedance spectra and voltammograms of PB films in NH<sub>4</sub>Cl and CsCl aqueous solutions, *Electrochim. Acta*, 43 1045-1052.

# X-ray Photoemission Spectroscopy Study of (3-mercaptopropyl)trimethoxysilane and n-propyltriethoxysilane on Rutile TiO<sub>2</sub> (110)

S. Chaudhary,<sup>1</sup> A. R. Head,<sup>1</sup> J. Schnadt<sup>1</sup>

<sup>1</sup>Division of Synchrotron Radiation Research, Lund University, Box 118, 221 00 Lund, Sweden

**Abstract:** Organo-silane terminated oxide surfaces are being used in semiconductor devices, biosensors and dye sensitized solar cells. Titanium dioxide is one of the widely studied oxide surfaces for model systems due to its wide range of properties (Diebold *et al.* 2003). We have studied the adsorption of two silane coupling agents, (3-mercaptopropyl) trimethoxysilane (MPTMS) and n-propyltriethoxysilane (PTES) (Figure 1), on rutile TiO<sub>2</sub>(110) using X-ray photoelectron spectroscopy (XPS). The molecular thin films were deposited by chemical vapour deposition and the doses were defined in Langmuirs (1 L= 10<sup>-6</sup> Torr × sec). Presence of S 2p (in case of MPTMS) and Si 2p spectra (both in MPTMS and PTES) confirms the adsorption of molecules. The coverage calculated with respect to attenuation of titanium signal for MPTMS is 0.55 for 121 L whereas for PTES the coverage for 111 L is 0.90. The line shapes of C 1s core level reflects that both PTES and MPTES binds dissociatively on TiO<sub>2</sub> surface. The intensity ratios for chemically different carbons were found to be different from the molecular form of molecules. Angle dependent XPS measurements on MPTES suggest the thiol group is pointing away from the surface, whereas in the case of PTES, the propyl chain is found to be more towards the surface compared to methoxy groups. Temperature programmed XPS measurements suggest that the oxy groups of both molecules desorb from the surface at 550 K, which is in accordance with literature (Gamble *et al.*, 1993). The present study can provide information on how silane coupling agents bind and their molecular orientation on oxide surfaces.

**Keywords:** (3-Mercaptopropyl) trimethoxysilane, n-propyltriethoxysilane, Molecular film, metal oxide chemical vapor deposition, X-ray photoelectron spectroscopy.

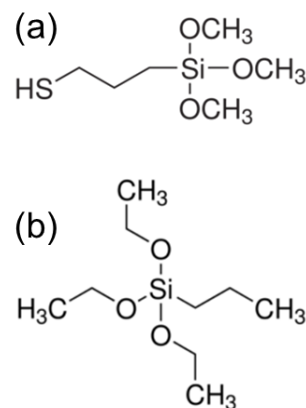


Figure 2: Schematic of silane coupling molecules: (a) (3-mercaptopropyl) trimethoxysilane (b) n-propyltriethoxysilane ..

## References:

- Gamble, L., Hugenschmidt, M. B., Campbell, C. T., Teresa Jurgens, A., and Rogers, J. W. Jr. (1993), Adsorption and Reactions of Tetraethoxysilane (TEOS) on Clean and Water-Dosed Titanium Dioxide (110), *J. Am. Chem. Soc.*, 115, 12096-12105.
- Diebold, U. (2003), The surface science of titanium dioxide, *Surf. Sci. Rep.* 48, 53.

# Smooth Polydimethylsiloxane Brush Surfaces Showing Unusual Dynamic Dewetting Behavior

A. Hozumi, D. F. Cheng, C. Urata, B. Masheder

National Institute of Advanced Industrial Science and Technology (AIST)  
2266-98 Anagahora, Shimoshidami, Nagoya 463-8560, Japan.  
[a.hozumi@aist.go.jp](mailto:a.hozumi@aist.go.jp)

## Abstract

Improvement of liquid droplet motion on various solid surfaces is a key factor in a wide variety of advanced applications, such as microfluidics, micro-/nano-electromechanical systems (MEMS/NEMS), self-cleaning surfaces and window coatings. In the ongoing effort to control the motion of liquid droplets on solid surfaces, dynamic contact angles (CAs) and tilt angles (TAs) rather than static CAs ( $\theta_s$ ) are more useful because the latter only provides information about the general surface energy of the solid surface. To understand the actual surface hydrophobicity and the ease of liquid droplet mobility on tilted solid surfaces, it is necessary to estimate the dynamic dewetting behavior (both TAs and CA hysteresis (difference between the advancing ( $\theta_A$ ) and the receding ( $\theta_R$ ) CAs)) [1].

In this study, we report a simple and effective principle to regulate the ease of mobility of liquid droplets on tilted surfaces. Vinyl-terminated polydimethylsiloxane (PDMS) with six different molecular weights (MWs) were grafted to hydride-covered Si wafers to form chemically- and topographically-identical polymer melt brush films. In the case of low MW PDMS (MW 6000), the resulting brush film surface was considerably flat (Figure1) and showed a liquid-like nature because of the high mobility of the surface-tethered polymer chains: both water and alkane droplets moved at low TAs [2]. By selecting PDMS with the appropriate MW, motion of probe liquids, either rolling off the surface at low TAs or remaining pinned on the surface, could be arbitrarily controlled. In addition, the polymer chain mobility in bulk melts also increases with temperature, as is evident by the decrease in the polymer melt viscosity with increasing temperature. The increase in the temperature of our PDMS surfaces from 25 °C to 70 °C resulted in greater ease of drop mobility, such that these probe liquids are capable of sliding off a surface at lower TAs than those at 25 °C (Figure2) [2]. Our principle reported here is simple and effective, and based on the chemical, rheological and physical properties of smooth polymer melt brush films of linear PDMS.

## References

- [1] Hozumi, A. et al., *Langmuir*, **26** (2010) 2567.  
[2] Hozumi, A. et al., *Angew. Chem. Int. Ed.*, **51** (2010) 2956.

## Figures

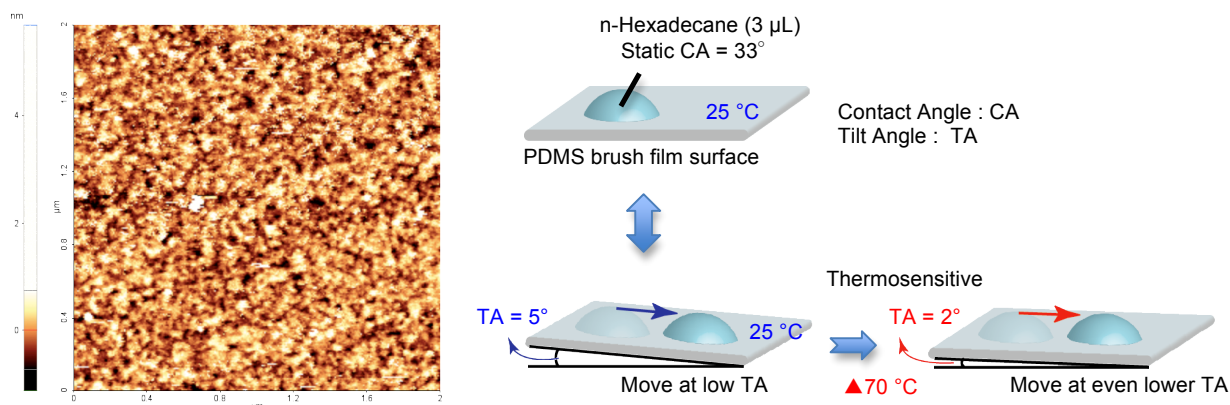


Figure 1 Typical AFM image of PDMS brush film surface (MW 6,000, 2 x 2 μm<sup>2</sup>) Figure 2 Changes in dynamic dewetting behavior of our PDMS brush film surface before and after heating.

# Preparation and Characterization of PEG bis(amine) grafted SPION/PMMA nanocomposite

Y. Wanna<sup>1,4,\*</sup>, R. Puingam<sup>1</sup>, J. Nukeaw<sup>1</sup>, A. Chindaduang<sup>2</sup>, G. Tumcharer<sup>2</sup>, S. Porntheerapat<sup>3</sup>, and S. Pratontep<sup>1</sup>

<sup>1</sup>College of Nanotechnology, King Mongkut's Institute of Technology Ladkrabang, Bangkok 12120 Thailand

<sup>2</sup>National Nanotechnology Center (NANOTEC), 111 Thailand Science Park, Pahol Yothin Rd, Klong Luang, Pathumthani 12120 Thailand

<sup>3</sup>Thai Microelectronics Center (TMEC), 51/4 Moo 1, Wangtakien District, Amphur Muang, Chachoengsao, Thailand 24000

<sup>4</sup>Nara Machinery Co., Ltd. 2-5-7, Jonan-Jima, Ohta-ku, Tokyo 143-0002, JAPAN

**Abstract:** The development of magnetic nanoparticles applied to rapid separation of heavy metal in water is a major goal in waste treatment application (Dave *et al.*; 2014). In this study, we report a novel of polymeric magnetic nanocomposite and surface modification. The composite particles of superparamagnetic iron oxide nanoparticles (SPIONs)/Polymethylmethacrylate (PMMA) were prepared by emulsion polymerization process in the aqueous suspension of SPIONs. In addition, the carboxyl(-COOH) groups were functionalized to the PMMA coated SPIONs and then grafting of Polyethylene glycol *bis(amine)* were functionalized investigated. The morphology and size distribution of SPIONs/PMMA was determined by transmittance electron microscopy (TEM) (Figure 1), scanning electron microscope and atomic force microscope (AFM) respectively. The metal concentration in the solution after separation nanoparticles was determined by inductivity coupled plasma optical emission spectrometer (ICP-OES). We have successfully prepared SPIONs/PMMA nanocomposite and surface functionalization for heavy metal ion chelation approach. Furthermore, we demonstrate that metal extraction using composite magnetic nanoparticles such as Cu(II), Mn(II), Pb(II), Zn(II), Cd(II), Pb(II), Co(II) and Ni(II). We have found that seven kinds of heavy metal percentage of extraction as 80, 58, 54, 35, 32 and 30 for Cu(II), Mn(II), Pb(II), Zn(II), Cd(II), Pb(II), Co(II) and Ni(II) respectively. The results show the composite nanoparticles surface modified are extremely promising for heavy metal ion separation.

**Keywords:** SPIONs, nanocomposite, surface modification, heavy metal removal application

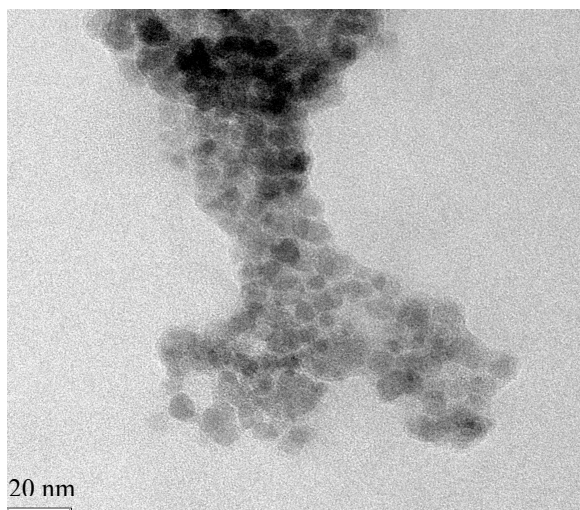


**Figure 1:** HR-TEM image of PEG bis(amine) grafted SPION/PMMA nanoparticles.

## References:

- Dave P. and Chopda L. (2014) Application of iron oxide nanomaterials for the removal of heavy metals. *J. Nanotechnol.* 2014, 1-14.
- Xu P., Zeng G.M, Huang D. , Feng C. , Hu.S, Zhao M., Lai C., Wei Z., Huang C., Xie G., and Liu Z. (2012) Use of iron oxide nanomaterials in wastewater treatment: A review. *Sci. Total Environ.* 424, 1-10

# Synthesis and Optical Characterization of $\text{Ca}_2\text{PO}_4\text{Cl}:\text{Tb}^{3+}$ and $\text{Mn}^{2+}$ Green Emitting phosphor for solid state lighting.

N.S.Kokode\*<sup>1</sup>, V.R.Panse<sup>2</sup> and S. J. Dhoble<sup>2</sup>

<sup>1</sup>N.H.College,Bramhapuri,Gondwana University Gadchiroli-441205,India

<sup>2</sup>Department of Physics, RTM Nagpur University, Nagpur -440033, India

\*<sup>1</sup>Corresponding Author: [drns.kokode@gmail.com](mailto:drns.kokode@gmail.com)

## Abstract:

The trivalent rare earth activated compounds and their luminescence properties have received great attention in the field of solid state lighting as well as white LED [1–2]. Solid-state lighting using light-emitting diode (LED) and phosphor material to generate white light is the current re-search focus in the lighting industry. Solid-state lighting technology has several advantages over conventional fluorescent lamps such as reduced power consumption, compactness, efficient light output, and longer lifetime. Solid-state lighting will have its impact on reducing the global electricity consumption. White light-emitting diodes (LEDs) can save about 70% of the energy and do not need any harmful ingredient in comparison with the conventional light sources, such as incandescence light bulbs and the luminescent tubes. Therefore white LEDs have a great potential to replace them and are considered as next generation solid state light devices [3-4]. Rare earth ions are characterized by an incompletely filled 4f shell, which can absorb the excitation energy to be at the excited state and then return to the ground state, resulting in emitting state in the visible region [5-6]. These feature transitions within the 4fn configuration have been found an important application in lighting and display (color television).  $\text{Tb}^{3+}$  and  $\text{Mn}^{2+}$  activated  $\text{Ca}_2\text{PO}_4\text{Cl}$  phosphor synthesized with the help of wet chemical method with extra heat treatment. Here we used the all the compound are from A.R. grade from merk such as  $\text{Ca}(\text{NO}_3)_2$ ,  $\text{NH}_4\text{Cl}$  and  $\text{NH}_4\text{H}_2\text{PO}_4$ ,  $\text{Tb}_4\text{O}_7$  and  $\text{Mn}(\text{NO}_3)_2$  with purity 99.99 %. Photoluminescence emission peaks of  $\text{Ca}_2\text{PO}_4\text{Cl}:\text{Tb}^{3+}$  phosphor excited by 380 nm found emission at 545 nm in the strong green region of the spectrum, and The prepared  $\text{Ca}_2\text{PO}_4\text{Cl}:\text{Mn}^{2+}$  phosphors were excited by 330 nm then we found that the characteristics emission of Mn ions at 511

nm. The increase in the luminescence intensity with the increase in concentration of Tb and Mn ion .The phosphors were characterized using X-ray diffraction (XRD), scanning electron microscopy and photoluminescence (PL) spectroscopy. Thermoluminescence (TL) spectroscopy.All the characterization was done at room temperature.The phase formation of the compound  $\text{Ca}_2\text{PO}_4\text{Cl}$  prepared by a wet chemical method was confirmed by the X-ray powder diffraction (XRD) pattern and it is found that it is well matched with the standard JCPDS data file (72-0010).The Chromaticity coordinates for the  $\text{Tb}^{3+}$  can be found as ( $C_x=0.265$ ,  $C_y=0.723$ ) and for  $\text{Mn}^{2+}$  as ( $C_x=0.019$ ,  $C_y=0.765$ ). The Thermoluminescence glow curve can be measured for the determination of kinetic parameter such as order of kinetics, activation energy and frequency factor for both the activator.Effect of temperature on the prepared phosphor was also studied.The intact study reveals that the present phosphor have promising applications in the lamp industry especially for solid state lighting (mercury-free excited lamp phosphor) and white light LED.

**Keywords:** Phosphor, Photoluminescence, Thermoluminescence, XRD, SEM, FTIR, Kinetic Parameter, Chromaticity,

## References:

- [1] A.N. Yerpude, S.J. Dhoble, J. Lumin. 132 (2012) 1781–1785.
- [2] K.N. Shinde, S.J. Dhoble, J. Fluorescence 21 (2011) 2053–2056.
- [3] H.A. Hoppe Angew, Chem. Int. Ed. 48 (20) (2009) 3572–3582.
- [4] T.S. Chan, R.S. Liu, B. Ivan, Chem. Mater. 20 (4) (2008) 1215–1217.
- [5] D.M. Burland, R.D. Miller, C.A. Walsh, Chem. Rev. 94 (1) (1994) 31–75.
- [6] L. Hesselink, S.S. Orlov, A. Liu, A. Akella, D.nLande, R.R. Neurgaonkar, Sciencen282 (1998) 1089–1094.

# Effect of electron beam on thermal, morphological and anti-oxidant properties of kraft lignin

T.Venkatappa Rao<sup>1\*</sup>, N.RajeswaraRao<sup>1</sup>, SVS Ramana Reddy,<sup>1</sup> B.Sanjeeva Rao<sup>2</sup>

<sup>1</sup>National Institute of Technology, Warangal, INDIA

<sup>2</sup>Govt. Degree College, Mulugu, Warangal, INDIA

\*Corresponding author Email address: tvraokmm@yahoo.co.in

**Abstract:** Lignin is a tridimensional phenolic polymer built from phenyl-propane units linked together by different bonds, is among the most abundant biopolymer on earth. Lignin is increasingly considered as a potential source for chemicals and studies on its thermal and antioxidant properties receive much interest. A strong interest have been manifested in the analytical characterization of kraft lignin. The present study was conducted to evaluate the effect of electron beam irradiation at doses of 30, 60 and 90 kGy on physical, thermal and antioxidant properties of kraft lignin. Under the treatment of electron beam, lignin undergo radical initiated reactions such as fragmentation and cleavage (Lepifre *et al.*, 2004). These reactions leave the compound open to interaction with a number of different resin systems, changing both the mechanical properties and biodegradability of the resulting composite. Irradiation of lignin is known to produce peroxy and poly-conjugated radicals which have different thermal stabilities. Figure 1 shows the Electron spin resonance (ESR) spectra of electron beam irradiated lignin of various doses which is superposition of peroxy and poly-conjugated radicals.

Keywords: electron beam, glass transition temperature, antioxidant activity

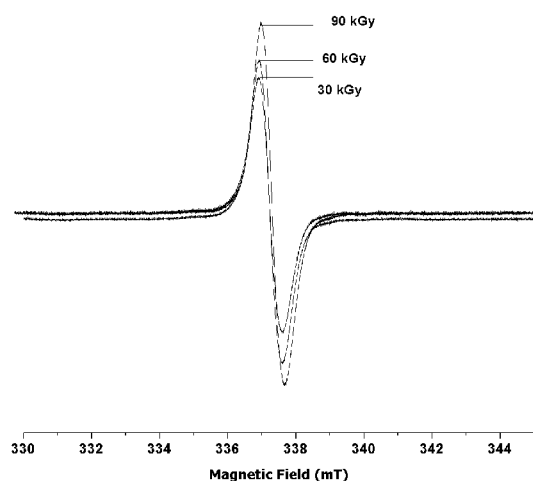


Figure 1: Figure illustrating the singlet ESR spectra of electron beam treated lignin irradiated to various doses.

Differential scanning calorimeter (DSC) thermograms of unirradiated and irradiated lignin are shown in Figure 2. Unirradiated thermogram of lignin consists of a first order transition around 130°C corresponding to glass transition temperature (T<sub>g</sub>) of lignin (Bouajila *et al.*, 2006). On

irradiation, there is a slight decrease in the value of T<sub>g</sub> and at highest dose i.e. 90 kGy there is a significant decrease in T<sub>g</sub> of lignin. Variation in T<sub>g</sub> of lignin is attributed to the plasticization effects in its molecular chains. SEM micrographs indicate the development of micro-cracks on the surface of granules of lignin on irradiation. Lignin aromatic structures suggests that it is well suited as a radical scavenger in existing commodity thermoplastics. Free radicals formed in plastic by irradiation with UV light which are the major causes of quick degradation of plastics, so kraft lignin can be substituted for more expensive UV stabilizers in polyethylene for minor effects on mechanical properties (Gosselink *et al.*, 2004). Anti-oxidant assays were carried out to check the anti-radical activity of lignin on electron beam treatment with DPPH and reducing power. There is a significant increase in the % inhibition values with the increase of radiation dose.

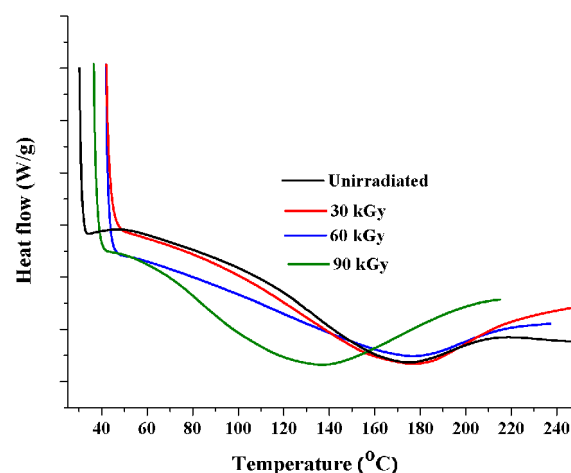


Figure 2: DSC thermograms of unirradiated electron beam treated lignin of doses 30, 60 & 90 kGy.

## References:

Lepifre, S., Froment, M., Cazaux, F. (2004) Lignin Incorporation Combined with Electron-Beam Irradiation Improves the Surface Water Resistance of Starch Films. *Biomacromolecules*, 5, 1678-1686.

Bouajila J, Dole P, Joly C, Limare A (2006) Some laws of a lignin plasticization. *J. Appl. Polym. Sci*, 102: 1445-1451.

Gosselink RJA, Snijder MBH, Kranenbarg A, Keijsers ERP, de Jong E, Stigsson LL (2004) Characterization and application of NovaFiber lignin. *Industrial Crops and Products*, 20: 191-203.

# Porosity Effect on Stoichiometry of GaN Nanostructures by Plasma Enhanced Chemical Vapor Deposition

M. Gholampour,<sup>1</sup> A. Abdollah-zadeh,<sup>1,\*</sup> R. Poursalehi<sup>1</sup>, L. Shekari<sup>2</sup>

<sup>1</sup>Nanomaterials Group, Department of Materials Engineering, Tarbiat Modares University, P.O. Box 14115-143, Tehran, Iran

<sup>2</sup>Faculty of Energy Engineering and New Technologies, Shahid Beheshti University, Tehran, Iran

**Abstract:** Porous Silicon (PSi) Substrate was direct affect on morphology and stoichiometry of deposited top layers by phase vapor deposition methods (Ishikawa et al., 2008). In this report, Gallium nitride (GaN) nanostructures were synthesized by direct current plasma enhanced chemical vapor deposition (PECVD) on PSi. Gallium (Ga) metal and nitrogen plasma have used as precursors. Plasma significantly affects on synthesis temperature of GaN nanostructures. The GaN nanostructures were grown based on the direct reaction between Ga atoms and excited nitrogen species in the plasma environment on PSi substrate. The result was obtained using X-ray diffraction (XRD) shows that the grown GaN nanostructures have the hexagonal wurtzite type structure. FESEM image indicates that PSi substrate has nano scales porous under 100nm. Line energy dispersive spectroscopy (EDS) shows that the effect of porous surface on the increasing of Ga and nitrogen atoms to form the GaN nanostructures (Figure 1). In our previous report, we have explained the growth mechanism of GaN nanostructures with and without gold catalyst by PECVD method (Gholampour et al., 2014). PECVD method is green, inexpensive, simple and flexible (Hou et al., 2008).

**Keywords:** GaN, nanostructures, plasma, PECVD.

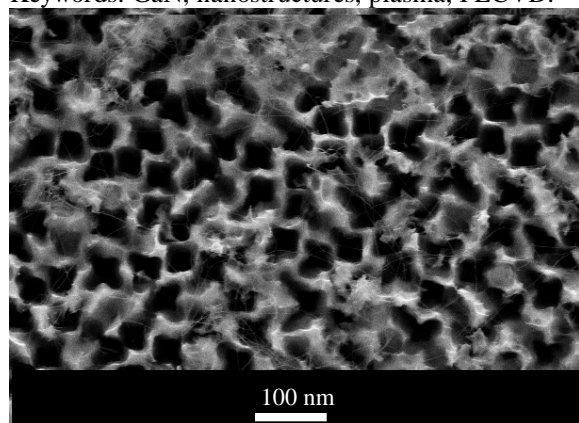


Figure 1: FESEM image of PSi nanostructures.

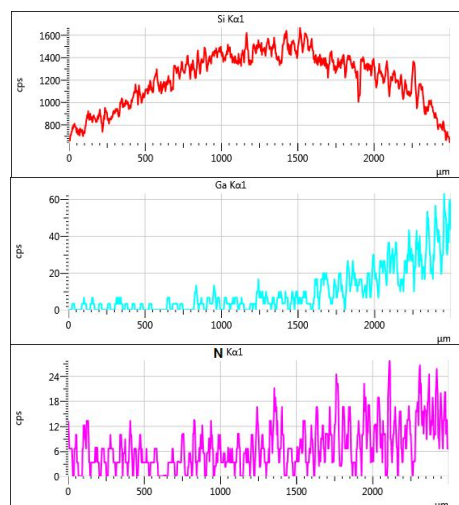
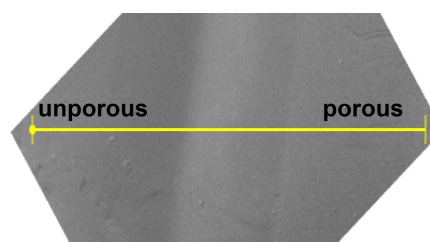


Figure 2: Line EDS analysis of GaN nanostructures grown on PSi via PECVD.

## References:

- Gholampour, M., Abdollah-zadeh, A., Poursalehi, R., and Shekari, L. (2014), Gold catalyst effect on the morphological and structural properties of GaN nanostructures deposited by plasma enhanced chemical vapor deposition, *Mater Lett.*, 120, 136–139.
- Hou, W.C., Chen, L.-Y., and Hong F. C.-N, (2008), Fabrication of Gallium Nitride Nanowires by Nitrogen Plasma: *Diam. Relat.Mater.*, 17, 1780–1784.
- Ishikawa, H., Shimanaka, K., Tokura, F., Hayashi, Y., and Hara, Y, (2008), MOCVD growth of GaN on porous silicon substrates: *J. Cryst. Growth.*, 310, 4900–4903.

# Poster Presentations

# Visible-Light-Activated Photocatalytic Hydrogen Production by Hybridized TiO<sub>2</sub> with Tin(IV) Porphyrin Complexes

Sung Hyun Kim, Gi-Seon Lee, Beom Hyeok Park, Hee-Joon Kim\*

Department of Applied Chemistry, Kumoh National Institute of Technology, Gumi 730-701, Republic of Korea

**Abstract:** Photocatalytic processes using TiO<sub>2</sub> as a photocatalyst have been introduced in the seventies. However, despite its advantages, TiO<sub>2</sub> must be excited in the UV region, which means that it can absorb only 3% of solar energy it receives. Therefore a photocatalyst that is active under visible light is of paramount importance as an essential element of solar photoenergy utilization. Diverse approaches are being made in search of visible light-sensitized photocatalysts. Porphyrins and metalloporphyrins, the synthetic structural analogue of chlorophyll in plant photosynthesis, have been widely investigated for their photochemical activity for various applications such as environmental photocatalysis, hydrogen production, and solar cell because of their strong absorption in the wide visible region. We have studied visible light-sensitized photocatalysts with tin(IV) porphyrins. Hydrogen gas was successfully produced under visible light in SnP/Pt-TiO<sub>2</sub> system in the wide pH range (pH 3-11), in which the apparent photonic efficiency for H<sub>2</sub> evolution in SnP/Pt-TiO<sub>2</sub> system was estimated to be 35% with the monochromatic radiation of  $\lambda = 550 \pm 10$  nm. This is clearly contrasted with the common ruthenium complex-sensitized TiO<sub>2</sub> system where the adsorption of the sensitizer complex is essentially required and the hydrogen production is limited to the acidic condition where the adsorption of the sensitizers on TiO<sub>2</sub> is allowed. Being less expensive, less toxic, and consisting of a more abundant element unlike the Ru-based sensitizers, SnP can be developed and utilized as a practical sensitizer for solar chemical conversion. We also prepared tin(IV) porphyrin incorporated-TiO<sub>2</sub> nanotubes (Figure 1) which exhibits visible-light-activated photocatalytic production of H<sub>2</sub>. We have been recently interested in an approach to incorporate tin(IV) porphyrins as visible light absorbing sensitizers at the TiO<sub>2</sub>/H<sub>2</sub>O interface. The surface of TiO<sub>2</sub> particles coated with perfluorosulfonate polymer (Nafion) can bind water-soluble cationic tin(IV) porphyrins within the Nafion layer through electrostatic attraction (Figure 2). The visible-light-induced production of H<sub>2</sub> by this hybrid photocatalyst is far more efficient than that on based TiO<sub>2</sub>.

Keywords: Photocatalysis, Hydrogen Production, Tin(IV) Porphyrin, Hybridized TiO<sub>2</sub>.

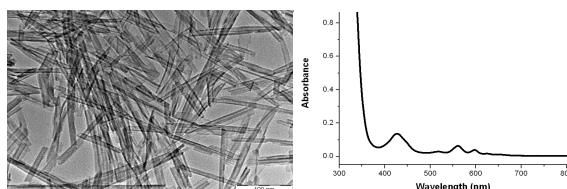


Figure 1: TEM image of tin(IV) porphyrin incorporated-TiO<sub>2</sub> nanotubes and its UV-vis spectrum.

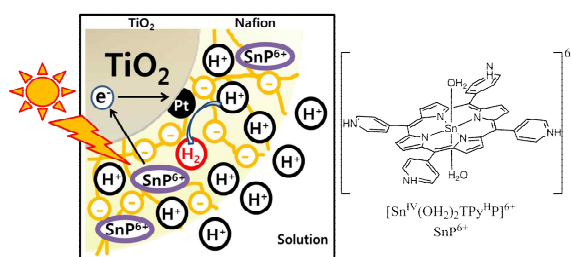


Figure 2: Illustration for visible-light-sensitized photocatalytic production of H<sub>2</sub> on Nafion-coated TiO<sub>2</sub> with tin(IV) porphyrin complexes.

## References:

- Jang, J. H., Jeon, K.-S., Oh, S., Kim, H.-J., Asahi, T., Masuhara, H., Yoon, M. (2007), Synthesis of Sn-Porphyrin-Intercalated Trititanate Nanofibers: Optoelectronic Properties and Photocatalytic Activities, *Chem. Mater.*, 19, 1984-1991.
- Kim, W., Park, J., Jo, H. J., Kim, H.-J., Choi, W. (2008), Visible Light Photocatalysts Based on Homogeneous and Heterogenized Tin Porphyrins, *J. Phys. Chem. C*, 112, 491-499.
- Kim, W., Tachikawa, T., Majima, T., Li, C., Kim, H.-J., Choi, W. (2010), Tin-porphyrin sensitized TiO<sub>2</sub> for the production of H<sub>2</sub> under visible light, *Energy Environ. Sci.*, 3, 1789-1795.
- Kim, H., Kim, W., Mackeyev, Y., Lee, G.-S., Kim, H.-J., Tachikawa, T., Hong, S., Lee, S., Kim, J., Wilson, L. J., Majima, T., Alvarez, P. J. J., Choi, W., Lee, J. (2012), Selective Oxidative Degradation of Organic Pollutants by Singlet Oxygen Photosensitizing Systems: Tin Porphyrin versus C<sub>60</sub> Aminofullerene Systems, *Environ. Sci. Tech.*, 46, 9606-9613.

# Establishment of Optimized Metallic Contacts on Porous Silicon for Thermoelectric Applications

O. Abbes,<sup>1,\*</sup> A. Melhem,<sup>1</sup> K. Snabi,<sup>1</sup> C. Leborgne,<sup>1</sup> N. Semmar,<sup>1</sup>

<sup>1</sup>GREMI CNRS-Université d'Orléans, 14 Rue d'Issoudun, 45067 Orléans, France

**Abstract:** While the world's need of energy is rising with a decrease of fossil fuel supplies, it becomes crucial to develop smart materials that can supply clean and sustainable energy to meet the needs of the future. Thermoelectric materials are currently investigated as a promising pathway, they allow the conversion of temperature gradients into electricity, which provides power generation without refrigerant or moving parts. During last years, nanostructured silicon demonstrated a great potential to ameliorate thermoelectric figure of merit  $ZT$  (Lee *et al.*, 2008). In addition, porous silicon (por-Si) exhibits interesting properties, such as good features of electroluminescence and photoluminescence in the visible and IR spectra (Hamadeh *et al.*, 2008 and Fauchet *et al.*, 1996). A lot of effort has been devoted to boost the material's figure of merit, however, in a realistic device, metallic contacts are needed to extract electricity. Those contacts could gradually lower the resulting current, in the case of high electrical contact resistivity. Therefore, optimizing the metallic contacts grown on porous Silicon is of a high interest, toward their integration in thermoelectric applications.

In this work we present a study of the effect of several metallic contacts on the figure of merit, using a new process, and comparing the different factors influencing the electrical and thermal conductivities. Besides, a thermoelectric micro-generator was produced, and several masks were used in order to optimize metallic contacts on thermoelectric elements (Figure 1).

**Keywords:** thermoelectricity, metallic contacts, porous Silicon, figure of merit, thermal conductivity, electrical resistivity.

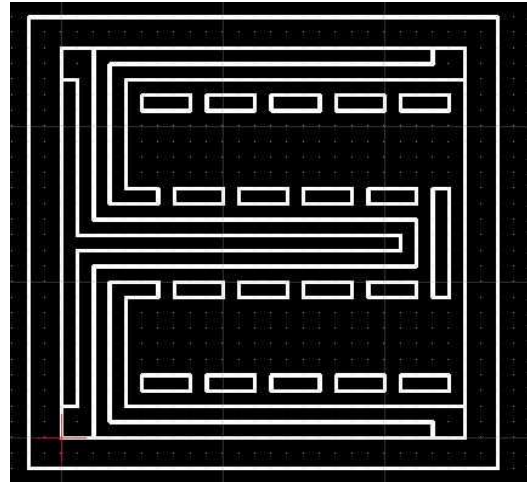


Figure 1: Figure illustrating the mask used in order to realize low resistive contacts on thermoelectric elements.

## References:

- Lee, J.H., Galli, G.A., Grossman, J.C., (2008) Nanoporous Si as an Efficient Thermoelectric Material, *Nano Letters*, 8, 3750-3754.
- Hamadeh, H., Naddaf, M., Jazmati, A., (2008) Near infrared photoluminescence properties of porous silicon prepared under the influence of light illumination, *Journal of Physics D: Appl. Phys.*, 2008, 41, 245108.
- Fauchet, P. M., (1996) Photoluminescence and electroluminescence from porous silicon, *Journal of Luminescence*, 70, 294-309.

# Photoresponse of Composites of Zinc Oxide and Poly(3-hexylthiophene) under Selective UV and White-Light Illumination

P. Pattamang<sup>1</sup>, P. Piyakylawat<sup>2</sup>, U. Asawapirom<sup>2</sup>, S. Porntheeraphat<sup>3</sup>, K. Tantisantisom<sup>2</sup>  
J. Nukeaw<sup>1,4</sup> and S. Pratontep<sup>1,4\*</sup>

<sup>1</sup>College of Nanotechnology, King Mongkut's Institute of Technology Ladkrabang, Chalongkrung Rd., Ladkrabang, Bangkok 10520, Thailand

<sup>2</sup>National Nanotechnology Centre, National Science and Technology Development Agency Thailand Science Park, Patumtani 12120, Thailand

<sup>3</sup>National Electronics and Computer Technology Center, National Science and Technology Development Agency Thailand Science Park, Patumtani 12120, Thailand

<sup>4</sup>ThEP Center, CHE, 328 Si Ayutthaya Rd., Bangkok 10400, Thailand

**Abstract:** We investigate charge transport in UV sensing devices based on organic-inorganic semiconductor composites with the metal-semiconductor-metal (MSM) structure. Composite materials of zinc oxide (ZnO) nanoparticles and poly(3-hexylthiophene) (P3HT) at different ratios were prepared by drop-casting their colloidal mixture in chloroform onto low-cost interdigitated copper electrodes with a gap size of approximately 150 microns. The current-voltage characteristics of the devices were investigated under both dark and illuminated conditions in the UV-visible range. The highest photoresponse of over 50 folds was observed for an optimal ZnO:P3HT ratio of 8:1 w/w in the wavelength range between 310 and 380 nm. The dynamic response was investigated by pulsing a 365 nm UV lamp with a long period (minutes) to reveal the response time of 4 s and the recovery time of less than 1 s. The photoresponse of the materials was also investigated for a shorter period of UV pulsing, using a rotating chopper. The response time and recovery time for the short UV pulse were found to be approximately 20 ms and 25 ms, respectively. Such variable response time should stem from the presence of two types of semiconductor materials, namely ZnO with a high electron mobility and P3HT with a moderate hole mobility. To probe the charge generation and transport mechanisms, we further investigate the photoresponse using UV pulsing under background white light of different intensities, and vice versa. The background white light was found to deteriorate the UV photoresponse of the materials. On the other hand, the background UV illumination produced an anomalous photoresponse pattern with the white light pulsing (Fig. 1). The results may be explained by considering three main charge transport channels for the composite materials, namely, highly mobile electrons in ZnO, holes in P3HT, and charge transfer between ZnO and P3HT, with the characteristic photoresponses in the UV and the visible range, respectively. In the presence of background white light, an accumulation of electrons in P3HT is likely to occur

and limit the hole current. This accumulation should explain the sharp pikes in the photoresponse characteristics (Fig. 1). Understanding the charge transport mechanisms is highly important for future applications in low-cost UV sensors and tunable optoelectronic devices..

**Keywords:** Zinc Oxide, poly(3-hexylthiophene), Composite film, UV sensor

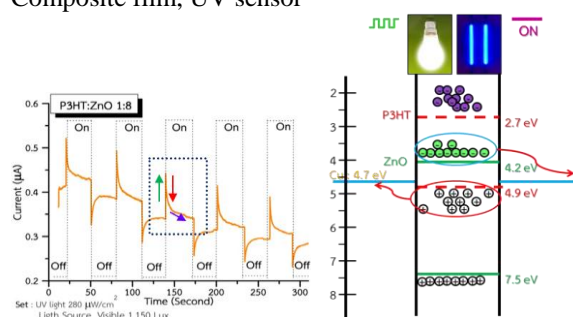


Figure 1: Photoresponse (left) and charge transport model (right) of ZnO:P3HT composites under white light pulsing with background UV illumination.

## References:

- H. G. Li, G. Wu, M. M. Shi, L. G. Yang, H. Z. Chen, and M. Wang (2008), ZnO/poly(9,9-dihexylfluorene) based inorganic/organic hybrid ultraviolet photodetector, *App. Phys. Lett.*, 93, 153309.
- J. H. Jun, H. Seong, K. Cho, B. M. Moon and S. Kim (2009), Ultraviolet photodetectors based on ZnO nanoparticles, *Ceramics International*, 35, 2797–2801.
- L. Wang, D. Zhao, Z. Su, F. Fang, B. Li, Z. Zhang, D. Shen and X. Wang (2010), High spectrum selectivity organic/inorganic hybrid visible-blind ultraviolet photodetector based on ZnO nanorods, *Organic Electronics*, 11, 1318–1322.

# Optical and magnetic properties of doped ZnO: Experiment and Simulation

Sakwiboon Jantrasee<sup>1</sup>, Pairot Moontragoon<sup>2,3</sup> and Supree Pinitsoontorn<sup>2,3\*</sup>

<sup>1</sup> Materials Science and Nanotechnology Program, Faculty of Science,  
Khon Kaen University, Khon Kaen 40002, Thailand

<sup>2</sup> Department of Physics, Faculty of Science, Khon Kaen University, Khon Kaen 40002, Thailand

<sup>3</sup> Nanotec-KKU Center of Excellence on Advanced Nanomaterials for Energy Production and Storage, Thailand

**Abstract :** Advancements in the ZnO research have fostered much interest in their magnetic and optical properties. In particular, Al- and Ga-doped ZnO have shown attractive electrical and optical properties (He *et al.*, 2013, Reddy *et al.*, 1998). On the other hand, Co-doped ZnO is well known as a diluted magnetic semiconductor showing ferromagnetism dependence of temperature (Maensiri *et al.*, 2006). In this work, the effects of Al-, Ga- and Co-doping in the ZnO system on the optical and magnetic properties are presented. The work is divided into the experimental and simulation sections. Firstly, nanosized powders of  $Zn_{1-x}M_xO$  ( $M = Al, Ga$  and  $Co$ ) were synthesized by the hydrothermal method. The XRD results show that the obtained powders are the single phases with hexagonal structure. The morphology of the samples revealed by SEM and TEM are different shape and size. The optical properties of the samples, measured by the UV-Vis technique, exhibited a strong absorption spectra below 400 nm in the UV region. This is equivalent to the band gap energy between 2.79-3.02 eV. The type and amount of dopants have an influential effect on the absorption spectra. The magnetization curves were investigated using the VSM technique from 50 K to 300 K. The undoped ZnO, Al- and Ga-doped ZnO exhibits purely diamagnetic behavior, whereas the Co-doped ZnO shows a combination of diamagnetism and ferromagnetism.

Secondly, the simulations were carried out using ABINIT, which is based on density functional theory (DFT). The energy band structures, density of states and magnetic properties of the doped-ZnO were investigated using PAW (projector-augmented plane wave) pseudopotential method within the local spin density approximation with the Hubbard model (LSDA + U). The optical and magnetic properties were extracted from the calculated results. The results from the simulation show good agreement with the experiments.

Keywords: doped- ZnO, optical properties, magnetic properties, DFT

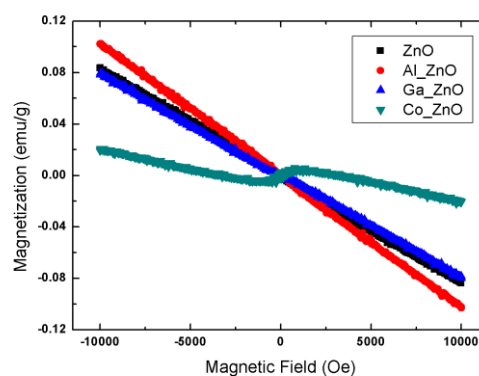


Figure 1: the magnetization of the undoped ZnO, Al-, Ga-, and Co-doped ZnO with Applied field.

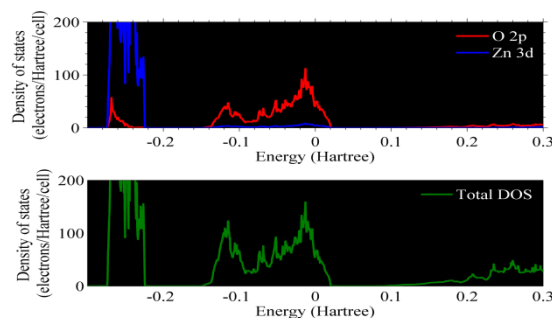


Figure 2: Partial density of states (PDOS) and total density of states (DOS) of pure ZnO.

## References:

H-Y, He., Z, He., Q, Shen., J, Lu., (2013) Optical transmittance enhancement and bandgap widening of ZnO:Al powders by W codoping, *J Mater Sci.*, 48, 316-321.

Reddy, K.T.R., Miles, RW., (1998) Growth and characterization of sprayed ZnO:Ga thin films, *J Mater Sci Lett.*, 17, 279-281.

Maensiri, S., Sreesongmuang, J., Thomas, C., Klinkaewnarong J., (2006) Magnetic behavior of nanocrystalline powders of Co-doped ZnO diluted magnetic semiconductors synthesized by polymerizable precursor method, *J Magn Magn Mater.*, 301, 422-432.

# Newly designed $\pi$ -conjugated thiazolo [5,4-*d*]thiazole based oligomer for efficient small molecule organic solar cells

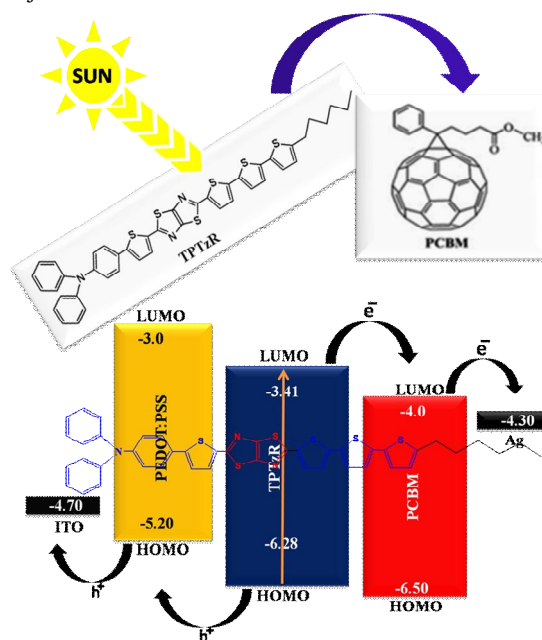
Mohammed Nazim, Sadia Ameen, Hyung-Kee Seo, Minwu Song, Doo-Ri Park, Hyung-Shik Shin\*  
Energy Materials & Surface Science Laboratory, Solar Energy Research Center, School of Chemical Engineering, Chonbuk National University, Jeonju, 561-756, Republic of Korea

\*E-Mail- hsshin@jbnu.ac.kr

**Abstract:** Small molecules organic  $\pi$ -conjugated oligomers have depicted as a great alternatives to organic polymers in solution-processed bulk heterojunction (BHJ) organic solar cells (OSCs) due to various advantages as light weight, low band gap, ease of purification as well as synthetic process with reproducibility, cost effective fabrication and good solubility in common organic solvents (Heeger et al., 2012). Oligomers containing thiazolo[5,4-*d*]thiazole acceptor have shown good electron-accepting tendency and high thermal stability due to the presence of C=N- backbone and coplanar fused heterocyclic ring system, and therefore ensures extended  $\pi$ -electron delocalization of electron in the conjugated system. Various types of D-A-D or A-D-A oligomers of thiazolo[5,4-*d*]thiazole has shown the good photovoltaic properties for solution-processed small molecule organic solar cells (Zhan et al., 2012). In this study, organic  $\pi$ -conjugated oligomer (TPTzR) featuring thiazolo[5,4-*d*]thiazole-core acceptor with triphenylamine (D<sub>1</sub>) and terminal alkylated bithiophene (D<sub>2</sub>) as donors was synthesized via Suzuki coupling and applied in solution-processed small molecule organic solar cells (SMOSCs). The synthesized oligomer has displayed liquid-crystal property which might be due to the presence of terminal alkyl chain and shown a molecular order of film morphology which results in the homogenous and uniform film morphology for the solution-processed fabrication (Yang et al., 2013). The thin film morphology of the blended active layer played a significant role in solution-processed fabrication and affects the performance of the solar cell devices (Bazan et al., 2011). The fabricated organic solar cell devices displayed a good power conversion efficiency of ~2.43 % with high J<sub>sc</sub> of ~12.05 mA/cm<sup>2</sup>.

**Keywords:** solution-processed,  $\pi$ -conjugated oligomers, bulk-heterojunction, thiazolo[5,4-*d*]thiazole,  $\pi$ -electron delocalization, electron-accepting, liquid-crystal, film morphology, power conversion efficiency.

Figure 1: Illustrating the fundamental principle of organic solar cell operation.



## References:

- Mishra, A., Bauerle, P., (2012), Small molecule organic semiconductors on the move: promises for future solar energy technology, *Angew. Chem., Int. Ed.*, 51,2020-2067.
- Sun, Y., Welch, G. C., Leong, W. L., Takacs, C. J., Bazan, G. C., Heeger, A. J., (2012), Solution-processed small-molecule solar cells with 6.7% efficiency, *Nature Mater.*, 11,44–48.
- Lin, Y., Fan, H., Li, Y., Zhan, X., (2012), Thiazole-based organic semiconductors for organic electronics, *Adv. Mater.*, 24,3087-3106.
- Liu, Y., Chen, C.-C., Hong, Z., Gao, J., Yang, M., Zhou, H., Dou, L., Li, G., Yang, Y., (2013), Solution-processed small-molecule solar cells: breaking the 10% power conversion efficiency, *Sci. Rep.*, 3:3356,1-8.
- Liu, X., Sun, Y., Perez, L. A., Wen, W., Toney, M. F., Heeger, A. J., Bazan, G. C., (2012), Narrow-band-gap conjugated chromophores with extended molecular lengths, *J. Am. Chem. Soc.*, 134,20609-20612.

# Fully inorganic tin halides perovskite as light harvesting materials

S. Del Gobbo, J. Eid, I. Gereige, S. Masala

Solar and Photovoltaic Engineering Research Center (SPERC), King Abdullah University of Science and Technology (KAUST), Thuwal, Saudi Arabia

**Abstract:** Post-transition metal halide perovskite has emerged as extraordinary materials for light harvesting and thus for photovoltaic applications [1,2]. Nowadays this class of material has supplanted the organic dye in standard DSSC but it still lacks of the needed chemical stability to be used in commercial applications. Moreover, being these materials lead-based, several environmental and health hazards might arise. As an alternative to lead-halide perovskites we investigated tin-based fully inorganic iodide perovskites doped with other halogens,  $\text{CsSnI}_{3-x}\text{X}_x$  and with metals such as Cu, Ag and Tl,  $\text{Cs}_{1-x}\text{M}_x\text{SnI}_3$ . The advantage of halogen doping is two-fold, firstly it stabilizes the structure and improves the stability of the material against the effects of moisture and oxygen [2]. Secondly it allows the fine tuning of the bandgap to better match the solar spectrum.

The doping of  $\text{CsSnI}_3$  by more covalent metals such as Cu, Ag, Tl has not quite well investigated so far, yet it is expected to contribute to the improved material stability against moisture and oxygen [3] without considerably changing the optoelectronic property of the material.

Among numerous compounds tested, the one that shows the highest stability is  $\text{CsSnIBr}_2$ . This compound is characterized by high degree of crystallinity and therefore gave us the best performance in terms of photoconversion. Its organic/inorganic analogue,  $\text{CH}_3\text{NH}_3\text{SnIBr}_2$ , has been already reported in [4] but suffers of a quick degradation after exposure to humidity.

Photovoltaic (PV) devices based on these materials were prepared by spin coating a solution of the salts dissolved in a polar solvent with the correct stoichiometric ratio followed by post-deposition annealing. As substrates we used FTO glass coated with a thin film of rutile  $\text{TiO}_2$  that works as a hole blocking layer and a mesoporous layer of  $\text{TiO}_2$  that allows to enhance the interfacial contact with the perovskite. The top anode contact was constituted by a thin layer of hole transporting material (HTM) embedded in an electrolytic medium and finished with gold pads deposited by thermal evaporation.

The major issue for these PV devices comes from the HTM that seems to chemically interact with the underlying perovskite film damaging it and thus dramatically reducing the power conversion efficiency of the device. This occurs mostly during the HTM deposition due to the solvent used, e.g. acetonitrile, that dissolves the perovskite. To solve this problem we have developed several strategies to reformulate

the HTM composition, in particular avoiding polar solvents. Additionally, we are currently exploring the advantages of fully inorganic HTM such as  $\text{CuSCN}$ . In conclusion, this study enlightens the potentiality of fully inorganic tin halides perovskite as a more stable light harvesting material compared to the organic cation-containing perovskite. However, still some device optimization work must be done in order to exceed the power conversion efficiency obtained by PV devices based on organic/inorganic lead-halide perovskite.

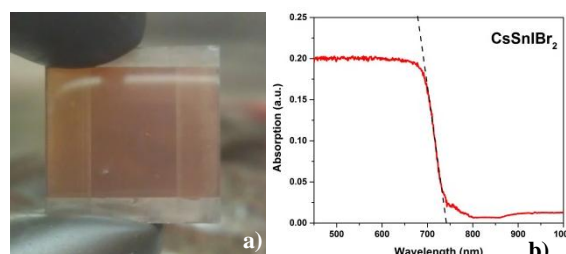


Figure 1: a) picture of a PV device with  $\text{CsSnIBr}_2$  as light harvesting material. b) Optical absorption  $\text{CsSnIBr}_2$  measured by diffuse reflectance spectroscopy. The estimated band-gap is of 1.67 eV, lower than the analogue  $\text{CH}_3\text{NH}_3\text{SnIBr}_2$  (1.75 eV) [4].

**Keywords:** Photovoltaic, solar cell, perovskite, tin halide perovskite, lead-free perovskite, titanium dioxide, hole transporting material.

## References:

- [1] Kojima, A., Teshima, K., Shirai, Y., and Miyasaka, T. (2009) Organometal Halide Perovskites as Visible-Light Sensitizers for Photovoltaic Cells. *J. Am. Chem. Soc.*, 131, 6050–6051.
- [2] Liu, M., Johnston, M.B. and Snaith, H.J., (2013) Efficient planar heterojunction perovskite solar cells by vapour deposition, *Nature*, 501, 395-398
- [3] Chung, I., Song, J.H., Im, J., Androulakis, J., Malliakas, C. D., Li, H., Freeman, A.J., Kenney J.T., and Kanatzidis M.G., (2012) *J. Am. Chem. Soc.*, 134, 8579-8587
- [4] Hao F., Stoumpos C.C., Cao, D. H., Chang Robert P. H., and Kanatzidis G.M. (2014), Lead-free solid-state organic–inorganic halide perovskite solar cells, *Nature Phot.*, 8, 489-494.

# Designing Hierarchical Nanostructures for Enhanced Gas Sensing Properties

Mohammad R. Alenezi

Public Authority for Applied Education and Training, College of Technological Studies,  
P.O. Box 42325 Shuwaikh, (Kuwait)

[Mr.alenezi@paaet.edu.kw](mailto:Mr.alenezi@paaet.edu.kw)

## Abstract:

Controlling the morphology of nanostructures is known to have a great impact on controlling its functional properties, which will help in enhancing the device performance[1-4]. Different methods have been reported to control the morphology of nanostructures grown via hydrothermal synthesis.

Rationally controlled multistage hydrothermal methods have been developed to prepare different types of hierarchical zinc oxide (ZnO) nanostructures with high surface-to-volume ratios and more exposed polar facets. Four types of hierarchical ZnO nanostructures, nanobrushes (ZNBs), nanoleaves (ZNLs), hierarchical nanodisks (HNDs) and nanoflakes (ZNFs) assembled from initial monomorphological nanostructures, nanowires (ZNWs) and nanodisks (ZNDs), were produced from sequential nucleation and growth following a hydrothermal process using zinc nitrate and zinc sulphate as the source of zinc ions. Compared to their initial monomorphological counterparts, the grown hierarchical nanostructures demonstrate superior gas sensing properties. ZNLs and ZNFs show significant improvement in sensitivity and fast response to acetone. In addition to the high surface-to-volume ratio due to the ultrathin sheet building blocks, the enhanced gas sensing properties of ZNLs and ZNFs are chiefly ascribed to the increased proportion of exposed (0001) polar facets. The current study offers the path for structure induced development of gas sensing properties by designing a necessary nanostructure, which could be used to fabricate high performance nanostructured gas sensors based on other metal oxides.

**Keywords:** Nanostructure, hierarchical, ZnO, Gas Sensor, Nanowire.

## References:

- Alenezi, M. R.; Alshammari, A. S.; Jayawardena, K. D. G. I.; Beliatis, M. J.; Henley, S. J.; Silva, S. R. P. *J. Phys. Chem. C* **2013**, 117, 17850–17858.
- Alenezi, M. R.; Abdullah S. Alshammari, Peter D. Jarowski, Talal H. Alzanki, Simon J. Henley, and S. R. P. Silva. *Langmuir*, **2014**, 30, 3913–3921.
- Alenezi, M. R.; Henley, S. J.; Emerson, N. G.; Silva, S. R. P. *Nanoscale*, **2014**, 6, 235–247.
- Alenezi, M. R.; Alzanki, T. H.; Almeshal, A. M.; *International Journal of Science and Research*. **2014**, 3, 588–591.

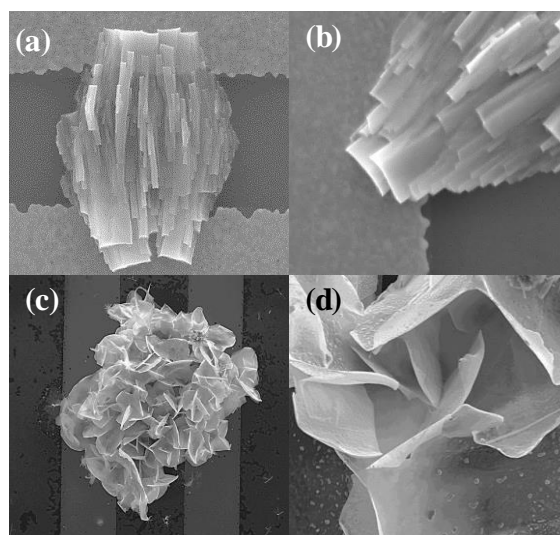


Figure 1. (a) Low magnification, (b) high magnification SEM image of a single ZNL; (c) low magnification, and (d) high magnification SEM image of single ZNF.

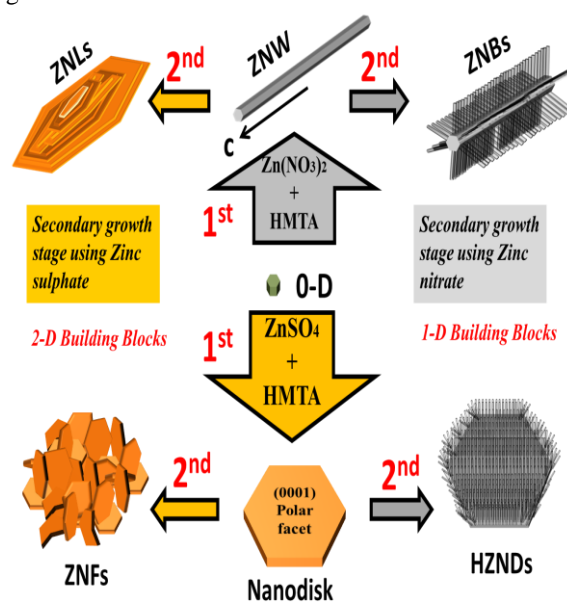


Figure 2: Summary of the impact of the zinc counter-ions in each growth stage on the final morphology of the produced ZnO nanostructure.

# The optical and surface properties of $Mg_{0.3}Zn_{0.7}O$ thin films deposited by PLD methods on the PES substrate

HyunMin Lee<sup>1</sup>, SangHyun Kim<sup>1</sup>, JaeHeon Ock<sup>1</sup>, and Nakwon Jang<sup>1,a</sup>

<sup>1</sup> Division of Electrical and Electronics Engineering Korea Maritime and Ocean University, Busan, 606-791, Korea

<sup>a</sup>E-mail: nwjang@kmou.ac.kr

**Abstract:** Recently, ZnO, II-IV oxide semiconductor, has attracted great attention due to their physical, chemical properties. And it showed high optical transmittance in the visible region[1].

In generally Mg is used for band-gap engineering of ZnO.  $Mg_xZn_{1-x}O$  is tunable the band-gap ranges from 3.37 eV to 7.8 eV according to content of Mg, which is essential for application as a barrier layer or quantum wells in Zn/MgZnO heterostructures[2]. MgZnO can be applied to optoelectronic devices. But it is difficult to deposit to MgZnO on PES substrate.

Therefore, in this study, we deposited 30 mol % of MgZnO thin films on PES substrate using PLD methods according to the oxygen partial pressure. As the oxygen pressure increased, the band-gap energy of  $Mg_{0.3}Zn_{0.7}O$  turned from 3.3 eV to 3.59 eV. As the result of AFM, the grain size of  $Mg_{0.3}Zn_{0.7}O$  thin film decreased to 55.3 nm from 83.2 nm, the rms roughness is decreased to 1.35 nm from 3.78 nm.

Keywords: Flexible devices, PES substrate, TOS, MgZnO, Optical properties

## Acknowledgements

This research was supported by the MSIP(Ministry of Science, ICT&Future Planning), Korea, under the ITRC(Information Technology Research Center) support program supervised by the NIPA(National IT Industry Promotion Agency)(NIPA-2014-H0301-14-1016)

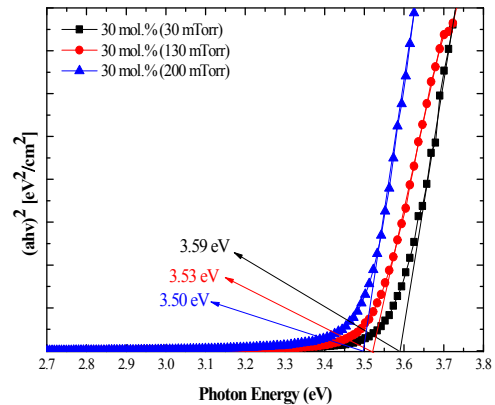


Figure 1: Figure is about the result of UV-visible spectrometer. The band gap energy change to 3.59 eV from 3.30 eV.

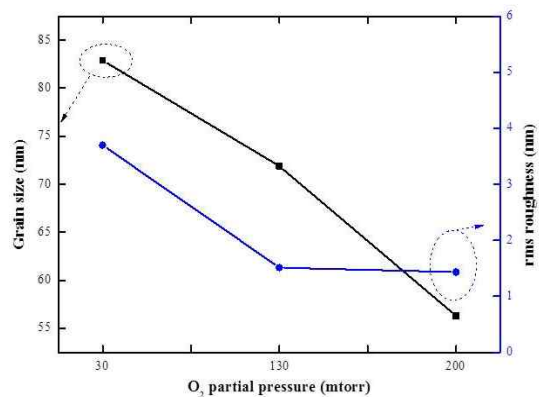


Figure 2 : Figure is about the result of AFM. The increasing of oxygen pressure, the grain size and rms roughness is decreased.

## References:

K. Nomura, H. Ohta, A. Takagi, T. Kamiya, M. Hirano, and H. Hosono, Nature, vol. 432, no. 7016, pp. 488-492, 2004.

T. Takagi, H. Tanaka, Sz. Fuita and Sg. Fujiuta, Jpn. J. Appl. Phys. 42, L401, 2003.

## Applicability of PEDOT:PSS Films for Highly Conductive Transparent Electrode by New Effective Dopant

Mi-im An, Se-jin Kwon, Seung Young Jeong, Gyo jic Shin, Kyung-ho Choi, Sangkug Lee

Korea Institute of Industrial Technology, 89, Yangdae-giro-gil, Ijangmyeon, Seobuk-gu, Cheonan-si, Chungnam, 331-822, Korea

skdlee@kitech.re.kr

### Abstract

The use of conductive PEDOT:PSS is rapidly increasing as one of the most widely used conducting polymers because of its conductivity and stability over the past decades. In addition, it is used in a various field of polymer electronics because these can be used as transparent, conducting electrode that can be processed in aqueous solution by techniques such as spin casting and inkjet printing. Furthermore, conductive PEDOT:PSS has many merits compared to other conducting polymers such as a high transparency in the visible range, thermal stability and it was possible to process in aqueous solution but conductivity exhibited very low  $0.2 \text{ S cm}^{-1}$ . Recently, to enhance the conductivity of PEDOT:PSS film have been proposed the various methods such as addition of polar organic solvent, inorganic acid, various nanoparticles, ionic liquid, and post-treatment of PEDOT:PSS film etc. These films are also essential to maintain the constant conductivity regardless of time and change of external conditions to realize practical application to transparent electrode.

In this paper, we investigated the *p*-toluenesulfonic acid as new dopant for the highly conductivity and superior transparency of PEDOT:PSS films. Particularly, Lifetime conductivity of PEDOT:PSS films with adding the resin was confirmed as a function of time for commercial applications. As a results, the conductivity of PEDOT:PSS films increased by approximately maximum three orders of magnitude compared to pristine PEDOT:PSS films and their conductivity for the lifetime stability also was confirmed to maintain the constant values regardless of time.

### References

- [1] C. Badre, L. Marquant, A. M. Alsayed, L. A. Hough. *Adv. Funct. Mater.*, **13** (2012) 2723.
- [2] Y. Xia, K. Sun, J. Ouyang. *Advanced Materials*, **18** (2012) 2436.
- [3] C. Gong, H. B. Yang, Q. L. Song, Z. S. Lu, C. M. Li. *Solar Energy Materials & Solar Cells*, **100** (2012) 115.

## Novel Photopolymer with High Photosensitivity and Superior Alignment Characteristics for 3D Retardation Film

Ju Hui Kang, Si Yeol Yang, Seung Yong Jeong, Sangkug Lee, Kyung Ho Choi, Gyo jic Shin

Korea Institute of Industrial Technology, 89, Yangdae-giro-gil, Ipjang-myeon, Seobuk-gu, Cheonan-si, Chungnam 331-822, Republic of Korea

[gyshin@kitech.re.kr](mailto:gyshin@kitech.re.kr)

### Abstract :

Photo-alignment is one of important technologies for making film-type patterned retarder (FPR) for the 3D display. That technology gives significant effect on the increase of productivity and the decrease of production cost. Photo-alignment materials are needed to have high photosensitive properties for high productivity on the continuous roll to roll process of retardation film. Photo-alignment is efficient method for aligning liquid crystal. Especially, photoisomerization and photodimerization were well known as reasonable methods for producing FPR because those reactions are occurred at lower polarized UV energy than photodegradation ( $3\sim 12.7\text{ J/cm}^2$ ). In general, photodimerization of photosensitive groups in the photopolymer was used to obtain a stable alignment of low molecular weight liquid crystal (LC) molecules. Additionally, photodimerization occurs by the exposure of relatively longer wavelength of the UV light to avoid partial degradation of photopolymer.

In the other hand, the chalconyl group is recognized to be a good photosensitive group and exhibits only photodimerization between the carbon double bonds in chalcone moieties. The photoreaction of chalconyl group takes place by irradiation with relatively longer wavelength UV light compare to cinnamoyl group. Photosensitive polymers with chalcone groups have been examined in the applications of photoalignment film. According to many works, good LC alignment was observed for the LC cell using the polymer film with chalcone moiety compared to the cinnamate polymer film when the deep UV light was cut-off. This result indicated that the chalconyl moiety is good photosensitive group. Accordingly, alignment behavior of LC molecules would be simply enhanced by the liquid crystalline polymer surface where mesogenic groups having similar chemical structure to that of the LC molecules existed. In addition, using RM instead of LCs has the simple and keeps advantages of photo-alignment, such as high alignment uniformity, easiness of alignment control, and precise patterning.

In this paper, we report newly synthesized photopolymer with back-bone imine linkage and chalconyl groups, PMCh, which have high sensitivity and superior photo-alignment to very low UV exposure energy. Especially, the higher sensitivity of LC alignment capability to low UV energy is essential to shorten exposure time in photo-alignment process for practical application to the retarder films.

### References

1. N. Koide, T. Mihara, Proc. of SPIE, 5003 (2003), 63-72.
2. T. Mihara, M. Tsutsumi, and N. Koide, Mol. Cryst. Liq. Cryst., 382 (2002), 53-64.
3. H. Tunell, M. Selo, K. Skarp, and J. Hilborn, Polymer. J., 38 (2006), 716-723.
4. K. H. Jung, S.-Y. Hyun, D.-M. Song, and D.-M. Shin, Optical Materials, 21 (2002), 663-666.

### Figures.

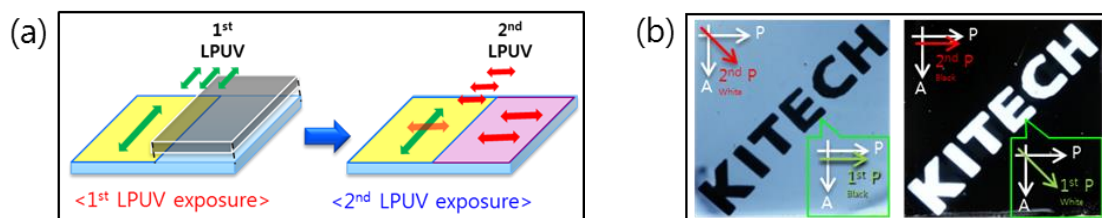


Figure. (a) The multi photo-patterning process on photosensitive PMCh, (b) Photograph of photoalignment film.

# Determination of Copper (II) Ions in Wastewater by Colorimetric Detection

P. Muensri,\* S. Danwittayakul

National Metal and Materials Technology Center, 114 Thailand Science Park, Paholyothin Rd., Klong 1, Klong Luang, Pathumthani, 12120, Thailand.

**Abstract:** Polyethylenimine (PEI) – Polyacrylonitrile (PAN) functionalized cellulose membranes were developed for determination of Cu(II) ions in wastewater. PAN was first coated on cellulose membrane by filtering method followed by PEI functionalization via the electrostatic self-assembly on the membranes by dipping PAN cellulose membranes into PEI solution for several hours. Excess PEI molecules were then totally removed by sonicating in deionized water for 1 hour. PEI-PAN cellulose membranes were selectively formed a blue cuprammonium complex at pH 7 with Cu(II) ions in water, then, the colorless PEI-PAN membranes turned into blue color ( $\lambda_{\max}$  at 650 nm) detected by naked eyes even at low concentration of 1 ppm. In this work we will report reliability of the PEI-PAN membrane for determining Cu(II) in wastewater.

**Keywords:** copper ions detection, test strip, polyethylenimine, polyacrylonitrile

## References:

Xu, J., Feng, X., Chen, P., Gao, C., (2012) Development of an antibacterial copper (II)-chelated polyacrylonitrile ultrafiltration membrane, *J. Membr. Sci.* 413-414, 62-69.

Monier, M., Akl, M.A., Ali, W.M., Modification and characterization of cellulose cotton fibers for fast extraction of some precious metal ions, 66, 125-134.

Wen, T., Qu, F., Li, N.B., Luo, Q. L., (2013) A facile, sensitive, and rapid spectrophotometric method for copper(II) ion detection in aqueous media using polyethylenimine, *Arabian J. Chem.*, In Press.

Navarro, R.R., Sumi, K., Fujii, N., Matsumura, M., (1996) Mercury removal from wastewater using porous cellulose carrier modified with polyethylenimine, *Wat. Res.* 30, 2488-2494.

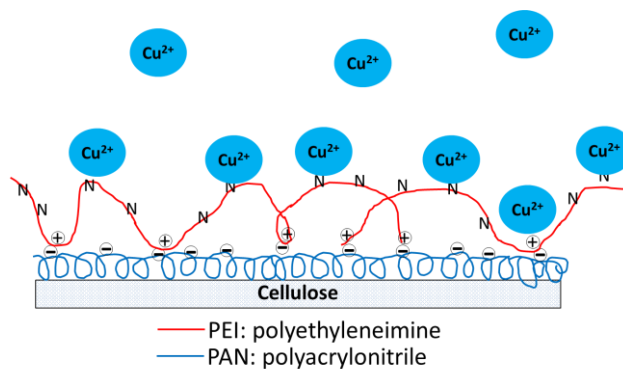


Figure 1: A graphical abstract of PEI-PAN membrane used for determination of copper (II) ion in water media.

# Hansen solubility parameters for an amphiphilic block copolymer selection for SU-8 modification through self-assembling

O. Mednova, K. Almdal

Denmark Technical University, Department of Nanotechnology, Copenhagen, Denmark

**Abstract:** SU-8 is a popular photoresist in the field of microelectromechanical systems (MEMS). It possesses excellent physical, chemical, noncorrosive and photo-plastic properties except low fracture resistance due to high cross-linking density. Brittle behavior limits the resin application and therefore, it has been proposed to modify mechanical properties of SU-8.

Great improvements of epoxies toughening were accomplished with a second phase incorporation in the cured epoxy matrix (Ryan *et al.*; 2008). As modifiers, various types of inorganic and organic fillers have been thoroughly tested and over last few decades amphiphilic block copolymers have been found to be universal (Kinloch; 2003, Hamley; 2004, 2005). A difference between block affinities toward a matrix promotes self-assembly and by changing blocks ratio and their molecular weight, different morphologies are possible to be obtained through phase reorganization. Correct morphology choice along with matrix miscible material selection is vital in order to achieve toughening result.

Hansen solubility parameters were applied to select suitable monomers, a block copolymer of which can undergo self-assembling in uncured and cured SU-8 matrix. In particular, a method based on relative sedimentation time and suspension was applied (Hansen; 2007). It can be assumed that maximum physical adsorption is accompanied by closely matching HSPs. Local adsorption by active groups (alcohol, acid, amine) having the required match, can give anchors on a surface that may no longer be soluble in the continuous media, and therefore will remain in place as required.

A tendency towards self-assembly can be estimated by controlling surface and interfacial energies with total cohesion energy and hydrogen bonding parameters. HSPs for SU-8 were found experimentally by testing the resin behavior in 27 solvents and are  $\delta_D$ ;  $\delta_P$ ;  $\delta_H$ = 18.88; 13.63; 7.82. These are not trivial parameters and only very few polymers have similar ones.

Poly(vinylpyridine) has been proposed as a SU-8 miscible block since its hydrogen bonding parameter is similar to SU-8. In order to equate total cohesion energies of SU-8 and a modifier, a second block with total energy smaller than  $25\text{MPa}^{1/2}$  and hydrogen bonding parameter lower than  $3,6\text{MPa}^{1/2}$  are re-

quired. Popular and easy synthesizing poly(ethyl ethylene) fits mentioned requirements. All chemical structures and HSPs are presented in Figure 1.

Four poly(ethyl ethylene)-poly(2-vinylpyridine) block copolymers with different block ratio and molecular weight were synthesized by living anionic polymerization. Blends with SU-8 will be detailed tested for self-assembling investigation which will prove or contradict the HSPs prediction.

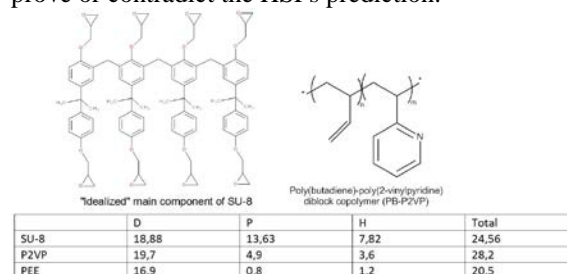


Figure 1: Structures and Hansen solubility parameters of SU-8 epoxy resin main “idealized” component and PEE-P2VP block copolymer.

**Keywords:** self-assembly, SU-8, epoxy, Hansen solubility parameters, mechanical properties modification, material modification toughening.

## References:

- Ruiz-Perez, L., Royston, G.J., Fairclough, J.P.A., Ryan, A.J. (2008) Toughening by nanostructure, *J. Polymer*, 49, 4475-4488
- Kinloch, A.J. (2003) Toughening Epoxy Adhesives to meet today’s challenges, *MRS Bulletin – Materials Research Society*, 28, 445-448
- Hamley, I.W. (2004) Developments in block copolymer science and technology, *J. Wiley*, ix, 367p
- Hamley, I.W. (2005) Block copolymers in solution: fundamentals and applications, *J. Wiley*, 288p
- Hansen, C. M. (2007). Hansen solubility parameters. A user's handbook, *CRC Press*, 519p

# Spectral selectivity of unbalanced magnetron sputtered TiN, TiAlN and TiAlSiN coatings: XRD, SEM and optical analyses

M. Mahbubur Rahman<sup>1\*</sup>, Zhong-Tao Jiang<sup>1</sup>, Chun Yang Yin<sup>2</sup>, Khalil Ibrahim<sup>1</sup>, Zhonghan Xie<sup>3</sup>, Zhi-feng Zhou<sup>4</sup>, Amun Amri<sup>5</sup>, Nick Mondinos<sup>1</sup>

<sup>1</sup>School of Engineering & Information Technology, Murdoch University, Murdoch, Western Australia 6150, Australia

<sup>2</sup>School of Science & Engineering, Teesside University, Borough Road, Middlesbrough, TS1 3BA, United Kingdom

<sup>3</sup>School of Mechanical Engineering, University of Adelaide, SA 5005, Australia

<sup>4</sup>Department of Mechanical and Biomedical Engineering, City University of Hong Kong, Kowloon, Hong Kong, China

<sup>5</sup>Department of Chemical Engineering, Riau University, Pekanbaru, Indonesia

**Abstract:** The photothermal industries require high quality and highly efficient solar selective coatings for the surface of solar energy converters. An efficient selective surface has high absorptance in the visible range and low emittance in the infrared~far-infrared range of the solar spectrum. The low emittance (or high reflectance) of such coatings would significantly reduce energy loss through infrared radiation.

In this paper, we highlight the recent development of utilizing transition metal nitride based coatings as solar selective surface, summarize their selective performances, address the challenges and issues relevant to such coatings and potential identification of the technical features to overcome these limitations for selective surface applications. TiN, TiAlN (Al concentrations vary from low to high atomic %) and TiAlSiN coatings synthesized on AISI M2 steel substrate via unbalanced magnetron sputtered technology were investigated for selective solar surface applications. X-ray diffraction, scanning electron microscopy, UV-Vis spectroscopy, FTIR spectroscopy were carried out to explore the crystalline structure, surface morphology, and optical selectivity of the coatings.

Optical studies showed that the optical absorptance, in the visible range, of the TiN coatings improved significantly from 25% to 74% with increasing Al-doping. However, an increase of optical absorptance of up to 50% resulted from coatings doped simultaneously with Al and Si. With the high Al-content, the optical emittance, in the infrared range, of TiN coatings decreased from 4.5% to 3.4% whereas simultaneous addition of Al and Si to the TiN coatings resulted in a reduction of the emittance down to 4%. The highest optical selectivity of 21.76 was achieved with Al

doping and 12.50 with simultaneous Al and Si doping to the TiN matrix.

**Keywords:** magnetron sputtering, thin film coatings, optical properties, solar absorptance, solar emittance, optical selectivity, selective solar surface, scanning electron microscopy, UV-Vis spectroscopy, FTIR spectroscopy.

# Immobilization of Urease Based on Adsorption in Eggshell Membrane for Urea Biosensor Application

Thanarat Suwanchaituch, Supranee Imthong, Kornvalai Panpae\*

Department of Chemistry, Faculty of Science, King Mongkut's University of Technology Thonburi, KMUTT, Bangkok, Thailand

**Abstract:** In aqueous solutions, biomolecules such as enzymes lose their catalytic activity rather rapidly, because enzymes can suffer oxidation reactions or its tertiary structure could be destroyed at the air/water interface, hence making the use of enzyme and reagents both expensive and complex. These problems can be minimized considerably by enzyme immobilization. By attachment to an inert support material, bioactive molecules may be rendered insoluble, retaining catalytic activity, thereby extending their useful life. In view of the above necessity and advantages, since the 1960s, an extensive variety of techniques have been developed to immobilize biomolecules, including adsorption, covalent attachment and entrapment in various polymers (Gupta et al; 2007). In general, adsorption techniques are easy to perform, but the bonding of the biomolecules is often weak and such biocatalysts lack the degree of stabilization and easy leakage from the matrix. A biosensor is an analytical tool that comprises two essential components—an immobilized biocomponent, in intimate contact with a transducer that converts a biological signal into a measurable electrical signal (Turdean; 2011). Some reports (D'Souza et al; 2012, Marzadori, et al; 1998) on biosensors have been published using eggshell membrane as a supporting matrix for immobilization of enzymes such as D-amino oxidase, catalase, myrosinase, tyrosinase and glucose oxidase. The technique, which mostly used for immobilization of enzyme on eggshell membrane, involved adsorption followed by cross-linking with glutaraldehyde. In this study, a novel immobilization based on adsorption method employing eggshell membrane from hard-boiled eggs and fresh eggs as supporting matrices and polyethyleneimine (PEI) as a carrier system was investigated using Jack bean urease as a model enzyme. Eggshell membranes were studied differentiation of morphology after urease immobilization by SEM. They were studied the changes in IR spectra after urease immobilization by FTIR. Immobilized membrane was attached with a standard pH-electrode. Biosensors of eggshell membrane from fresh egg and hard-boiled egg response urea concentration range from 7.5 mM to 200 mM. The response time of biosensors was 300 s. Biosensors can be reused more than 10 times with no significant decreasing of activity. The efficiency of urease immobilization on fresh membrane is as well as that of boiled egg membrane.

**Keywords:** Potentiometric biosensor, eggshell membrane, urease immobilization, urea biosensor.

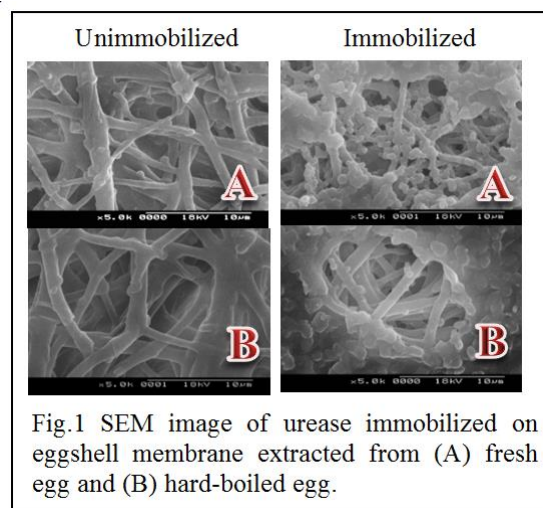


Fig.1 SEM image of urease immobilized on eggshell membrane extracted from (A) fresh egg and (B) hard-boiled egg.

Figure 1: Fig.1 SEM image of urease immobilized on eggshell membrane extracted from (A) fresh egg and (B) hard-boiled egg.

## References:

- D'Souza, S.F., Kumar, J., Jha, S.K., Kubal, B.S. (2012), Immobilization of the urease on eggshell membrane and its application in biosensor, Mater. Sci. Eng.C, 33, 850-854.
- Gupta, R., Chaudhury, N.K. (2007), Entrapment of biomolecules in sol-gel matrix for applications in biosensors: Problems and future prospects, Biosens. Bioelectron., 22, 2387-2399.
- Turdean, G.L. (2011), Design and development of biosensors for the detection of heavy metal toxicity, Int. J. Electrochem., 2011, Article ID 343125, 15 pages.

# Effect of the combined radiation and oxidation pretreatment on the surface properties of lignocellulosic materials

D.P. Melnikov<sup>1</sup>, Ya.A. Masyutin<sup>1</sup>, A.V. Beskorovaynyy<sup>1,\*</sup>, D.S. Kopitsyn<sup>1</sup>, A.A. Novikov<sup>1</sup>, V.A. Vinokurov<sup>1</sup>  
<sup>1</sup>Gubkin Russian State University of Oil and Gas, Department of Physical and Colloid Chemistry, Moscow, Russia

**Abstract:** Biofuel production from lignocellulosic feedstock is the promising way to a greener economy. However, hydrolysis of lignocellulose remains the significant problem. The thorough research of different types of feedstock and different types of pretreatment is necessary to achieve maximum yield of valuable products (ethanol, furan derivatives, etc.). There is a number of lignocellulose pretreatment methods based on the physical, physical-chemical, chemical and biological processes. One must carefully select the pretreatment method, because the pretreatment typically represents about 18% of the total cost of cellulosic ethanol production (Zhang & Shahbazi, 2011). Therefore, it is necessary to choose the less time-consuming, less reagent-consuming and effective method for the pretreatment of lignocellulosic feedstock. The promising method of pretreatment is the combination of irradiation and hydrothermal treatment, which leads to high yields of reducing sugars after subsequent hydrolysis (Duarte *et al.*, 2012). Earlier, we tried to use 1,3-dialkylimidazolium and tetraalkylammonium ionic liquids for the efficient pretreatment of lignocellulose (Masyutin *et al.*, 2013), but the high cost of ionic liquids prevents their usage for the industry-scale pretreatment processes.

In this work, the combination of  $\gamma$ -irradiation and oxidation was employed for the pretreatment of pine wood chips, the model lignocellulosic substrate. We have found that certain combination of irradiation and oxidation by  $\text{H}_2\text{O}_2/\text{Fe}_2\text{O}_3$  leads to significant alteration of lignocellulose microstructure (see Figure 1) and increase of the surface area of the material. Somewhat counter-intuitively, the wet air oxidation of the irradiated wood chips leads to decrease of the surface area with the increase of the absorbed dose of  $\gamma$ -radiation (see Figure 2).

Thus, the large-surface-area materials could be produced by the combined  $\gamma$ -irradiation and oxidation pretreatment of lignocellulose, which opens the possibilities of efficient production of cellulosic ethanol, cellulose-based adsorbents and so on.

This work is supported by Ministry of Science and Education of Russian Federation (project 14.577.21.0070). The authors are thankful to Mikhail S. Kotelev for the SEM micrographs.

Keywords: wet air oxidation, irradiation pretreatment, surface area.

Figure 1: SEM micrographs of  $\gamma$ -irradiated wood chips before and after  $\text{H}_2\text{O}_2/\text{Fe}_2\text{O}_3$  oxidation:

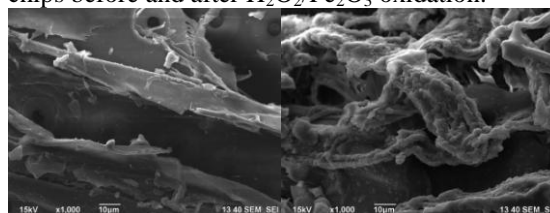
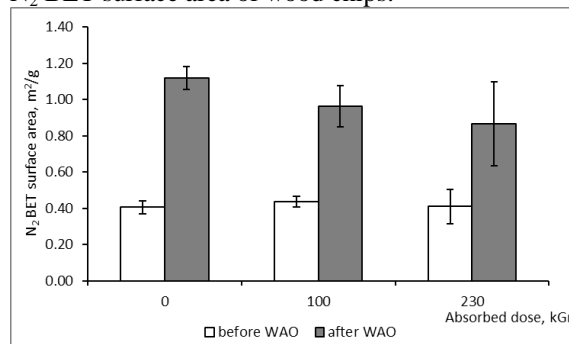


Figure 2: Effect of the wet air oxidation on the  $\text{N}_2$  BET surface area of wood chips:



## References:

- Zhang, B., Shahbazi, A. (2011) Recent Developments in Pretreatment Technologies for Production of Lignocellulosic Biofuels. *J Pet Environ Biotechnol*, 2, 111.
- Duarte, C.L., Ribeiro, M.A., Oikawa, H., Mori, M.N., Napolitano, C.M., & Galvão, C.A. (2012) Electron beam combined with hydrothermal treatment for enhancing the enzymatic convertibility of sugarcane bagasse. *Radiation Physics and Chemistry*, 81, 1008-1011.
- Masyutin, Ya.A., Golyshkin, A.V., Novikov, A.A., Vinokurov, V.A. (2013) Synthesis of ionic liquids based on cations of 1,3-dialkylimidazolium and tetraalkylammonium for pretreatment of lignocellulosic raw material to increase its hydrolyzability. *Lesotechnicheskiy zhurnal*, 3, 107-114 (in Russian) DOI: 10.12737/2188.

# Antibiotic-Labelled Nanomaterials for the Rapid Detection of Microorganisms by Surface-Enhanced Raman Spectroscopy

A.V. Beskorovaynyy<sup>1</sup>, D.S. Kopitsyn<sup>1</sup>, A.A. Novikov<sup>1,\*</sup>, E.A. Bochkova<sup>1</sup>, E.V. Ivanov<sup>1</sup>  
<sup>1</sup>Gubkin Russian State University of Oil and Gas, Department of Physical and Colloid Chemistry, Moscow, Russia

**Abstract:** Gold nanoparticles are very perspective diagnostic and therapeutic agents due to their unique optical properties, biocompatibility and a possibility to modify their surface and make it selective to certain bacterial cells. Usually it can be done by coupling nanoparticles with antibodies to bacterial antigens, but the high cost of antibodies severely constrains the usage of such conjugates (I. Cho *et al*, 2013). However, nanoparticles could be coupled with the much cheaper alternative – various antibiotics (R. Iyer *et al*, 2014, S. Karthick *et al*, 2013).

It was shown in our previous work (A. Beskorovaynyy *et al*, 2014), that antibiotic-coupled nanoparticles with penicillin, chloramphenicol, ciprofloxacin and amikacin have an affinity for bacterial cell wall, and these nanoconjugates can be used for detection of microorganisms such as *Escherichia coli* and *Staphylococcus aureus*. In the present work, rod-shaped gold nanoparticles (Fig. 1) were coupled with various antibiotics and their strong affinity to the cells wall (Fig. 2) was used for surface enhanced Raman scattering (SERS) experiments. It was shown that the bacteria contrasted by the nanoconjugates can be separated from liquid media and detected in trace amounts due to strong SERS signal of antibiotics on their surface (Fig. 3). Based on these evidences, we conclude that a new approach for rapid and selective detection of various microorganisms was proposed and its efficacy was demonstrated.

This work is supported by Ministry of Science and Education of Russian Federation (project 13.1812.2014/K). The authors are thankful to Denis A. Bakulin for the TEM micrographs.

**Keywords:** SERS, Surface enhanced Raman spectroscopy, gold nanoparticles, plasmon resonance, nanosensors, bacteria.

Figure 1: Transmission electron micrograph of the gold nanorods used for the coupling with bacteria

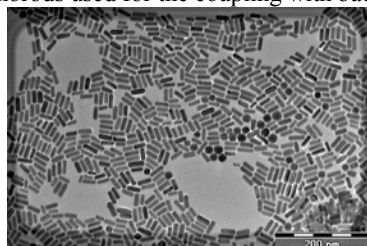


Figure 2: TEM micrograph of the *E. coli* cells with the chloramphenicol-coupled gold nanorods adsorbed on them; bar 0.5  $\mu\text{m}$

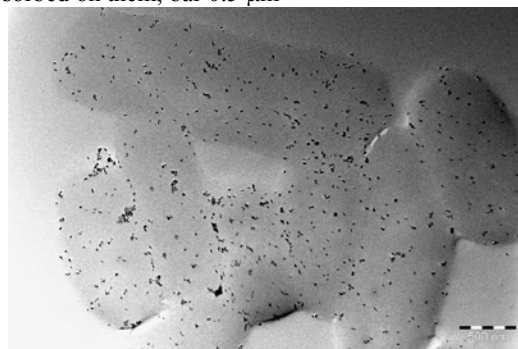
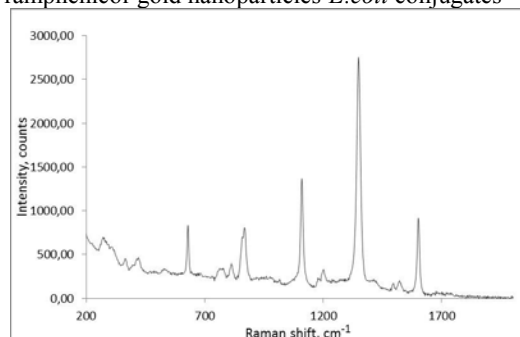


Figure 3: Surface enhanced Raman spectrum of chloramphenicol-gold nanoparticles-*E.coli* conjugates



## References:

- Cho, I. H., Irudayaraj, J. (2013). *In-situ* immuno-gold nanoparticle network ELISA biosensors for pathogen detection. *International journal of food microbiology*, 164(1), 70-75.
- Iyer, R. I., & Panda, T. (2014). Biogenic Synthesis of Gold and Silver Nanoparticles by Seed Plants. *Journal of nanoscience and nanotechnology*, 14(2), 2024-2037.
- Namasivayam, S. K. R., Samrat, K., & Ganesh, S. (2013). Preparation of chitosan stabilized ofloxacin-gold nano conjugate for the improved anti bacterial activity against human pathogenic bacteria. *Innovare Journal of Medical Science*, 1(2).
- A.V. Beskorovaynyy et al. (2013). Evaluation of antibiotics as the target-sensitive component of nanobiomarkers. *Nanotech Dubai 2013 International Conference Proceeding*, 12-13.

# Optimization of enzyme immobilization onto nano-structure materials for enhancing bio-gas production from anaerobic digestion

C. Kang,<sup>1</sup> K.Y. Lee,<sup>2</sup> S.J. Kim,<sup>2</sup> K.Y. Park,<sup>2</sup> H.S. Kim<sup>1\*</sup>

<sup>1</sup>Environmental Engineering, Konkuk University, Seoul, Korea

<sup>2</sup>Civil and Environmental System Engineering, Konkuk University, Seoul, Korea

\*Correspondance

**Abstract:** An enzyme (horseradish peroxidase, HRP) was immobilized by inorganic matrix of which inner pores are layered with nano-scale spacing planar to remove phenolic compounds. Clay materials and chemical and natural organic substances isolated and purified from soils, referred to as soil organic matter (SOM), were screened for the enzyme carrier (support) and binding agent (spacer), respectively. Montmorillonite and fulvic acid were found to be the best combination for the surface-activated carrier matrix since the 2:1 dioctahedral structure clay demonstrated the highest sorptive capacity for SOM and fulvic acid provided various stable chemical bonds with enzyme owing to the high content of various functional groups of SOM. Activities of immobilized and free enzymes were examined by their removal efficiencies for phenol. The Michaelis-Menten model parameters by free HRP were somewhat different from those by immobilized HRP ( $V_{max}$  of 96.6 mM/min and  $K_M$  of 8.4 mM for free HRP and  $V_{max}$  of 62.1 mM/min and  $K_M$  of 129.6 mM for immobilized HRP, respectively), but in general, the immobilized enzyme was almost as effective as free enzyme. While free HRP was slightly sensitive to the environmental factors such as pH, temperature, and ionic strength, fairly stable enzyme activities were observed from immobilized HRP even in large variations in environmental factors. The results of this study are expected to provide fundamental information for the development of an innovative and advanced biochemical treatment and/or remediation technology.

**Keywords:** enzyme immobilization; clay mineral; soil organic matter; phenol; horseradish peroxidase.

**Acknowledgements:** This research was supported by the Geo-Advanced Innovative Action Projects (2012000550002 and 2012000550008) and the Waste to Energy and Recycling Human Resource Development Project (YL-WE-12-001).

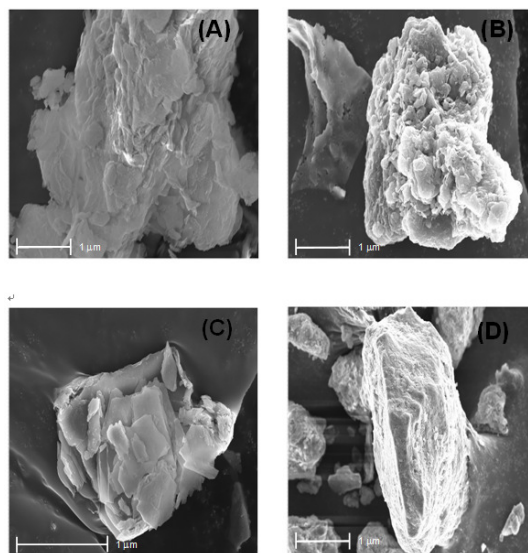


Figure 1: Figure illustrating the surfaces of clays: (a) montmorillonite before fulvic acid adsorption; (b) montmorillonite after fulvic acid adsorption; (c) vermiculite before fulvic acid adsorption; (d) vermiculite after fulvic acid adsorption.

## References:

- Alemzadeh, I., Nejati, S. (2009), Phenols removal by immobilized horseradish peroxidase, *J. Hazard. Mat.*, 166 (2-3), 1082-1086
- Feng, X., Simpson, A.J., Simpson, M.J. (2005), Chemical and mineralogical controls on humic acid sorption to clay mineral surfaces, *Org. Geochem.*, 36 (11), 1553-1566.
- Jafri, F., Saleemuddin, M. (1997), Immobilization of invertase on sepharose-linked enzyme glycosyl recognizing polyclonal antibodies, *Biotechnol. Bioeng.*, 55 (3), 171-179.
- Nazari, K., Esmaeili, N., Mahmoudi, A., Rahimi, H., Moosavi-Movahedi, A.A. (2007), Peroxidative phenol removal from aqueous solutions using activated peroxidase biocatalyst. *Enzyme Microb. Tech.*, 41 (3), 226-233.

# Needle-less Jet Injection System with Multi-Pore Nozzle for Viscous Drug Delivery Applications

Y. C. Jo,<sup>1\*</sup> H. K. Hong,<sup>1</sup> Y. S. Choi<sup>1</sup>, H. S. Kim<sup>2</sup>

<sup>1</sup>Korea Electronics Technology Institute, Medical IT Convergence Research Center, SeongNam-Si, South Korea

<sup>2</sup>Korea Electronics Technology Institute, Contents Research Center, SeongNam-Si, South Korea

**Abstract:** Jet injection is an important needle-free drug delivery method for insulin and vaccines[1-3]. Jet injections employ a high speed jet to puncture the skin and deliver drugs without the use of a needle. Although jet injections have been used for tens of years and continue to be researched for new applications. Needle-free jet injection constitute an important method of drug delivery, especially for beauty treatment. An experimental study was performed using a newly developed air-powered needle-free jet injector(Figure 1) to investigate the relationship between nozzle pore variation and delivered viscous liquid drug volume. The most important injector fuction for beauty treatment are the penetration depth and diffusion area which is related with jet velocity and nozzle pore number. The driver pressure of the air cylinder considered in this work ranged from 6 to 10 bar provided by an air compressor fitted with a precision regulator. Individual nozzle and pressure combinations were tested a minimum of ten times in order to ensure consistent and reliable results. Developed injector in this work is the first needle-free jet injector prototype with multi-pore nozzle for viscous drug delivery upto 12cps, 1% Hyaluronic Acid(HA) solution. The proposed injector has three types of nozzle structure, such as single pore, 4 pores array and 9 pores array nozzles(Figure 2). Experimental studies showed that the penetration depth and diffusion of drug into skin continue to decrease as the nozzle pore number increase(Figure 3, Figure 4).

**Keywords:** Needle-free, Jet injector, Drug delivery, Skin, High viscosity, Beauty treatment

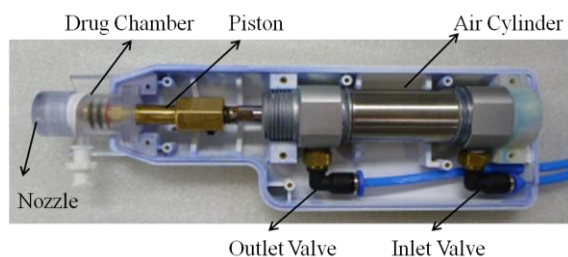


Figure 1: A New needle-free jet injector developed in these work. The injector is driven by a air compressor. The nozzle is made of clear thermoplastics.

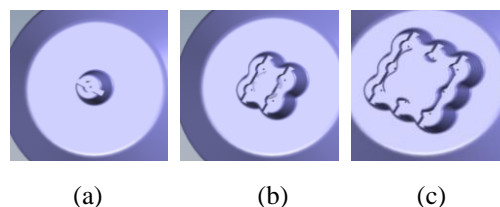


Figure 2: Design models of the injector nozzles of the proposed jet injector used in these experiments. Each nozzle has different pore number. (a) single pore, (b) 4 pores array (c) 9 pores array

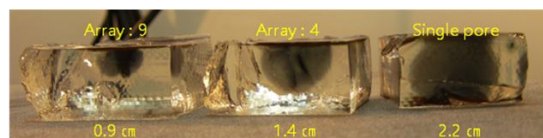


Figure 3: Sample pictures showing the jet penetration generated by the air-powered injector with three different nozzle configurations(9, 4 and single pore) into the 5% gelatin block. All of the pore diameter was 100 um in common and 1% Hyaluronic Acid(HA) solution was used for this experiments

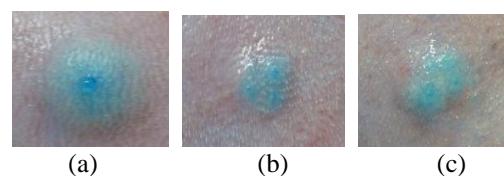


Figure 4: Guinea pig skin test results of the proposed device using designed nozzle with various pore number, (a) 1 pore, (b) 4 pores array (c) 9 pores array

## References:

Portaro, R., Dick Ng, Hoi. (2013) Experimental analysis of the performance of an air-powered needle-free liquid jet injector, *IEEE EMBS*.

Baxter, J., Mitragotri, S.(2005), Jet-induced skin puncture and its impact on needle-free jet injections : Experimental studies and a predictive model, *Int. J. Controlled Release*, 106, 361-373.

Baxter, J., Mitragotri, S.(2005), Needle-free jet injections : dependence of jet penetration and dispersion in the skin on jet power, *Int. J. Controlled Release.*, 97, 527-535.

# Simple Methods to Fabricate Multilayer Microfluidic Devices

T. Jiemsakul,<sup>1</sup> C. Kortchana,<sup>2</sup> S. Manakasettharn<sup>1,\*</sup>

<sup>1</sup>National Nanotechnology Center, Integrated Nanosystem Laboratory, Pathum Thani, Thailand

<sup>2</sup>King Mongkut's Institute of Technology Ladkrabang, College of Nanotechnology, Bangkok, Thailand

**Abstract:** Microfluidic devices have attracted wide attention with practical applications to microtechnology and nanotechnology, primarily due to their advantages such as low fluid volume consumption and compactness of the devices. Microfluidic devices can consist of one or more microchannels with at least one dimension less than 1 mm. In traditional two-layer microfluidic devices, the microchannels are fabricated on a substrate (the first layer) and are then sealed with a cover plate (the second layer). In multilayer microfluidic devices, longer microchannels can be fabricated to achieve more performances. This work presents two simple methods to fabricate multilayer microfluidic devices. For the first method, we have used a CO<sub>2</sub> laser beam to cut through 100- $\mu$ m-thick polyvinyl chloride (PVC) substrates to create microchannels. For the second one, we have used the CO<sub>2</sub> laser beam to engrave microchannels on 1-mm-thick poly(methyl methacrylate) (PMMA) substrates. The cover plates are made of the same material. For both methods, we have used thermal bonding to bond substrates and cover plates together. The PVC microchannels resulting from the first method have approximately rectangular cross-sections, whereas the engraved PMMA microchannels have approximately triangular cross-sections. The depth of the PVC microchannels is controlled by the thickness of the PVC substrates, whereas the depth of the engraved PMMA microchannels depends on laser power. The width of microchannels for both methods can be adjusted by varying the laser power. Compared to conventional photolithography, these two fabrication methods are simpler, faster, and cheaper. We hope that these two methods will be implemented to manufacture sophisticated multilayer microfluidic devices.

**Keywords:** microfluidic devices, microchannels, multilayer, fabrication, CO<sub>2</sub> laser, polyvinyl chloride, PVC, poly(methyl methacrylate), PMMA.

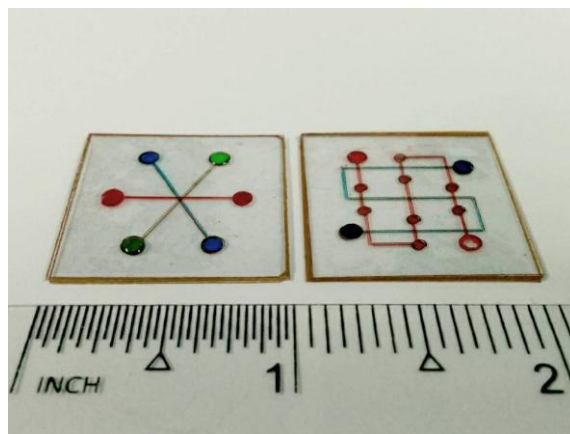


Figure 1: Two fabricated 0.7-mm-thick seven-layer microfluidic devices next to the ruler. (Left) The seven-layer microfluidic device with three (red, green, and blue) microchannels crossing over and under each other. (Right) The seven-layer microfluidic device with the red microchannel alternately crossing over and under the blue microchannel.

# Effect of Annealing Temperature on Microstructure and Optical Properties of ZnO Thin Films with Mg Dopant

Kartikey Verma\*, Babulal Chaudhary and Mahendra Kumar  
Nanomaterial and Environmental Sensors Research Laboratory  
Department of Physics, University Of Lucknow, Lucknow-226007, India

**Abstract:** Polycrystalline  $Zn_{1-x}Mg_xO$  thin-films have been prepared by spin-coating technique annealed at 400°C and 500°C. The prepared thin films were characterized by suitable techniques viz. XRD, SEM, AFM etc. UV-visible and photoluminescence studies of these thin films were also investigated to disclose their optical behaviour. In the present investigation, the 10% content of Mg was used in ZnO for doping. The SEM image of the prepared thin films reveals the existence of fiber-like streaks of 20 nm dimension. The uniformity of the deposited thin films was further confirmed by the AFM study. The polycrystalline nature of the film was proved by the XRD analysis. The prepared thin films show transmittance up to 93% with the optical band gap of 3.42eV. The effect of annealing temperature on the thin films was also observed. The present study indicates the surface properties of the prepared thin films strongly depends on the annealing temperature. The increase in annealing temperature decreases the grain of the films. The dopant concentration (Mg content in ZnO) also affect the surface properties of the films. The prepared thin films are also suitable for various opto-electronic devices.

**Keywords:** sol-gel, XRD, SEM, spin coating, doping, ZnO

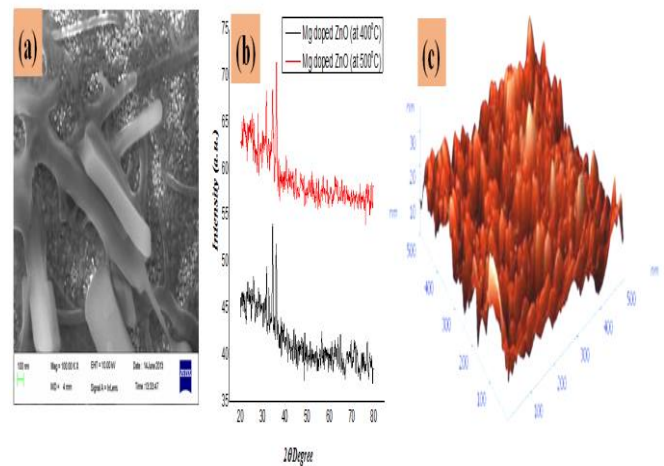
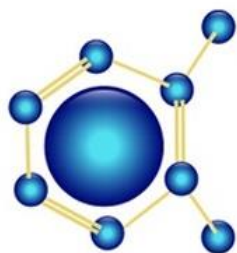


Figure 1: (a) SEM image of Mg doped ZnO thin film, (b) XRD spectra of Mg doped ZnO thin film annealed at 400° and 500° C, and (c) AFM image of Mg doped ZnO thin film. The content of Mg in ZnO is 10%.

## References:

- C. H. Chia, Y. J. Lai, T. C. Han, J. W. Chiou, Y. M. Hu, and W. C. Chou, *Appl. Phys. Lett.* 96, 081903 (2010).
- Salam A. Yousif , Nadir F. Habubi, Abdulla A. Rasheed : *J. Electron Devices*, Vol. 16, 2012, pp. 1347-1355
- M. Wei, R. C. Boutwell, J. W. Mares, A. Scheurer, and W. V. Schoenfeld : *Appl. Phys. Lett.*, 98, 261913 (2011)





**S M S**  
Smart Materials and Surfaces  
B A N G K O K 2 0 1 4  
26 - 28 August 2014

Sheraton Grande Sukhumvit Hotel - Bangkok-Thailand

[www.setcor.org](http://www.setcor.org)